CHALCONE BASED DITHIOCARBAMATE DERIVATIVE INCORPORATED SOL-GEL FOR THE REMOVAL AND PRE-CONCENTRATION OF AQUEOUS MERCURY(II) ION

KHOR SOO WEI

FACULTY OF SCIENCE
UNIVERSITY OF MALAYA
KUALA LUMPUR

2018

CHALCONE BASED DITHIOCARBAMATE DERIVATIVE INCORPORATED SOL-GEL FOR THE REMOVAL AND PRE-CONCENTRATION OF AQUEOUS MERCURY(II) ION

KHOR SOO WEI

DISSERTATION SUBMITTED IN FULFILMENT OF THE REQUIREMENTS FOR THE DEGREE OF MASTER OF SCIENCE

DEPARTMENT OF CHEMISTRY
FACULTY OF SCIENCE
UNIVERSITY OF MALAYA
KUALA LUMPUR

2018

UNIVERSITY OF MALAYA

ORIGINAL LITERARY WORK DECLARATION

Name of Candidate: Khor Soo Wei

Matric No : SGR150046

Name of Degree : Master of Science (Except Mathematics & Science Philosophy)

Title of Dissertation ("this Work"):

Chalcone based dithiocarbamate derivative incorporated sol-gel for the removal and pre-concentration of aqueous mercury(II) ion

Field of Study : Environmental Chemistry

I do solemnly and sincerely declare that:

(1) I am the sole author/writer of this Work;
(2) This Work is original;
(3) Any use of any work in which copyright exists was done by way of fair dealing and for permitted purposes and any excerpt or extract from, or reference to or reproduction of any copyright work has been disclosed expressly and sufficiently and the title of the Work and its authorship have been acknowledged in this Work;
(4) I do not have any actual knowledge nor do I ought reasonably to know that the making of this work constitutes an infringement of any copyright work;
(5) I hereby assign all and every rights in the copyright to this Work to the University of Malaya ("UM"), who henceforth shall be owner of the copyright in this Work and that any reproduction or use in any form or by any means whatsoever is prohibited without the written consent of UM having been first had and obtained;
(6) I am fully aware that if in the course of making this Work I have infringed any copyright whether intentionally or otherwise, I may be subject to legal action or any other action as may be determined by UM.

Candidate's Signature Date:

Subscribed and solemnly declared before,

Witness's Signature Date:

Name:

Designation:

CHALCONE BASED DITHIOCARBAMATE DERIVATIVE INCORPORATED SOL-GEL FOR THE REMOVAL AND PRE-CONCENTRATION OF AQUEOUS MERCURY(II) ION

ABSTRACT

This study demonstrated the application of chalcone based dithiocarbamate derivative as metal capturing ligands for the removal and pre-concentration of mercury ion (Hg^{2+}). Chalcones are a group of naturally occurring compounds, which can be extracted from fruits, vegetables, plants, and spice. In the first part of this work, chalcone was first chemically modified to produce dithiocarbamate derivative, 3-oxo-1,3-diphenylpropyl-2-(naphthalen-2-ylamino) ethylcarbamodithioate (ODPPNE). After that, chalcone incorporated sol-gel (SG-C) and ODPPNE incorporated sol-gel (SG-ODPPNE) were prepared and used as adsorbents to remove Hg^{2+}. The result showed that with the presence of dithiocarbamate functional group, SG-ODPPNE exhibited the high selectivity toward Hg^{2+} adsorption as compared to other metal ions. The effect of operating conditions (such as the size of adsorbent, adsorbent dosage, contact time, the initial concentration of Hg^{2+} and pH of solution) were examined for the adsorption of Hg^{2+} by SG-ODPPNE. The adsorption data were fitted well to Langmuir isotherm, and the monolayer adsorption capacity was found to be 13.5 mg/g. In the adsorption kinetic study, the obtained data were well fitted to pseudo-second order model. According to intraparticle diffusion model, the adsorption process of Hg^{2+} by SG-ODPPNE involves film diffusion, intraparticle diffusion, and equilibrium stages. For the second part of this study, ODPPNE incorporated silica was coated onto magnetic nanoparticle (ODPPNE@MNP). This ODPPNE@MNP was used as the solid phase in magnetic dispersive micro-solid phase extraction method (D-μSPE) for the pre-concentration and determination of trace amount of Hg^{2+} ion in water samples. Under optimized condition, this method achieved low

method detection limit (4.0 ng/L), wide linearity (50.0-5000.0 ng/L), high pre-concentration factor (100), a good coefficient of regression (0.9985) and good repeatability (4.5-6.5%). This proposed method was also successfully utilized for determination of Hg^{2+} in drinking water, tap water and surface water with good extraction efficiency (90.1-99.0%) as well as the relative standard deviation value for intra-day and inter-day study of 0.7-8.8% and 1.1-7.7%, respectively. In conclusion, the natural product based ODPPNE is an effective and selective ligand, which can be used to determine Hg^{2+} in aqueous samples and to remove Hg^{2+} from the water.

Keywords: Chalcone, dithiocarbmate derivative, sol-gel, mercury, adsorption

TERBITAN DITIOKARBAMAT BAGI KALKON YANG DIGABUNGKAN DENGAN SOL-GEL UNTUK PENYINGKIRAN DAN PEMEKATAN ION RAKSA(II) ION DALAM LARUTAN AKUEUS.

ABSTRAK

Kajian ini menunjukkan penggunaan terbitan ditiokarbamat bagi kalkon sebagai ligan untuk penyingkiran dan pra-pemekatan ion raksa (Hg^{2+}) dalam air. Kalkon merupakan sebatian semulajadi yang boleh diperolehi daripada buah-buahan, sayur-sayuran, tumbuhan dan rempah. Di bahagian pertama kajian ini, kalkon telah diubah suai secara kimia untuk menghasilkan terbitan ditiokarbamat, 3-okso-1,3-difenilpropil-2-(naftalena-2-ilamino) etilkarbamoditioat (ODPPNE). Seterusnya, sol-gel yang bergabung dengan kalkon (SG-C) dan sol-gel yang bergabung dengan ODPPNE (SG-ODPPNE) disintesiskan sebagai penjerap untuk Hg^{2+}. Hasil kajian ini menunjukkan bahawa dengan kehadiran kumpulan berfungsi ditiokarbamat, SG-ODPPNE menunjukan kepilihan yang tinggi terhadap penjerapan Hg^{2+} berbanding dengan ion logam yang lain. Kesan daripada parameter seperti saiz penjerap, jumlah penjerap, masa, kepekatan Hg^{2+} dan pH larutan bagi penjerapan Hg^{2+} oleh SG-ODPPNE telah dikaji. Data penjerapan yang diperolehi adalah patuh kepada isoterma Langmuir dan muatan jerapan ekalapis yang diperolehi ialah 13.5 mg/g. Dalam kajian kinetik jerapan, data eksperimen adalah padan dengan model tertib pseudo kedua. Menurut kepada model resapan intrazarah, proces penjerapan Hg^{2+} oleh SG-ODPPNE melibatkan resapan tipisan, resapan intrazarah dan peringkat keseimbangan. Untuk bahagian kedua kajian ini, nanopartikel bermagnet telah disalutkan dengan gel silika yang digabungkan dengan ODPPNE (ODPPNE@MNP). ODPPNE@MNP telah digunakan sebagai fasa pepejal dalam kaedah pengekstrakan fasa pepejal bermagnet secara penyebaran (D-μSPE) untuk permekatan dan penentuan Hg^{2+} dalam sampel air. Dibawah keadaan optimum, kaedah ini berjaya mencapai had

pengesanan kaedah yang rendah (4.0 ng/L) , julat linear yang luas (50.0-5000.0 ng/L), faktor pra-pemekatan yang tinggi (100), pekali regresi yang baik (0.9985) dan keterulangan yang memuaskan (4.5-6.5%) . Kaedah ini juga telah berjaya digunakan dalam penentuan Hg^{2+} dalam air minuman, air paip dan air permukaan dengan pemisahan keupayaan yang baik (90.1-99.0%). Sisihan piawai relatif bagi analisis intraday dan interday adalah 0.7-8.8% dan 1.1-7.7% masing-masing. Kesimpulannya, ODPPNE berasaskan sebatian semulajadi merupakan ligan yang berkesan dan berpilih dalam penentuan Hg^{2+} dan penyingkiran Hg^{2+} dalam air.

Kata kunci: Kalkone, terbitan ditiokarbamat, sol-gel, raksa, penjerapan

ACKNOWLEDGEMENT

First at all, I wish to convey my gratitude and thank to all those who gave me the possibility to complete this dissertation. I would like to express my sincere appreciation to my supervisor Dr. Tay Kheng Soo for his constant guidance and support provided throughout this research study. I am also grateful to Prof. Dr. Mhd. Radzi Bin Abas and Dr Lee Yan Kee for their constructive suggestions and inputs that contributed to my research study.

Besides that, I would like to thank my entire colleagues from lab L5-21/23 for their kindness and support. My sincere gratitude is extended to all the staff from the Department of Chemistry, Faculty of Science, University of Malaya for their informative and knowledgeable advices.

Last but not least, I am truly grateful towards my beloved family for the encouragements, constant supports and motivation throughout my life.

TABLE OF CONTENTS

LIST OF FIGURES

LIST OF TABLES

LIST OF SYMBOLS AND ABBREVIATIONS

%E	:	Recovery efficiency
%R	:	Removal percentage
AAS	:	Atomic absorption spectroscopy
AC	:	Activated carbon
Ag-NP	:	Silver-nanoparticle
APTES	:	3-aminopropyltrimethoxysilane
ATR/FTIR	:	Attenuated total reflection/ Fourier-transform Infrared
B_f	:	Freundlich constant
B_L	:	Langmuir constant
Bt	:	Mathematical function for fraction of Hg^{2+} adsorbed at different time
C_e	:	Equilibrium concentration
CF-CVAAS	:	Continuous-Flow Cold Vapor Atomic Absorption Spectrometry
C_{id}	:	Constant related to the thickness of the boundary layer
CNT	:	Carbon nanotube
C_o	:	Initial concentration
CPTS	:	3-chloropropyltriethoxysilane
C_r	:	Extracted concentration
CV-AAS	:	Cold Vapor Atomic Absorption Spectrometry
CV-ETAAS	:	Electrothermal Atomic Absorption Spectrometer
DMA	:	Direct mercury analyser
D-SPE	:	Dispersive solid phase extraction
DTA	:	Differential thermal analysis

DWQS	:	Drinking Water Quality Standard
D-μSPE	:	Dispersive micro-solid phase extraction
EC	:	Electrocoagulation
F	:	Fraction of Hg^{2+} adsorbed at different time
Fe_3O_4-SiO_2	:	Silica gel coated iron oxide magnetic nanoparticle
FI-MSPME	:	Flow injection magnetic solid phase micro-extraction
GO	:	Graphene oxide
ICP-OES	:	Inductively Coupled Plasma Optical Emission Spectrometry
k_1	:	Pseudo-first order rate of reaction
k_2	:	Pseudo-second order rate constant
k_{id}	:	Intra-particle diffusion rate constant
LOD	:	Limit of detection
LOQ	:	Limit of quantitation
MA	:	Mercury analyser
MCLG	:	Maximum contaminant level goal
MDL	:	Method of detection limit
MNP	:	Magnetic nanoparticle
MOHM	:	Ministry of Heath Malaysia
MPTS	:	Methacryloxypropyltriethoxysilane
MWCNT	:	Multiwalled carbon nanotube
n	:	Adsorption intensity constant
NWQS	:	National Water Quality Standards
ODPPNE	:	3-oxo-1,3-diphenylpropyl-2-(naphthalen-2-ylamino) ethylcarbamodithioate
ODPPNE@MNP	:	ODPPNE-silica coated magnetic nanoparticle

PEUF	:	Polymer enhanced ultrafiltration
PMO	:	Periodic mesoporous organosilica
Q_e	:	Adsorption capacity at equilibrium
$Q_{e,cal}$	:	Calculated adsorption capacity at equilibrium
$Q_{e,exp}$	:	Experimental adsorption capacity at equilibrium
Q_m	:	Maximum adsorption capacity
Q_t	:	Amount of adsorbed sorbate at time *t*
R'''	:	Organic functionalities
R_L	:	Dimensionless constant
SG	:	Blank sol-gel
SG-C	:	Chalcone incorporated sol-gel
SG-ODPPNE	:	3-oxo-1,3-diphenylpropyl-2-(naphthalen-2-ylamino) ethylcarbamodithioate incorporated sol-gel
SiO_2	:	Porous silica frameworks
SiO_2@MNP	:	Silica coated magnetic particle
SPE	:	Solid phase extraction
SPME	:	Solid phase micro-extraction
SWCNT	:	Single walled carbon nanotube
TGA	:	Thermogravimetric analysis
UNICEF	:	United Nations Children's Fund
USEPA	:	United States Environmental Protection Agency
V_0	:	Initial volumes of aqueous solution
V_f	:	Volume of desorption agent
WEPA	:	Water Environment Partnership in Asia
WHO	:	World Health Organization
χ^2	:	Chi-square values

LIST OF APPENDICES

CHAPTER 1: INTRODUCTION

1.1 Background Study

Clean drinking water is a basic human need. Unfortunately, 748 million people around the world still facing the lack access to the improved drinking-water (WHO and UNICEF, 2014). This problem is particularly acute in the developing countries (WHO, 2017). There are numbers of threats to drinking water which include chemicals, animal wastes, pollutants and human wastes which have been frequently contaminated the sources of drinking water (USEPA, 2004). Among various pollutants, metal contamination in the aquatic environment has attracted global attention owing to its toxicity and persistence in the environment (Islam et al., 2015). Small amounts of heavy metal are commonly found in our environment and diet. Some of these metals are necessary for diet; for example, living organism required various amounts of heavy metal such as iron, cobalt, copper, manganese, molybdenum and zinc (Singh et al., 2011) for metabolism process (Abbaspour et al., 2014; Bost et al., 2016; Fenech, 2001; Mendel, 2013; Roohani et al., 2013; Seo and Park, 2008). However, due to the bioaccumulation and biomagnifications in the food chain, metals and metalloids from natural and anthropogenic sources are continuously posing the serious threat to human and ecological health (Rahman et al., 2012). Most of the metals are entering to the natural water system through the anthropogenic activities such as mining, disposal of untreated and partially treated effluents which containing toxic metals, metal chelates from different industries, indiscriminate use of heavy metal-containing fertilizer and pesticides in agricultural fields (Reza and Singh, 2010). Table 1.1 shows the heavy metal pollution status in several surface water sources in Malaysia and other countries. The amount of some heavy metal such as aluminum (Al), arsenic (As), boron (B), cadmium (Cd), chromium (Cr), iron (Fe), lead (Pb), manganese (Mn), mercury (Hg) and selenium (Se) have been found at the level which is higher than the quality standard regulated by National Water Quality Standards

for Malaysia (NWQS), Drinking Water Quality Standard for Malaysia (DWQS) and World Health Organization (WHO) Guidelines for Drinking-water Quality.

Table 1.1: Heavy metal pollution status of some rivers and lakes in Malaysia and other countries

Heavy metal that exceeded the water quality standard	Location
Hg [a, b, c, 1]	Langat River Basin, Selangor
Fe and Mn [a, b, c, 2]	Well, river and tap water, Sungai Buloh village, Selangor.
Al and Fe [a, b, c, 3]	Selangor River, Selangor
As [a, b, c, 1]	Klang River Basin, Kuala Lumpur
Fe, Pb and Se [a, b, c, 4]	Curtin Lake, Miri Sarawak
As, Cd, Cr and Pb [c, 5]	Dhalai Beel , Bangladesh
As ,Cd, Cr and Pb [c, 5]	Bangshi River, Bangladesh
As and B [c, 6]	Chasicó Lake, Argentina
Al, Cd and Pb [c, 7]	Ismailia Canal, Nile River, Egypt
Pb [c, 8]	Siling Reservoir Watershed in Zhejiang Province, China
As and Pb [c, 9]	Shadow Lake of Yangtze River region, China
Hg [c, 10]	River in Artisanal gold mining site, Asutifi District, Ghana
As and Hg [c, 11]	Can Tho/Hau Giang provinces, Mekong Delta, Vietnam

[a]NWQS (WEPA, 2006), [b]DWQS (MOHM, 2010), [c]WHO Guidelines for Drinking-water Quality (WHO, 2011)

[1]Poon et al., 2016, [2]Ambu et al., 2014, [3]Daniela and Kawasaki, 2016, [4]Prasanna et al., 2012, [5]Rahman et al., 2014, [6]Avigliano et al., 2015, [7]Goher et al., 2014, [8]Naveedullah et al., 2014, [9]Liu and Li, 2011, [10]Adjei-Kyereme et al., 2015, [11]Wilbers et al., 2014

Among various heavy metals, one of the serious threats to human health is associated with the exposure to mercury (Hg) and this metal is required to be removed to very low levels during water treatment. Hg has been found to bioaccumulate in the living organism to a level that produced adverse effects (Hennebery et al., 2011). In the environment, mercury can exist and circulate in several chemical forms which include elemental mercury (Hg^0), mercury ions (Hg^+ and Hg^{2+}) and organomercury (CH_3Hg^+) as shown in Figure 1.1.

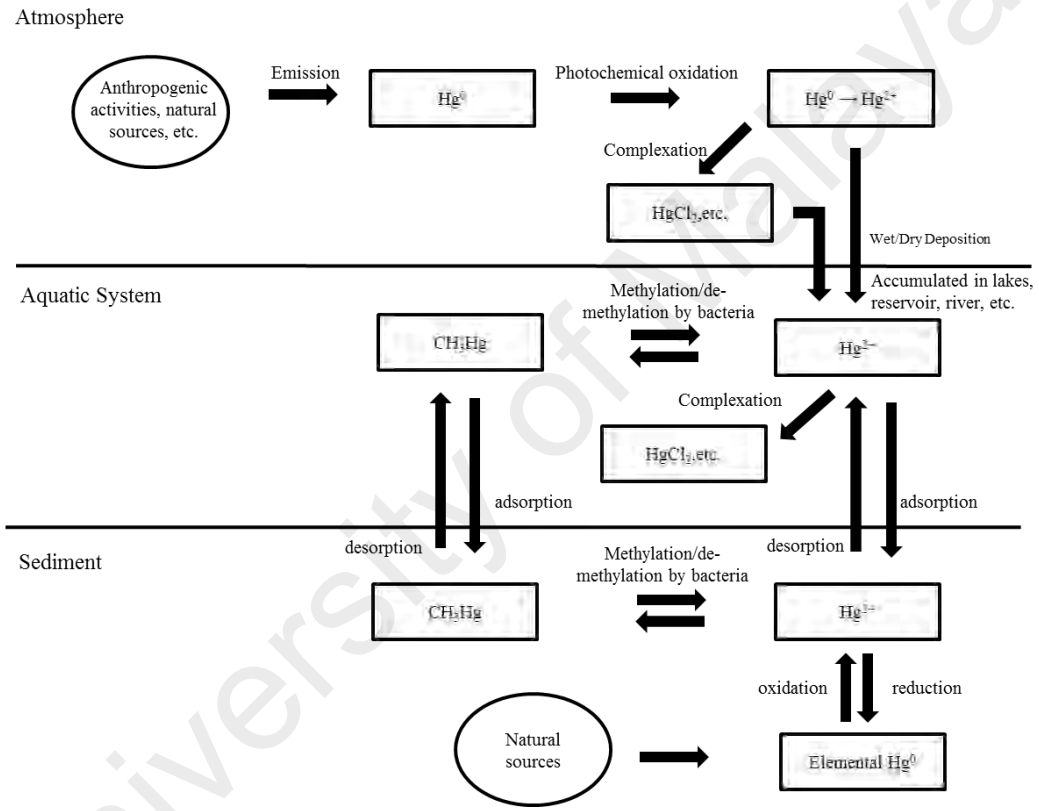

Figure 1.1: Mercury species exist in environment system.

Elemental Hg^0 is the predominant form of mercury in the atmosphere (Lamborg et al., 2002) with natural and anthropogenic activities as the major sources (Strode et al., 2007). The atmospheric half-life of Hg^0 vapour is within 0.5 to 1 year. Due to the long half-life, Hg^0 can spread globally in the atmosphere (Selin, 2009; Weiss-Penzias et al., 2016). For the human, the poisoning of Hg^0 vapour is mainly through inhalation (Lambertson, 2005). In Prestea, Ghana, 46.7% of small-scale gold miners inhaled high

level of Hg^0 vapour that released from gold mining activities were experienced high Hg^0 concentration in their urine (Mensah et al., 2016). The chronic exposure of Hg^0 vapour can damage the central nervous system and kidneys (Lambertson, 2005). On the other hand, the absorption of Hg^0 through ingestion and the dermal process has been found to be poor and limited (Park and Zheng, 2012).

Inorganic mercury in the form of mercuric (II) ion (Hg^{2+}) is the most abundant mercury species in the aquatic environment (Bridges and Zalups, 2010). Conversion of elemental Hg^0 to gaseous inorganic mercury Hg^{2+} or particle bound Hg^{2+} compounds can be occurred through photochemical oxidation of Hg^0 in the atmosphere (Selin, 2009; Weiss-Penzias et al., 2016). Hg^{2+} species with shorter half-life and water-soluble behaviour is then deposited in the aquatic system (Stein et al., 1996; Zhang et al., 2012). Thus, the Hg^{2+} was predominantly found in freshwater and sea water system (Karthiga et al., 2016). Mercurous (Hg^+) and mercuric (Hg^{2+}) complexes can be found in the aquatic system resulted from the complexation between deposited Hg^+ or Hg^{2+} with anions in water such as chloride and hydroxide ions (Lambertson, 2005). On the other hand, the atmospheric Hg^{2+} tends to form complex also with the other ions such as chloride ion in the atmosphere (Stein et al., 1996). The main Hg^{2+} intake route for the human is by Hg^{2+} contaminated food or drink (Bridges and Zalups, 2010). The study by Monteiro et al. (2013) also showed that, inorganic mercury has the potential to undergo bioaccumulation through the food chain in the aquatic system. The toxicity of Hg^{2+} complexes is largely depending on their solubility in water. Hence, the low water-soluble forms of Hg^+ complexes are less poisonous than water soluble Hg^{2+} complexes (Langford and Ferner, 1999). The corrosive feature of inorganic mercury enhances the gastrointestinal permeability and absorption. Oral exposure to mercury salt causes the syndrome like burning chest pain, darkened discoloration of the oral mucous membrane and severe

gastrointestinal symptoms and follow by signs of mercurial stomatitis and impaired kidney function (Park and Cheng, 2012).

Organic mercury such as methyl mercury (CH_3Hg^+) is the most toxic mercury form as compared to Hg^0, Hg^+ and Hg^{2+} (Hong et al., 2012). Methyl mercury is forms through methylation of Hg^{2+} in the aquatic system by microorganism such as sulfate and iron reducing bacteria (Gilmour et al., 2013). The hazardous methylmercury is intake by the aquatic organism and initiates the bioaccumulation of mercury in the food chain. Methyl mercury intake by human body can happen through the contaminated aquatic organism such as fish which are consumed and as food. (Hong et al., 2012). Methyl mercury with high lipid-soluble properties can permeate into the blood and reach the brain and placental barrier which ended up at central nervous system (Lambertson, 2005).

This study was focused on the removal and pre-concentration of Hg^{2+}. World Health Organization (2005) reported that almost all mercury in drinking water present in the form of Hg^{2+}. The Hg mostly presences in the air as Hg^0 vapour while the organic mercury such as methyl mercury is mainly accumulating in biota. Moreover, methyl mercury is not produced until the methylation of inorganic mercury (Hong et al., 2012) in water. Due to the hazardous effect of mercury, the maximum allowable concentration of mercury in drinking water is keep under 0.001 mg/L by Drinking Water Quality Standard of Malaysia (DWQS) (MOHM, 2010), 0.002 mg/L by the United States Environmental Protection Agency (USEPA) (USEPA, 2009) and 0.001 mg/L by World Health Organization (WHO) (WHO, 2011).

Conventional water treatment methods for mercury ion (Hg^{2+}) removal that have been developed are such as coagulation and flocculation (Henneberry et al., 2011), chemical precipitation (Lewis, 2010; Sumesh et al., 2011), electrochemical methods (Wang et al., 2011), membrane filtration (Bessbousse et al., 2010; Song et al., 2012) and adsorption process (Dong et al., 2016). Among these methods, adsorption process is

receiving high attention because of its high efficiency, technical flexibility and cost-effectiveness (Dong et al., 2016). A variety of adsorbents for heavy metal removal had been studied and discussed by many researchers. These adsorbents are such as activated carbon, bioadsorbent, agricultural wastes and clay material (Abu-Eishah, 2008; Ghorbani et al., 2011; Kavand et al., 2014; Khoramzadeh et al., 2013; Monier and Abdel-Latif, 2012; Najafi et al., 2012). On the other hand, these materials have its own limitation such as low loading capacities, relatively small metal ion binding constant and less selectivity (Najafi et al., 2012). Recently, the used of porous silica frameworks (SiO_2) or so-called sol-gel as adsorbent in the removal of toxic substances such as heavy metal have become a popular method due to the simplicity in preparation, low cost, large surface areas, excellent thermal and mechanical stability, rapid adsorption kinetics, and excellent anti-swelling properties (Niu et al., 2015; Zhao et al., 2012). In addition, the sol-gel is readily modified by a variety of functionalities ligand for selective removal of the target metal ion such as aqueous Hg^{2+} (Esmaeili Bidhendi et al., 2014; Khor et al., 2017)

A wide range of sol-gel based adsorbents has been developed for the adsorption of heavy metals and the sol-gel with incorporated metal capturing ligand has been reported as one of the effective adsorbents (Zhao et al., 2012). This material has become an attractive adsorbent due to its simplicity in preparation (Zaitoun et al., 2014). Thus far, various ligands such as *N*-(dipropylcarbamothioyl) thiophene-2-carboxamide, polyamidoamine dendrimers, trioctylmethylammonium 1-phenyl-3-methyl-4-benzoyl-5-onate, 2-aminothiazole, 1,4,10,13-tetraoxa-7,16-diazacyclooctadecane- 7,16-bis(malonate), and dithizone have been synthesized for the removal and also the determination of metals ions (Mehmood et al., 2013; Sun et al., 2014; Turanov et al., 2016; Tzvetkova and Nickolov, 2012; Yost et al., 2000; Zhang et al., 2014). These ligands are often synthesized through a series of organic reactions, which is not environmental friendly. On the other hand, numerous studies also have shown the ability of natural

products such as rutin (Ikeda et al., 2015) and curcumin (Picciano and Vaden, 2013) to form complexes with metal ions.

The first part of this study demonstrated the application of a natural product called chalcone as a ligand for the removal of Hg^{2+} in water. Chalcone contains two aromatic rings linked by a three-carbon α, β-unsaturated carbonyl system (Figure 1.2a). Chalcone-type of natural products can be obtained from fruits (e.g., citruses, apples), vegetables (e.g., tomatoes, shallots, bean sprouts, and potatoes), various plants and spices (Orlikova et al., 2011; Patil et al., 2009). Chalcone was selected because of its low-toxicity, eco-friendly, and possible chemical modification (Ghouila et al., 2012; Hsieh et al., 2012). In this study, the chemical modification was also carried out on chalcone to increase its selectivity towards the removal of Hg^{2+}. Among various functional groups, dithiocarbamate functionalized ligands have been found to be selective towards the interaction with Hg^{2+} (Figueira et al., 2011; Tavares et al., 2013). Therefore, in this study, chalcone was modified into dithiocarbamate derivative, 3-oxo-1,3-diphenylpropyl-2-(naphthalen-2-ylamino) ethylcarbamodithioate (ODPPNE) (Figure 1.2b). The ODPPNE was then incorporated on the sol-gel to generate the effective adsorbent in removal aqueous Hg^{2+}.

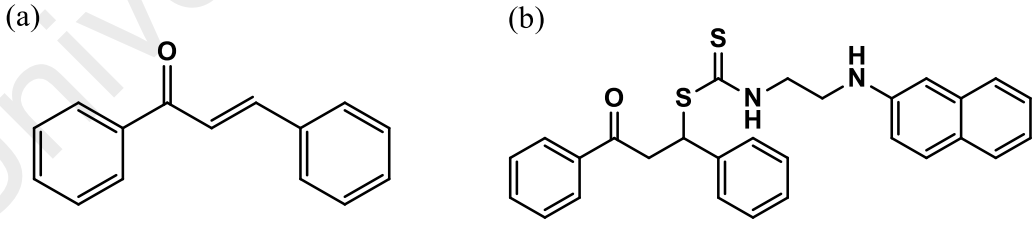

Figure 1.2: (a) Chalcone and (b) ODPPNE.

The concentration of total dissolved mercury in natural water samples could be varying from pg/L to ng/L (Zhang et al., 2014). However, the detection limits for inorganic mercury for common instruments such as Atomic Absorption Spectrometry (AAS) are at the μg/L level (WHO, 2005). Therefore, an appropriate pre-concentration

method is required before Hg^{2+} determination. The application of solid phase extraction method that employing modified magnetic particles as adsorbents in analytical chemistry has increased significantly in recent years (Wierucka and Biziuk, 2014; Ríos and Zougagh, 2016). When magnetic particle-based adsorbents are used for the extraction, super paramagnetic properties of these materials allow it to be separated from water by an external magnetic field. As a result, the duration of sample preparation can significantly shorten and simplified. A wide range of magnetic adsorbents have been developed for selective determination of Hg^{2+} (e.g. Adlnasab et al., 2014; Abolhasani et al., 2015; Alonso et al., 2016; Cui et al., 2015; Es'haghi et al., 2016; López-Garcia et al., 2015; Sobhi et al., 2017; Zhang et al., 2014). Most of these magnetic adsorbents were produced through a series of reactions. These reactions are such as synthesis of iron oxide (Fe_3O_4) magnetic nanoparticle, coating of Fe_3O_4 with silica layer, functionalization of silica coated Fe_3O_4 and bonding of selected ligand onto the functionalized silica coated Fe_3O_4 (Alonso et al., 2016; Cui et al., 2015; Sobhi et al., 2017). Some of this reactions involved high temperature reflux and also time consuming. Hence, the second part of this study demonstrated the coating of sol-gel doped with ODPPNE ligand onto Fe_3O_4 to produce an adsorbent (ODPPNE@MNP) for pre-concentration of Hg^{2+}. This method simplifies the preparation of adsorbent by incorporating the ligand during the coating of Fe_3O_4 with silica layer. The performance of ODPPNE@MNP as solid phase for Hg^{2+} pre-concentration and determination was evaluated through a series of experiment.

1.2 Objective of Study

The objectives of this study were:

a) to prepare and characterize the ODPPNE incorporated sol-gel (SG-ODPPNE) and the magnetic nanoparticle coated with ODPPNE incorporated sol-gel (ODPPNE@MNP).
b) to evaluate the Hg^{2+} adsorption performance of the adsorbents
c) to investigate the capability of selected adsorbent (ODPPNE@MNP) for pre-concentration of Hg^{2+}.
d) to develop a Hg^{2+} pre-concentration method for analysis water sample by using ODPPNE@MNP as solid phase in magnetic dispersive micro-solid phase extraction technique (D-μSPE).

1.3 Research scope

Generally, this research study can be divided into two parts. First part of the study was consisted of the synthesis of of SG-ODPPNE as adsorbent for the removal of Hg^{2+} in water sample. In the second part of the study, ODPPNE incorporated silica gel which showed the greatest selectivity towards the adsorption of Hg^{2+} was used as the coating material for iron oxide magneric nanoparticle (MNP) to produce ODPPNE@MNP. The ODPPNE@MNP was used as an adsorbent for dispersive micro-solid phase extraction technique (D-μSPE) to pre-concentrate Hg^{2+} in water sample.

CHAPTER 2: LITERATURE REVIEW

2.1 Conventional treatment methods for Hg^{2+} removal in water

Generally, the conventional treatment methods which have been used for Hg^{2+} removal are include coagulation-flocculation, co-precipitation, electrochemical treatment, membrane filtration and adsorption (Dong et al., 2016; Henneberry et al., 2011; Huang et al., 2016; Nanseu-Njiki et al., 2009; Santhosh et al., 2013).

2.1.1 Coagulation and Flocculation

The coagulation-flocculation process is a common technique used for the removal of suspended solids in water during water and wastewater treatment (Lanciné et al., 2008). During coagulation, coagulants such as ferric chloride and alum are added to the water. The cation species such as Al^{3+} and Fe^{3+} are neutralized the negatively charged suspended solids. The suspended solids are then allowed to agglomerate into larger settable flocs during flocculation (Amuda and Amoo, 2007; Folens et al., 2017; Lanciné et al., 2008). The flocs are then precipitated as sludge. Positively charged heavy metals are known to form the strong complexes with organic based suspended solids (Muresan et al., 2011). Haitzer et al. (2002) reported that the Hg^{2+} bind favourably to organic matter that containing the sulphur atom. Hence, the certain fraction of Hg^{2+} can be removed from the water when the suspended solids are removed through coagulation-flocculation. For Hg removal, Henneberry et al. (2011) reported the efficiency of three different coagulants namely ferric sulfate ($FeSO_4$), ferric chloride ($FeCl_2$) and poly aluminium chloride (PAC) in the removal of inorganic mercury (Hg^{+} and Hg^{2+}) in surface water by using coagulation-flocculation process. They found that 96, 97, and 84% of inorganic mercury were removed when $FeSO_4$, $FeCl_2$, and PAC were used as the coagulant. Although the coagulation-flocculation method was widely used it's generally facing some limitation. This method required high operation cost due to chemical consumption (Kurniawan et al., 2006) and the further treatment of the sludge that generated during the process (Teh

et al., 2016). Furthermore, the usage of the conventional coagulant such as alum was limited by its dosage due to the high dosage of alum-based coagulant released and increased the amount of toxic aluminium species in water (Teh et al., 2016).

2.1.2 Co-precipitation

The co-precipitation method was performed by the addition of the co-precipitation reagent such as sodium hydroxide and iron sulphide into the metal contaminated water. The metal ions are then reacted with the added reagent to form metal hydroxide or metal sulphide as insoluble precipitates (Santhosh et al., 2013). Besides that, heavy metal in water also can be removed as the insoluble metal-ligand precipitate by the addition of synthetic ligand into the water (Blue et al., 2008). The insoluble precipitates can be separated from aqueous solution by filtration or sedimentation. For Hg^{2+} removal through the co-precipitation method, a previous study reported the application of hydrogen sulphide and alkali metal sulphide salts as co-precipitation reagents (Ebadian, 2001). This study reported that 99.9% of Hg^{2+} was removal from water. In another study, Blue et al. (2008) applied a synthetic ligand called dipotassium salt of 1,3-benzendiamidoethanethiol (K_2BDET) to treat Hg^{2+} contaminated ground water. The Hg^{2+} was found to bind with the $BDET^{2-}$ and subsequently, formed the insoluble Hg-BDET complex as the precipitate. They found that 99.9% of Hg^{2+} was removed. Although this method showed high efficiency in Hg^{2+} removal, it also has its own weaknesses. For example, the co-precipitation process tends to produce the large amount of low-density sludge, which is difficult to remove from water (Fu and Wang, 2011). In addition, the metal sulphide based precipitate tends to form the colloidal system, which may cause difficulties in the separation process (Fu and Wang, 2011). Moreover, the evolution of toxic H_2S fumes may occur under acidic condition if the sulphur-type of co-precipitation reagents was used (Fu and Wang, 2011).

2.1.3 Electrocoagulation

Electrocoagulation (EC) is a technique that applies the electrochemical method for the treatment of polluted water (Ferniza-García et al., 2017; Hakizimana et al., 2017). In EC process, the electric current is applied to water through an electrode (anode) which commonly consisted of iron or aluminum material. The electrochemical dissolution of anode electrode generates the coagulants species such as Fe^{3+} or Al^{3+}, which have the capability coagulate the soluble or suspended particles to form the settleable floc (Ferniza-García et al., 2017). On the other hand, the reduction of water at cathode will release the hydroxide ion (OH^-) and hydrogen gas (H_2) (Bazrafshan et al., 2012). The OH^- reacts with Al^{3+} to form aluminum hydroxide ($Al(OH)_3$) as floc. The $Al(OH)_3$ floc with high surface area, acts as a trap for the contaminant such as metal ions in water (Nouri et al., 2010; Nanseu-Njiki et al., 2009). Meanwhile, the released H_2 gases enhanced the removal of flocculated particles from water (Bazrafshan et al., 2012). According to Nanseu-Njiki et al. (2009), Hg^{2+} also can be removed by EC from the water. In this study, the electrode consisted of iron or aluminum was used as the anode. The metal ion released from anode was found to react with OH^- to form hydroxide species of Hg^{2+}. The reported result showed that 99.9 to 100% of aqueous Hg^{2+} were removed. The main concern of this method was the large initial capital investment due to long term operation and costly electricity supply which may restrict its applicability (Arbabi and Golshani, 2016; Fu and Wang, 2011).

2.1.4 Membrane Filtration

Membrane technology such as ultrafiltration (UF), nanofiltration (NF), and reverse osmosis (RO) is one of the popular methods for water purification (Bessbousse et al., 2010). During the membrane filtration process, the water is passing through the permeable membrane with pore size varying from 0.5 to 20 nm. This membrane can retain macromolecule and suspended solid (Barakat et al., 2011). The low-molecular weight solutes and metal ions, which soluble in water are readily to pass through the membranes. Hence, removal of metal ions through membrane filtration always associated with the addition of metal chelating polymers to the water. Incorporation of the metal chelating ligand into the membrane is also another method that has been introduced for metal ions removal. Among various membrane filtration process, polymer enhanced ultrafiltration (PEUF) process is one of the techniques which have been applied in the removal of Hg^{2+} in water. In PEUF process, the water-soluble polymer such as polyvinyl alcohol (PVA), polyethylenimine (PEI), polyvinylamine (PVAm) and poly (acrylic acid) (PAA) (Huang et al., 2016; Jana et al., 2011) was added to the water to bind with Hg^{2+}. The water sample was then filtered through UF membrane where the Hg^{2+}-polymer complexes were rejected by the membrane (Huang et al., 2016). Jana et al. (2011) applied the combination of PVA and chitosan coated ceramic ultrafiltration membrane in UF process. The result shows that almost 100% of Hg^{2+} and As^{3+} were removed. Huang et al., (2015) reported that the combination of PVAm and pristine UF membrane managed to remove 99% of Hg^{2+} in water. Although, PEUF can be a good alternative for metal ions removal, however, membrane fouling by the water-soluble polymer is the main concern in this method. To resolve the fouling problem, the increase of pressure and periodical cleaning have to be carried out and consequently, the maintenance cost increases (Kabay and Bryjak., 2013).

2.1.5 Adsorption

Among various treatment methods, removal of heavy metal through adsorption process is receiving high attention because of its high efficiency, technical flexibility and cost-effectiveness (Dong et al., 2016). A wide range of silica-based and carbon-based adsorbents have been developed for the metal ions removal. The carbonaceous materials such as activated carbon (AC), graphene oxide (GO) and carbon nanotube (CNT) have been frequently reported as the effective adsorbents for the removal of the heavy metal ion in water (Arcibar-Orozco et al., 2015; Mubarak et al., 2014; Ren et al., 2013).In general, the carbonaceous materials are not selective materials. In order to enhance the selectivity in the adsorption of the specific metal ion such as Hg^{2+}, these carbonaceous materials were often modified with metal capturing groups. For example, Zhu et al. (2009) reported the application of AC that functionalized with the amine group in the removal of Hg^{2+}. According to the result obtained by Zhu et al. (2009), the removal efficiency of Hg^{2+} by the modified AC was much higher than when the unmodified AC. In another study, polypyrrole was intercalating into GO, and the maximum adsorption capacity of this adsorbent to the Hg^{2+} was 980 mg/g (Chandra and Kim, 2011). Pillay et al. (2013) demonstrated the application of sulphur containing MWCNT (S-MWCNT) and AC (S-AC) in the removal of Hg^{2+}. They reported that the maximum adsorption capacity was 72.8 μg/g for S-MWCNT and 44.7 μg/g for S-AC. The carbonaceous materials also suffer from a few drawbacks such as the high commercial cost and poor dispersal ability in water (Saka, 2012; Shawky et al., 2012). For example, low dispersal ability of GO in water causing the surface area of GO to decrease drastically in water (Hashim et al., 2016). Hence, the hybridized GO are often produced to overcome the concern on the dispersal ability (Hashim et al., 2016). Moreover, the synthesis processes hybridized carbonaceous materials was tedious and harsh reaction condition are often required.

2.2 Removal of aqueous metal ion by using sol-gel based adsorbent

2.2.1 Sol-gel and silica gel

A wide range of silica-based adsorbents has been developed for the removal of heavy metals in aqueous solution. The porous silica or metal frameworks (SiO_2) or so-called sol-gel have become a popular material for metal ions removal due to its simplicity in preparation, low cost, large surface areas, excellent thermal and mechanical stability, rapid adsorption kinetics, excellent anti-swelling properties and good dispersal ability in water (Niu et al., 2015; Zhao et al., 2012). A "sol" is a colloidal suspension of the dispersed solid particle in a dispersion medium or liquid. In this system, the dispersed solid is stable and does not precipitate through gravitational force. The condensation process of the dispersion medium leads to the formation of the cluster, and the bonding between the clusters leads to the formation of a single giant network called gel (Brinker and Scherer, 2013).

There are several routes in producing sol-gel. These processes are such as hydrolysis and condensation of metal or metalloid alkoxide precursor, Pechini's method, pyrolysis method, organic-hybrids method and non-hydrolytic reaction (Danks et al., 2016; Kumar et al., 2015; Sciancalepore et al., 2017; Wang et al., 2014; Wu et al., 2016). Among these methods, hydrolysis and condensation of various metal or metalloid alkoxide are the most widely used method for the preparation of sol-gel (Dimitriev et al., 2008; Brinker and Scherer, 2013). In hydrolysis and condensation method, various chemicals such as silicates, borate, aluminate and transition metal alkoxide have been used as the precursor (Brinker and Scherer, 2013). Silicon alkoxide such as tetraethoxysilane ($Si(OC_2H_5)_4$, TEOS) and tetramethoxysilane ($Si(OCH_3)_4$, TMOS) are the most common and thoroughly studied materials in sol-gel preparation (Brinker and Scherer, 2013). Sol-gel that produced from silicon alkoxides is also known as silica gel

The preparation of silica gel through hydrolysis and condensation of silicon alkoxide (Figure 2.1) begins with the hydrolysis of alkoxysilane ($Si(OR)_4$) group under the acidic or basic condition to form the silanol group (Si-OH) (Equation 2.1). This process continues with the formation of siloxane group (Si-O-Si) which constitute the entire silica networks by condensation between Si-OH group (Equation 2.2) or between Si-OH and $Si(OR)_4$ group (Equation 2.3) (Hench and West, 1990). Poly-condensation between Si-OH or Si-OH with $Si(OR)_4$ form the cluster and the collision between cluster finally forms large aggregate called gel (Brinker and Scherer, 2013). The aging process takes place after gelation process where the poly-condensation process continued to complete the formation of the gel. During the aging process, the gel shrinks due to the expulsion of liquid from the pores (Hench and West, 1990). Finally, the entrapped liquid in the pore network is removed by evaporation to form a xerogel. The gels also can be dried under supercritical conditions to produce aerogels (Danks et al., 2016).

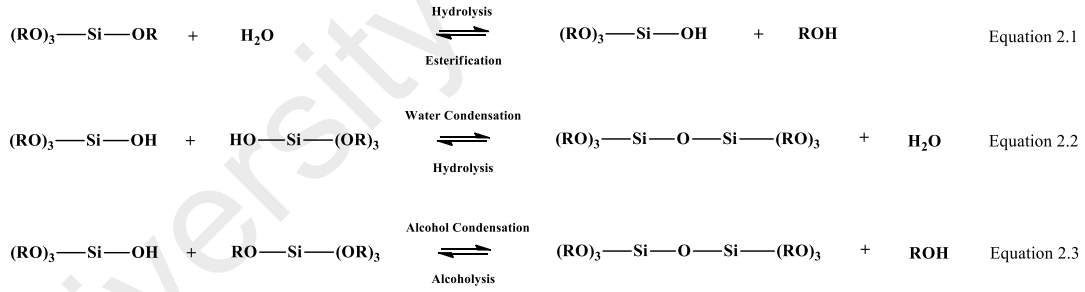

Figure 2.1: The mechanism for the formation sol-gel through hydrolysis and condensation of silicon alkoxides (Brinker and Scherer, 2013).

2.2.2 Modification of silica gel

Silica gel is a functional material with an impressive range of applications in controlled release process of drug delivery, protective coatings, adsorption, chromatography, separation, biotechnology, energy conservation, cultural heritage restoration, environmental remediation, and many other fields of contemporary technology (Ciriminna et al., 2013). In order to enhance the properties and effectiveness of silica gel in metal ions adsorption, this material is often modified through various surface functionalization process. The silica gel with the OH groups at the surface are often functionalized by grafting method, co-condensation method and the bridged organosilane as precursors (Hoffmann et al., 2006). To further improve the performance of the adsorbent in adsorption of metal ion, various metal capturing ligands also have been immobilized onto the functionalized silica gel or incorporated into the silica gel matrix.

2.2.2.1 Surface modification of silica gel through grafting method

The functionalization of mesoporous silica can be carried out by covalently immobilizing the organosilane or so-called silane coupling reagents onto the silica surface through grafting method (Yokoi et al., 2004). This process is achieved by reacting organosilanes such as 3-aminopropyltrimethoxysilane (APTES), 3-chloropropyltriethoxysilane (CPTS) and methacryloxypropyltriethoxysilane (MPTS) with the free silanol group of silica gel (Jal et al., 2004; Rahman and Padavettan, 2012) as shown in Figure 2.2.

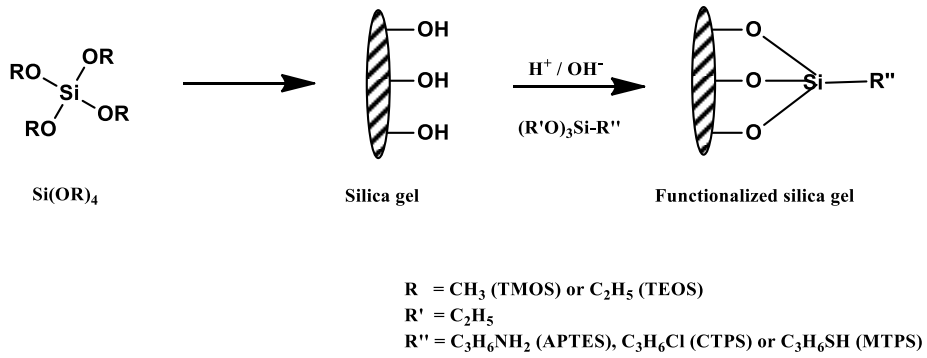

Figure 2.2: Surface functionalized silica gel through grafting methods.

Heidari et al. (2009) functionalized the nano-MCM-41 mesoporous silica using APTES (Figure 2.3a) to generate the amine functionalized silica-based adsorbent (Figure 2.3b) (nano NH_2-MCM 41) for the removal of Ni^{2+}, Cd^{2+}, and Pb^{2+} from ternary aqueous solution. The removal efficiency of this material was 92, 93 and 97% for Ni^{2+}, Cd^{2+}, and Pb^{2+}, respectively, by using 5.0 g/L of nano NH_2-MCM 41.

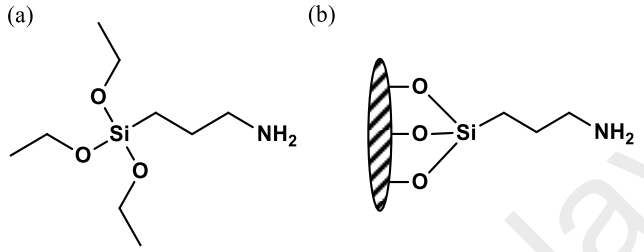

Figure 2.3: (a) APTES and (b) amine functionalized silica based adsorbent.

Fan et al. (2016) grafted the MPTS (Figure 2.4a) onto the surface of silica gel surface to study the adsorption ability of this mercapto-functionalized silica gel (Figure 2.4b) towards Sb^{3+}. This adsorbent showed high adsorption affinity toward Sb^{3+}, and it was suggested as an efficient adsorbent for the removal of Sb^{3+} from aqueous solution.

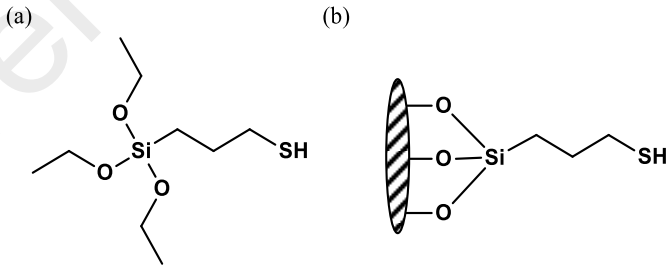

Figure 2.4: (a) MPTS and (b) mercapto-functionalized silica gel.

Diethylphosphatoethyltriethoxysilane (Figure 2.4a) was also grafted onto the silica gel to produce phosphorus acid-functionalized silica gel (Figure 2.4b) to produce an adsorbent for the adsorption of U^{6+} from aqueous solution. The maximum adsorption capacity of this material was found to be 76.9 mg/g (Zhou et al., 2016).

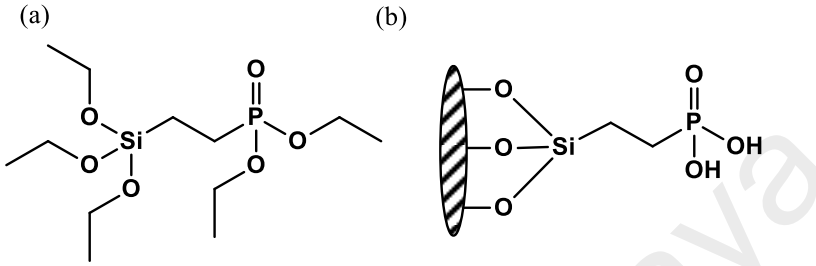

Figure 2.5: (a) Diethylphosphatoethyltriethoxysilane and (b) phosphorus acid-functionalized silica gel.

2.2.2.2 Surface modification of silica gel through co-condensation method

Co-condensation process (Figure 2.6) is another method for the functionalization of silica gel. In this method, the organic functionalities are covalently bonded onto the silica gel through one-pot synthesis. For the synthesis, the organosilanes that are containing specific functional group is mixed with the aqueous cationic surfactant and $Si(OR)_4$ during condensation process under basic condition (Trewyn et al., 2007). The cationic surfactant such as cetyltrimethylammonium bromide (CTMABr–$C_{19}H_{42}NBr$), tetradecyltrimethylammonium bromide (TTMABr–$C_{17}H_{38}NBr$) and trimethyloctadecylammonium bromide (DTMABr–$C_{21}H_{46}NBr$) act as structure directing agent, which is responsible to generate the porosity of silica gel matrix (Costa et al., 2014; Soto et al., 2016). Da'na and Sayari (2011) synthesized amine-functionalized mesoporous silica gel by mixing TEOS, APTES, and Pluronic P123 surfactant. This adsorbent was found to be highly selective and effective in removing of Cu^{2+}. On the other hand, Machida et al. (2012) investigated the ability of amino (NH_2), and mercapto (SH) functionalized mesoporous silica (HMS) for the adsorption of Cd^{2+} and Pb^{2+}. These

materials were synthesized through the co-condensation method by using TEOS, Dodecylamine (DDA) surfactant, APTES (for NH_2-HMS) and MPTS (for SH-HMS) (Machida et al., 2012). The result showed that NH_2-HMS adsorbed the highest amount of Cd^{2+} and Pb^{2+} with maximum adsorption capacity (Q_m) equal to 0.25 and 0.45 mmol/g respectively.

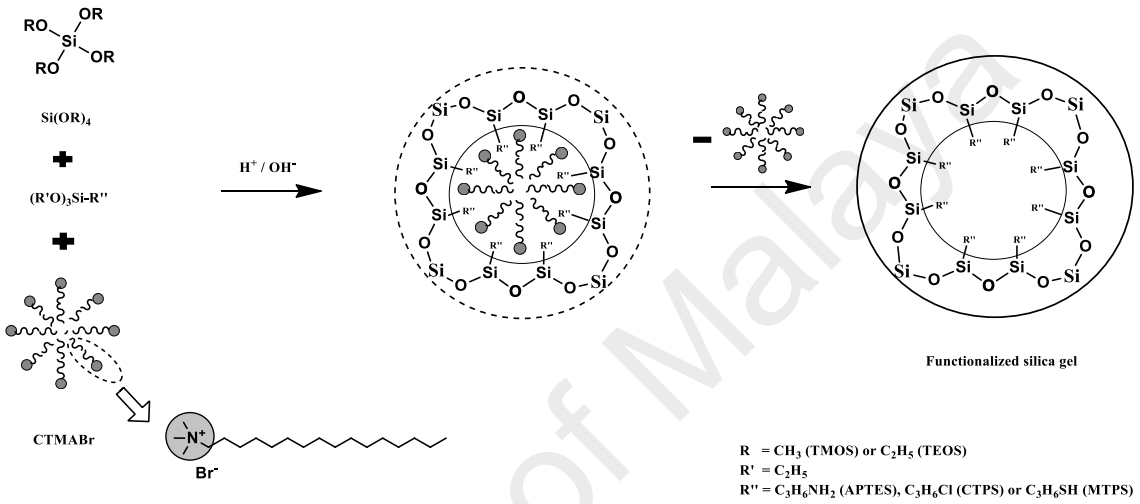

Figure 2.6: Formation pathways of functionalized silica gel through co-condensation method.

2.2.2.3 Modification of silica gel by using Periodic mesoporous organosilica

Grafting and co-condensation method are related to the surface modification of silica gel. On the other hand, functionalization of silica gel also can be carried out by using bridged organosilane precursors. Periodic mesoporous organosilica (PMO) are produced using bridged bi-silane, $(RO)_3Si\text{-}R'''\text{-}Si(OR)_3$. $(RO)_3Si\text{-}R'''\text{-}Si(OR)_3$ containing organic functionalities (R''') such as ethane, ethene, 2,5-thiophene, and 1,4-benzene (Dag et al., 2001) which connecting two silane groups. The R''' group is entrapped in the three-dimensional silica gel matrix (Figure 2.7). For example, Leng et al. (2013) used the bisilylated crown ether (Figure 2.8) alongside with TMOS to synthesize a PMO for the adsorption of Sr^{2+}. As shown in the result obtained by Leng et al. (2013), the PMO incorporated silica adsorbent was selective towards the adsorption of Sr^{2+} in the presence of the various interfering ions.

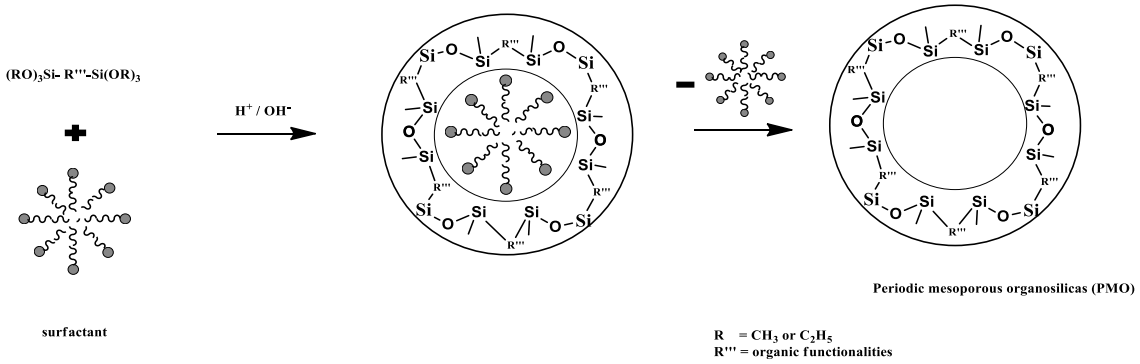

Figure 2.7: Formation pathways of periodic mesoporous organosilicas (PMO).

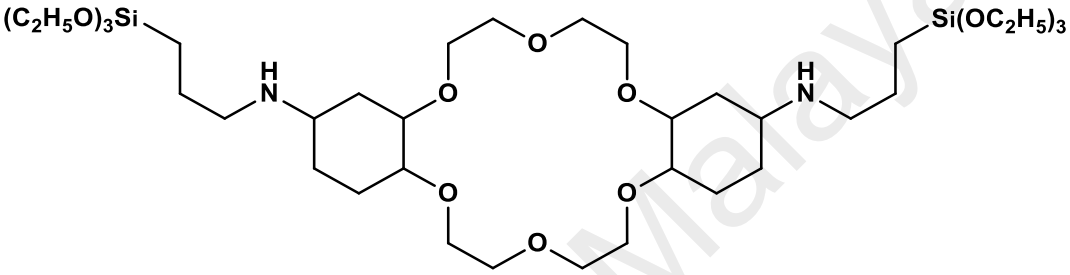

Figure 2.8: Bisilylated crown ether.

2.2.2.4 Immobilization of metal capturing ligand onto the surface of silica gel

Despite the direct functionalization of silica gel, various metal capturing ligands also have been immobilized onto silica gel. These metal capturing ligands tend to enhance the metal ions adsorption ability and selectivity of the functionalized silica gel. The ligands that exhibit strong affinity towards specific metal ion are widely available. For example, sulphur-containing ligands such as dithiocarbamate derivatives are often found to be the selective ligands toward the complexation with Hg^{2+}. Hence, these ligands can be immobilized onto the silica gel to produce selective adsorbents for Hg^{2+}.

Throughout the history, various selective adsorbents have been produced for the adsorption of specific metal ions. For example, in a study reported by Huang et al. (2008), the silica gel was first functionalized with chloro group (Figure 2.9a). Then, the tris(2-aminoethyl) amine ligand (Figure 2.9b) was immobilized onto this chloro-functionalized silica gel. The tris(2-aminoethyl) amine modified silica gel (Figure 2.9c) was applied as

the adsorbent for Cr^{3+}, Cd^{2+}, and Pb^{2+}. The reported maximum adsorption capacities were 32.7, 36.4 and 64.6 mg/g for Cr^{3+}, Cd^{2+}, and Pb^{2+}. In another study, a Schiff base, *N*-(2-hydroxyethyl) salicylaldimine (Figure 2.10a), was used as a ligand to modify the chloro functionalized SBA-15 mesoporous silica (Tadjarodi et al., 2015). This material (Figure 2.10b) removed 96% of La^{3+} in water (Tadjarodi et al., 2015).

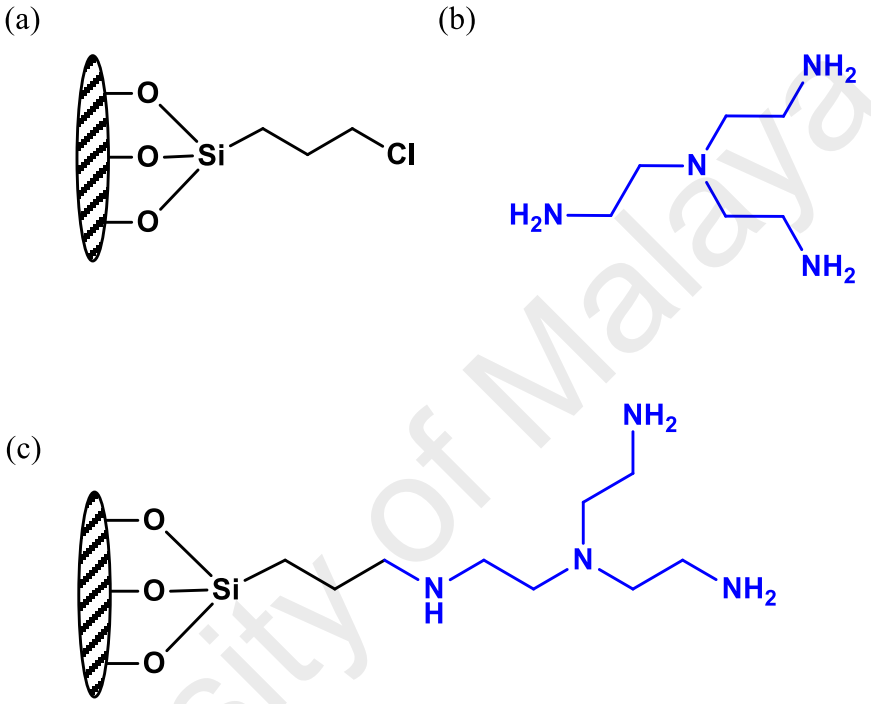

Figure 2.9: (a) Chloro functionalized silica gel, (b) tris(2-aminoethyl) amine and (c) tris(2-aminoethyl) amine modified silica gel.

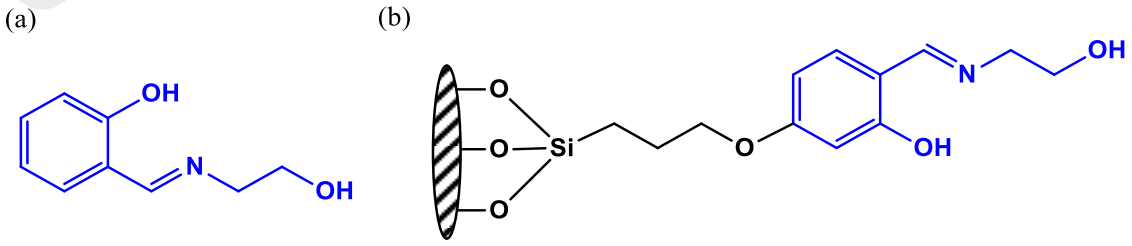

Figure 2.10: (a) *N*-(2-hydroxyethyl) salicylaldimine and (b) *N*-(2-hydroxyethyl) salicylaldimine-functionalized mesoporous silica gel.

Radi et al. (2014) immobilized a ligand called 1*H*-pyrrole-2-carbaldehyde (Figure 2.11a) onto an amine-functionalized silica gel to form a new adsorbent (Figure 2.11b). This adsorbent was found to be selective towards the adsorption of Cu^{2+}, Zn^{2+}, and Cd^{2+} from aqueous solution. The reported maximum adsorption capacity was 27.9, 24.2 and 20.3 mg/g for Cu^{2+}, Zn^{2+}, and Cd^{2+}. Banaei et al. (2015) reported the immobilization of bisaldehyde ligand,2,2'-(propane-1,3-diylbis(oxy))dibenzaldehyde (Figure 2.12a) onto the silica-coated magnetite particle to generate the bisaldehyde functionalized magnetic silica gel (Figure 2.12b). This material selectively removed more than 95% Ag^{+} from aqueous samples.

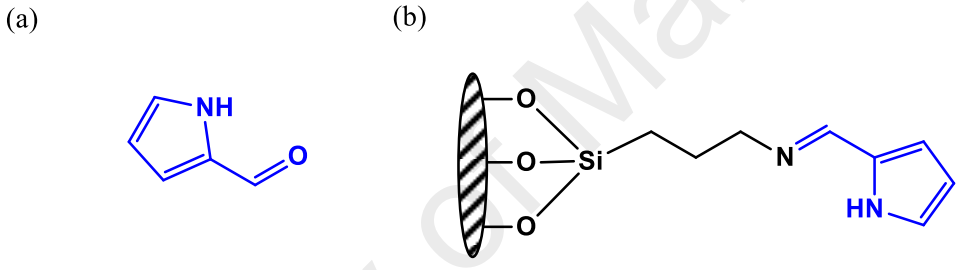

Figure 2.11: (a) 1*H*-pyrrole-2-carbaldhyde and (b) 1-(Pyrrol-2-yl)imine modified silica gel.

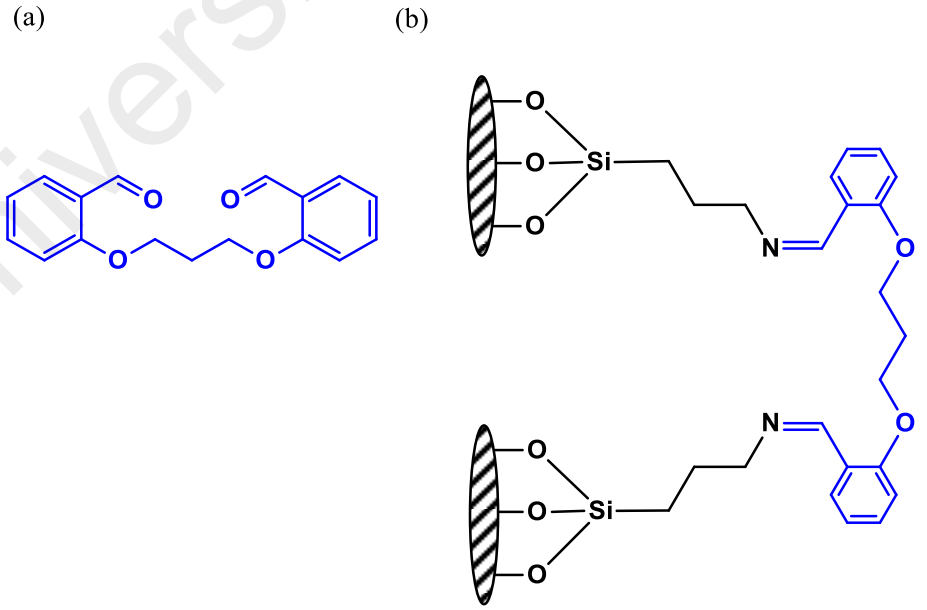

Figure 2.12: (a) 2, 2'-(propane-1,3-diylbis(oxy))dibenzaldehyde and (b) bisaldehyde modified silica gel.

In another study, 5-sulfosalicylic acid (Figure 2.13a) was bonded to dendrimer-like poly-amidoamine (PAMAM) modified silica gel (Wu et al., 2016). The immobilized 5-sulfosalicylic acid silica gel (Figure 2.13b) was used to adsorb Pb^{2+} in the water sample. Wu et al. (2016) revealed that almost 100% of Pb^{2+} was successfully removed from the water. Guo et al. (2017) immobilized the dibutyl (3-chloro-2-hydroxypropyl) phosphate (Figure 2.14a) onto the surface of mesoporous silica gel (Figure 2.14b). This material was used to remove U^{6+} in water. The result showed that this material was able to remove almost 100% of U^{6+}.

(a) (b)

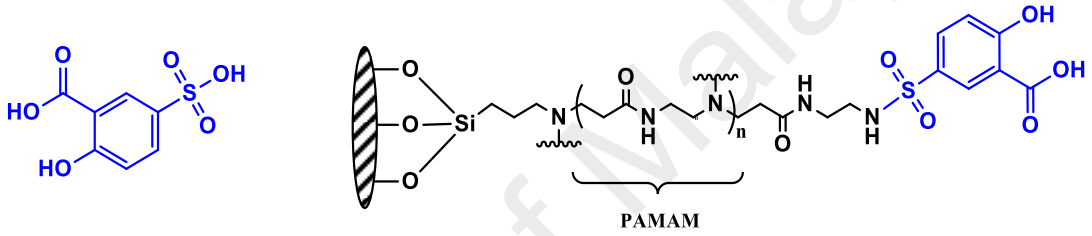

Figure 2.13: (a) 5-sulfosalicylic acid and (b) 5-sulfosalicyclic acid / PAMAM modified silica gel.

(a) (b)

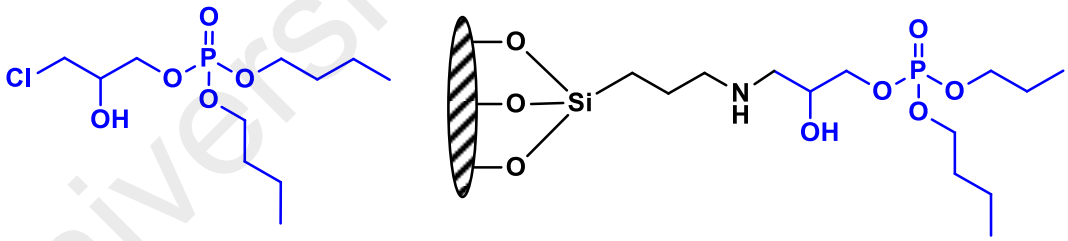

Figure 2.14: (a) Dibutyl (3-chloro-2-hydroxypropyl) phosphate and (b) phosphoryl modified mesoporous silica gel.

2.2.2.5 Metal capturing ligand incorporated silica gel

The modification of silica gel by immobilization of ligand involved multi-step reaction. Also, the functionalization of silica gel through grafting, co-condensation, and PMO methods often involved the use of various chemicals, which included silane coupling agent, structure directing reagent, solvents, and ligands. This may increase the chemical usage and the time of synthesis. Hence, to overcome such disadvantages, the approach to incorporate the metal capturing ligand into silica gel matrix during its preparation has been developed (Figure 2.15). In this approach, the ligand is entrapped into the silica gel matrix instead of covalently bonding it to the silica gel. Furthermore, the incorporated ligand or so-called doped-ligand was found to retained its chemical properties (Yost et al., 2000) and the synthesized route was relatively simple compared with the immobilization method.

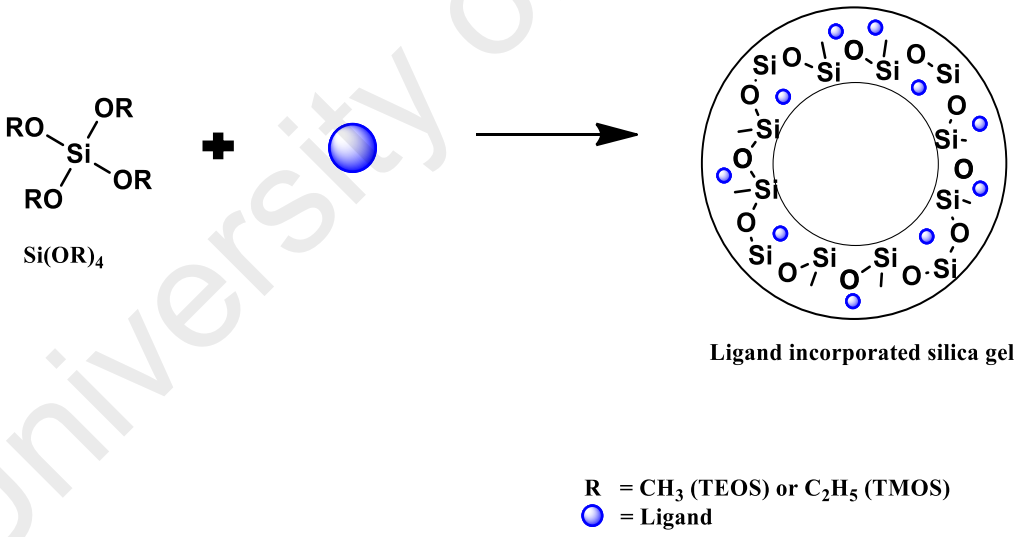

Figure 2.15: Formation pathways of metal capturing incorporated silica gel.

For example, by just using TEOS as a precursor, Mehmood et al. (2013) incorporated a ligand called *N,N*-(dipropylcarbamothioyl) thiophene-2-carboxamide (Figure 2.16a) into the silica gel matrix. This adsorbent managed to remove 95% of Cu^{2+} from Cu^{2+} solution with the concentration of 1 mg/L. The crown ether type of ligand, 1, 4, 10, 13-tetraoxa-7, 16-diazacyclooctadecane-7,-16-bis (malonate) (Figure 2.16b) was incorporated into the silica gel matrix. The selected ligand is selective toward the complexation with Sr^{2+} (Yost et al., 2000). The crown ether incorporated silica gel has been found to retain its chemical property where it was selective in the removal of Sr^{2+} in aqueous solution (Yost et al., 2000). Besides that, an organic ligand, 1,5-diphenylcarbazide (DPC) (Figure 2.16c) was doped into the silica gel matrix by Khan et al. (2006). The DPC tends to coordinate with Hg^{2+} to form the complex. This ligand has been found to be a promising material for Hg^{2+} extraction from the aqueous sample. Khan et al. (2006) reported that about 90% of Hg^{2+} was removed from water by the DPC incorporated silica gel.

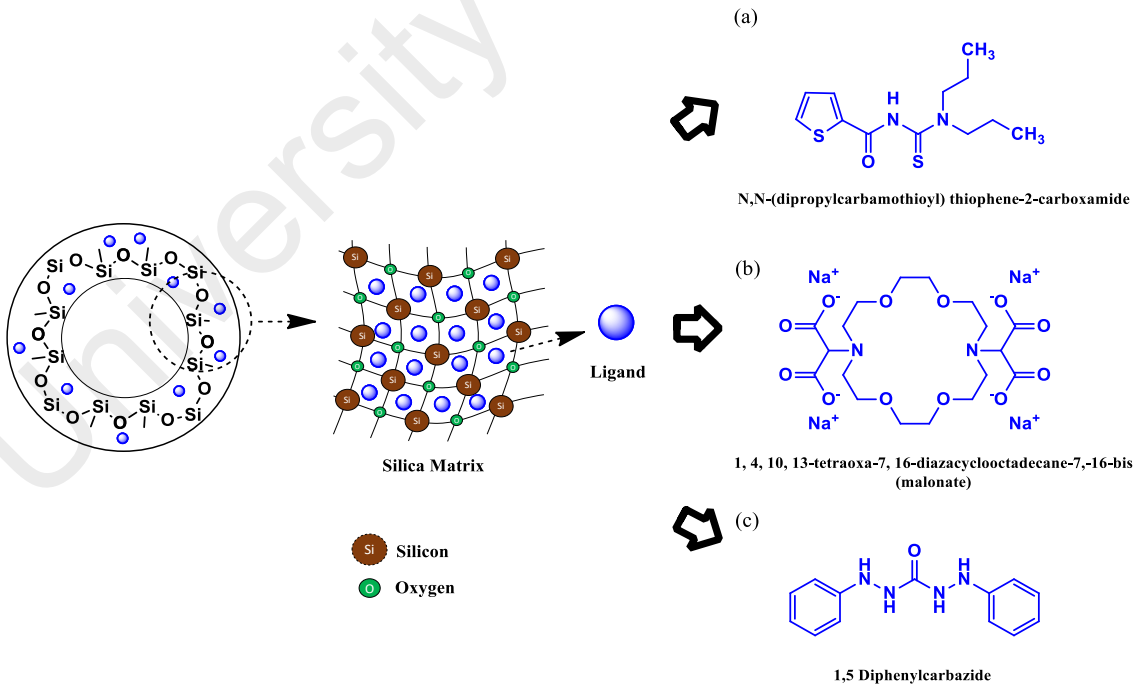

Figure 2.16: A variety of ligand used to incorporate into silica gel.

2.3 Sulphur containing ligand modified silica gel for the removal of aqueous Hg^{2+}

Sulphur containing compounds have frequently been used as the ligand to capture Hg^{2+} in aqueous solution (Qu et al., 2013). Hg^{2+} is a soft acid, and it tends to bind to the sulphur atom, which acts as the soft base through complexation (Wajima and Sugawara, 2011). Silica gel that modified with functional group that containing sulphur atom has also shown great chemical activity to remove Hg^{2+} in aqueous solution (Aguado et al., 2005; Antochshuk et al., 2003; Cestari and Airoldi, 1997; Evangelista et al., 2007; Johari et al., 2014; Prado et al., 2004; Puanngam and Unob, 2008).

The sulphur containing ligands are often grafted or incorporated on silica gel. For example, 1-furoyl thiourea (Figure 2.17a) was covalently anchored onto chloro-functionalized silica gel through co-condensation (Figure 2.17b) and grafting methods (Figure 2.17c) by Mureseanu et al. (2010) for the preparation of adsorbents for Hg^{2+}. The maximum adsorption capacity of the adsorbents that prepared through co-condensation and grafting methods were 56.2 and 122.4 mg Hg/g, respectively. Esmaeili Bidhendi et al. (2014) synthesized another ligand named 1,3,5-trithiane (Figure 2.18) and incorporated it into mesoporous silica gel matrix. This 1,3,5-trithiane doped silica gel showed a good capability in Hg^{2+} removal with the maximum adsorption capacity of 10 mg/g.

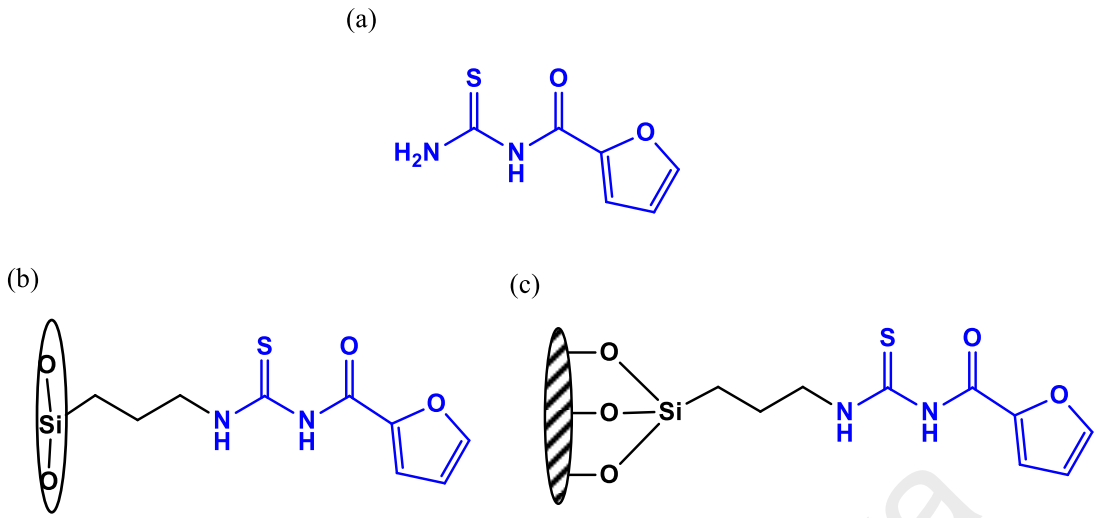

Figure 2.17: (a) 1-furoyl thiourea, (b)1-furoyl thiourea functionalized SBA-15 (co-condensation route) and (c) 1-furoyl thiourea functionalized SBA-15 (grafting method).

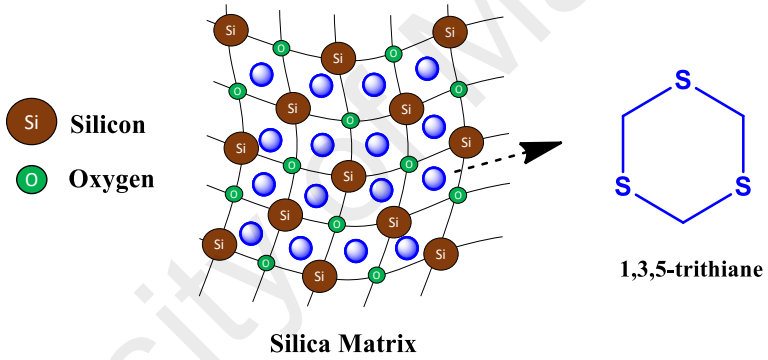

Figure 2.18: 1,3,5-trithiane doped in silica matrix.

Among the various sulphur containing ligands, the capability of dithiocarbamate (Figure 2.19) and its derivatives to complex with Hg^{2+} has been widely reported (Denizli et al., 2000; Figueira et al., 2011; Girginova et al., 2010; He et al., 2015; He et al., 2016; Say et al., 2008; Venkatesan et al., 2002). Silica gel that containing dithiocarbamate group (Si-DiTC) can be synthesized directly by modifying the functionalized silica gel with CS_2 (Venkatesan et al., 2002). For example, He et al. (2015) and He et al. (2016) functionalized the silica gel with diethylenetriamine, tetraethylenepentamine, diethylenetriamine-salicylaldehyde and tetraethylenepentamine-salicylaldehyde (Figure 2.20) to prepare amine groups functionalized silica gel. The amine groups functionalized

silica gel was then modified with CS_2 to produce Si-DiTC. With the presence of various metal ions, these synthetic adsorbents showed high maximum adsorption capacity ranging from 169.7 to 225.8 mg/g for Hg^{2+}.

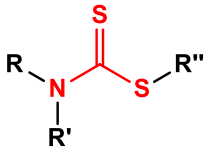

Figure 2.19: Common structure of dithiocarbamate compound.

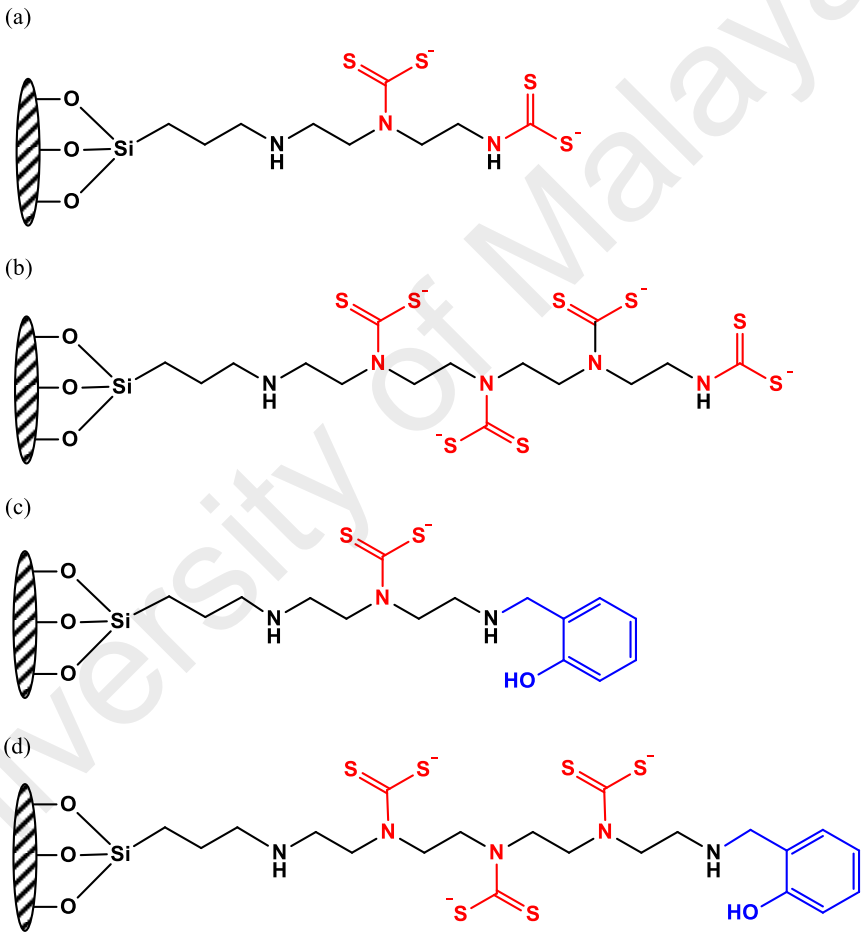

Figure 2.20: (a) CS_2 modified diethylenetriamine functionalized silica gel, (b) CS_2 modified tetraethylenepentamine-salicaldehyde functionalized silica gel, (c) CS_2 modified diethylenetriamine functionalized silica gel and (d) CS_2 modified tetraethylenepentamine-salicaldehyde functionalized silica gel.

On the other hand, the silica coated magnetite particles derivatized with dithiocarbamate groups (Figure 2.21) was synthesized by Girginova et al. (2010) by grafting the CS_2 on amine functionalized silica gel, and the high efficiency of Hg^{2+} uptake (74%) was recorded by this material.

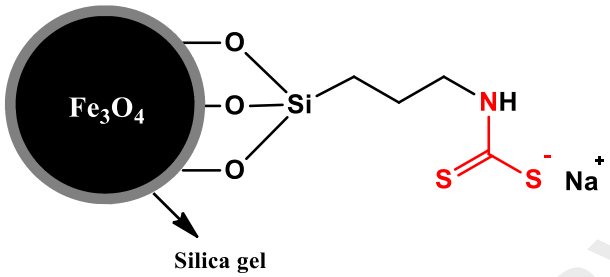

Figure 2.21: Silica coated magnetite particles derivatized with dithiocarbamate group.

Instead of grafting CS_2 to the functionalized silica gel, the Si-DiTC also can be obtained by converting the silane coupling agent such as APTES to dithiocarbamate derivative before the silica gel preparation (Tavares et al., 2013). The siloxydithiocarbamate (Figure 2.22a) compound was used as precursor material alongside with TEOS to coat the surface of magnetite particles (Figure 2.22b). This material successfully removed 99.8% of Hg^{2+} in the aqueous sample.

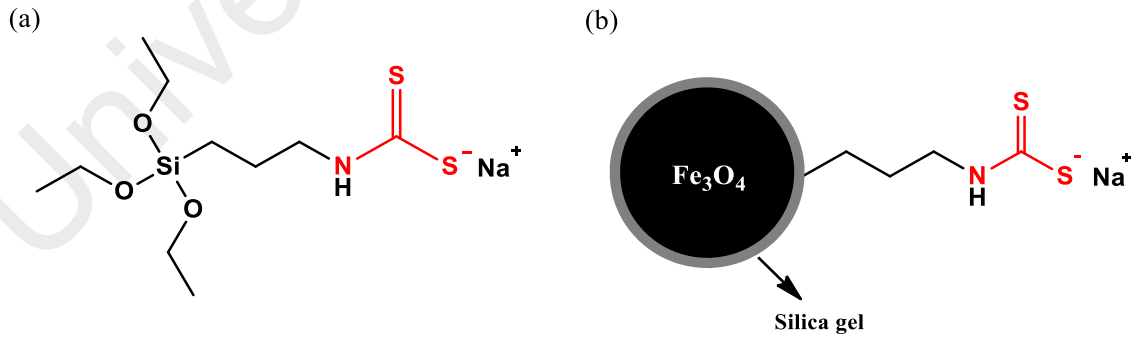

Figure 2.22: (a) Siloxydithiocarbamate compound, and (b) dithiocarbamate modified silica gel coated magnetite particle.

The reaction between CS_2 and amine group on silica surface are generally conducted under harsh conditions where the strong alkaline condition may cause the degradation of silica gel (Bai et al., 2011). In addition, to attach the dithiocarbamate group onto the silica gel, silica gel need to be functionalized with small molecular weight amine derivatives such as diethylenetriamine and tetraethylenepentamine (He et al., 2015; He et al., 2016) and this reduce the number of dithiocarbamate group on Si-DiTC (Bai et al., 2011).

2.4 Natural product based ligand

2.4.1 Metal capturing ability of natural products

So far, most of the doped or immobilized ligands onto the silica gel are mostly synthetic chemicals. Synthesis of ligands is not economic and not environmentally friendly since it involved multi-step reaction and required various chemicals. Therefore, it is worth to study the potential of natural products as metal capturing ligands. Natural products are organic compounds, which can be extracted from microbes, plants, and animals. These compounds have remarkable structural diversity and biological characteristics (Ding et al., 2016; Wang et al., 2016). Some natural products are containing various functional groups such as carbonyl, hydroxyl, amines, and ketone group as electron donating group. Consequently, these natural compounds also have the potential to complex with metal ions. The metal capturing ability of some natural products such as curcumin, quercetin, rutin, and morin also has been proven.

Curcumin (Figure 2.23a) is a hydrophobic polyphenol with the chemical structure called bis-R-unsaturated-diketone, which can be extracted from ginger (Arnand et al., 2007; Karri et al., 2015). The ability of curcumin and its derivatives to form complexes with several metals was reported by Wanninger et al. (2015). Picciano and Vaden (2013)

further proved the binding ability of curcumin toward Cu^{2+}. Rutin (Figure 2.23b) is a naturally occurring flavonoid, which consists of ketone and hydroxyl group. Due to the rich of functional group, natural rutin has been shown to have the capability to form the complexes with Cr^{3+}, Zn^{2+}, and Sn^{2+} (Ikeda et al., 2015; Panhwar and Memon, 2014; Zhai et al., 2014). Quercetin (Figure 2.23c) is another flavonoid that can be obtained from various plants. It tends to form complexes with Al^{3+} and Tb^{3+} (Dolatabadi et al., 2014; Furia et al., 2014). In addition, another natural product called morin (Figure 2.23d) was found to form a complex with Zn^{2+} (Sendrayaperumal et al., 2014). So far, most of these natural product based ligands are belong to a class of chemical named flavonoid. This study investigated the potential of another class of natural product named chalcone as metal capturing ligand.

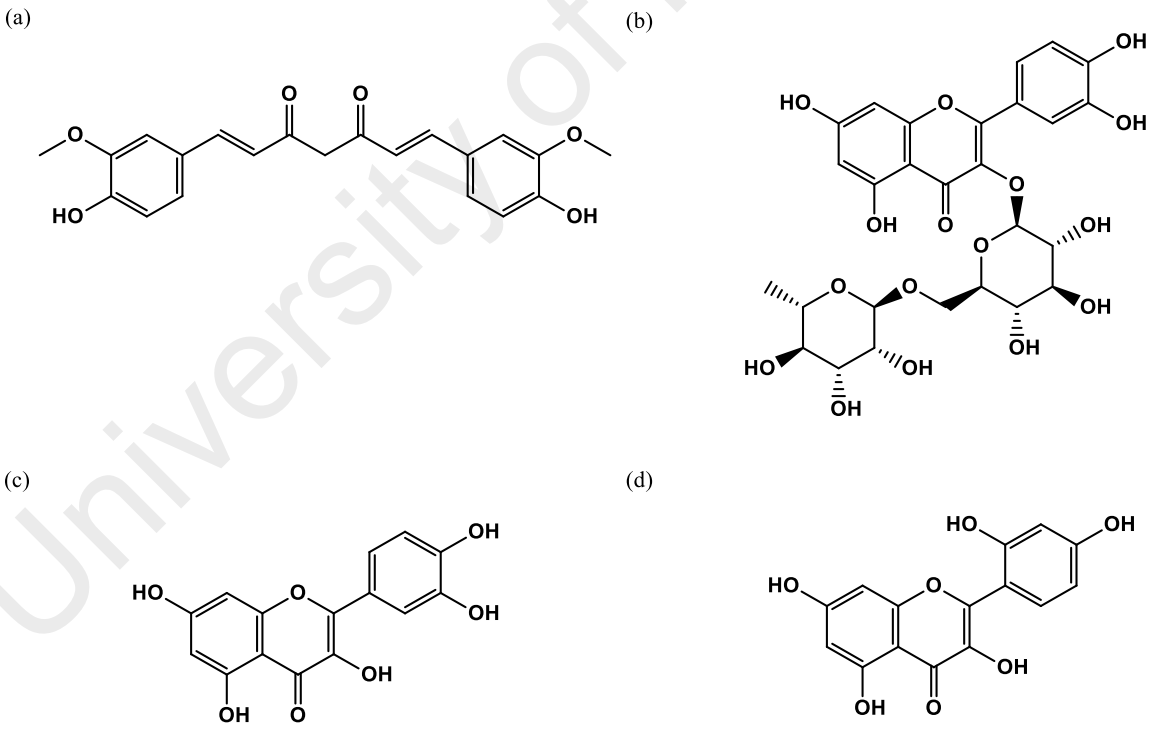

Figure 2.23: (a) Curcumin, (b) Rutin, (c) Quercetin and (d) Morin.

2.4.2 Chalcone

Chalcone (Figure 1.2a) is a type of natural product that containing two aromatic rings linked by a three carbons α, β-unsaturated carbonyl system. Chalcone-type of natural products can be obtained easily from fruits (e.g., citruses, apples), vegetables (e.g., tomatoes, shallots, bean sprouts, and potatoes), and spices (Orlikova et al., 2011; Patil et al., 2010). Chalcone and its derivative showed the remarkable biological activities such as anti-cancer, anti-inflammatory, anti-HIV, etc. (Singh et al., 2014) but the adsorption ability of chalcone for various metal ions has not been reported elsewhere. In this study, the chalcone was modified into dithiocarbamate derivative, ODPPNE, through reaction pathway shown in Figure 2.24. As mentioned previously, dithiocarbamate has the chelating ability towards Hg^{2+} (Heard, 2005; Kanchi et al., 2014). The synthesized ODPPNE was doped into the silica gel for the preparation of adsorbent for the removal of Hg^{2+} in water. ODPPNE was also incorporated onto the silica gel coated magnetic particles for the preparation of solid phase to pre-concentrate Hg^{2+} in water.

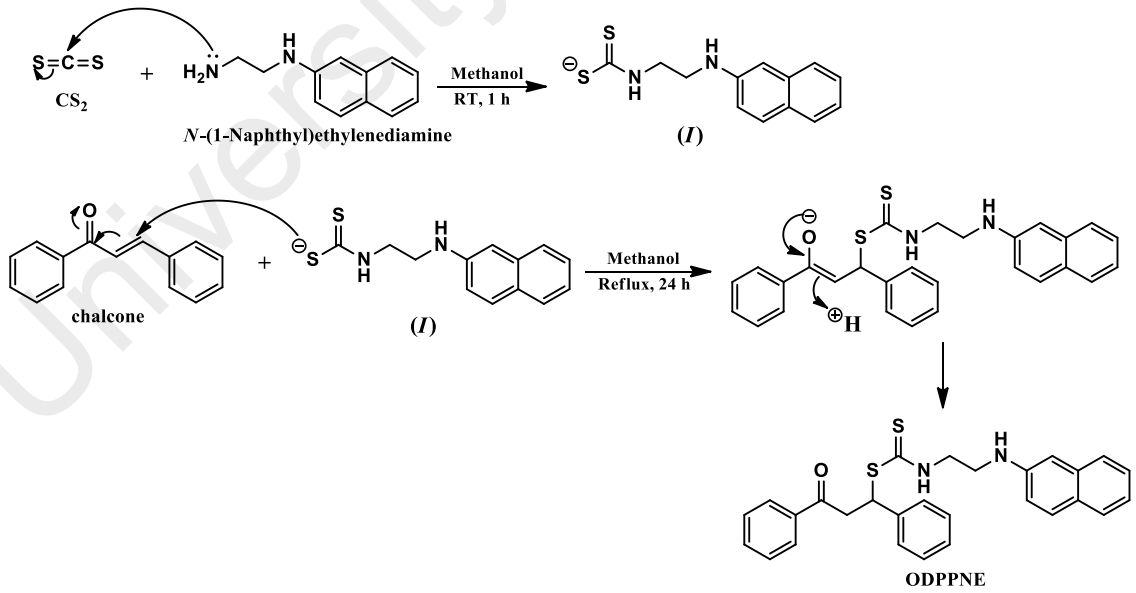

Figure 2.24: Synthesis pathway of ODPPNE.

2.5 Pre-concentration of trace heavy metal from aqueous sample.

Direct determination of trace pollutants such as heavy metal ions in water may require complicated sample preparation procedure due to the limitation of instruments (Wen and Zhu, 2014). For example, the concentration of Hg in natural water samples could vary from pg/L to ng/L (Zhang et al., 2014) while the detection limit for instruments which can be used to quantify Hg such as ICP and AAS are at the μg/L level (WHO, 2005). In addition, the matrix effect appears in the water sample may interfere with the analysis. Therefore, an appropriate pre-concentration method for trace metal analysis is required.

2.5.1 Solid phase extraction and solid phase micro-extraction as the pre-concentration method

Conventional solid phase extraction methods (SPE) have become the standard technique to pre-concentrate trace element in the aqueous sample due to its simplicity, less chemical consumption, rapid, and high enrichment factor (Hu et al., 2015; Pytlakowsk, 2016; Yilmaz and Soylak, 2014). In SPE process, the analytes are transferred from the water sample to the solid adsorbent phase (Hu et al., 2015). The analytes that retained on the adsorbent can be recovered by elution with specific solvent or reagent. The adsorbent phase employed in conventional SPE can consist of different materials such as polymer beads, silica gel, modified silica gel, activated carbon (Habila et al., 2014), molecularly imprinted polymer (Nestora et al., 2016) and metal-organic framework (Xie et al., 2015). These SPE adsorbents are contained in the cartridges, syringe barrels or disk (Wells et al., 2003).

In order to enhance the efficiency of conventional SPE, the manipulated SPE technique called solid phase micro-extraction (SPME) was developed. In SPME, the conventional adsorbents were replaced by the nano-size adsorbent in according to their high surface-area-to-volume ratio, simple derivatization procedure, and unique thermal,

mechanical or electronic properties (Zhang et al., 2013). Among the nano-size adsorbents, carbonaceous materials such as single wall carbon nanotube (SWMNT) (Asghari et al., 2016; Gutierrez et al., 2017), multiwall carbon nanotube (MWCNT) (Yilmaz and Soylak, 2014; Zhou et al., 2014), graphene oxide (GO) (Pourjavid et al., 2014; Yang et al., 2012) were widely used as adsorbent in SPME. However, the application of these nanoparticles in SPME can disrupt by several conditions. The nanoparticles may aggregate to cause the reduction of surface area of adsorbent, produced the back-pressure in extraction instrument and clogging SPME device resulted in the failure of extraction process (Pytlakowsk, 2016). Also, SPME method also suffers other drawbacks such as large secondary wastes, time-consuming, and complex equipment may be needed (Asgharinezhad et al., 2014). Therefore, to overcome the problems mentioned above, Anastassiades et al. (2003) have introduced an easy and rapid method called dispersive-solid phase extraction (D-SPE).

2.5.2 D-μSPE

In D-SPE, a small amount of adsorbent is directly added to the water sample. The nano-size adsorbents are dispersed in water using various agitation methods (Khezeli and Daneshfar, 2017). The dispersed adsorbent adsorbs the target analytes such as heavy metal ions in the water. Then, centrifugation or filtration is often applied to isolate the dispersed adsorbent. The analytes retained on the isolated adsorbent can be recovered through desorption process using suitable solvent or reagent (Xian et al., 2017). This approach enables the adsorbent to interact equally with all samples and greater capacity per amount of adsorbent can be achieved (Abdolmohammad-Zadeh and Talleb, 2012). Recently, dispersive micro-solid phase extraction method (D-μSPE) has been developed as the miniaturized extraction technique when nanoparticles with unique size and physical/chemical properties were used as the adsorbent (Pytlakowsk, 2016; Khezeli and Daneshfar, 2017).

2.5.3 D-μSPE as pre-concentration method for heavy metal ions in water

The application of D-μSPE as the pre-concentration process of trace metal ion in aqueous solution has been widely reported. The conventional adsorbents used in D-μSPE can consist of the nanoparticle materials such as carbon nanotube (CNT) (Krawczyk and Jeszka-Skowron, 2016), graphene (Kocot and Sitko, 2014), graphene oxide (GO) nanosheet (Ghazaghi et al., 2016). Application of these materials in D-μSPE usually required the addition of metal capturing ligand to enhance the selectivity. For example, Feist (2016) incorporated a chelating reagent named 1,10-phenanthroline to the oxidized MWCNT. This adsorbent was to pre-concentrate Cd^{2+} and Pb^{2+}. In another method, ammonium pyrrolidine dithiocarbamate (APDC) was applied as the metal capturing ligand for Cd^{2+} and Pb^{2+} in the D-μSPE process (Kocot et al., 2013). In this method, the obtained Cd^{2+}-APDC and Pb^{2+}-ADDC complex was then adsorbed by the dispersed MWCNT to form the sediments which was isolated from the water sample (Kocot et al., 2013). Another modification process was reported by Bahadir et al. (2015) where an anionic exchanger tricaprylmethylammonium chloride (Aliquat 336) was loaded onto the MWCNT in order to extract Cr^{6+} in drinking water through D-μSPE. Pytlakowsk (2016) reported that another D-μSPE process where Cr^{3+}, Co^{2+}, Cu^{2+}, Ni^{2+}, Pb^{2+} and Zn^{2+} in water samples was pre-concentrated using an azo dye named 2-(5-bromo-2-pyridylazo)-5-diethylaminophenol (5-Br-PADAP), as a complexing reagent and the GO nanoparticles as an adsorbent. Zawisza et al. (2016) reported the application of ethylenediamine modified GO (EDA-GO) as a solid phase for the pre-concentration Fe^{3+}, Co^{2+}, Cu^{2+}, Ni^{2+}, Pb^{2+}, and Zn^{2+} in the real water sample. This material was synthesized through the suspension of GO in ethylenediamine and refluxed with *N,N*-dicyclohexylcarbodiimide (Zawisza et al., 2016).

Instead of the carbonaceous nanoparticle, other nanomaterials such as halloysite nanotube (Krawczyk et al., 2016), silica-nanoparticle (Shirkhanloo et al., 2016), and silver-nanoparticle (Krawczyk and Stanisz, 2015) also have been employed as the adsorbent phase in D-μSPE. Krawczyk et al. (2016) reported the application of dendrimer modified halloysite nanotubes as an adsorbent for ultrasound-assisted D-μSPE for the pre-concentration of Cd^{2+} and Pb^{2+} in the water sample. For selective extraction of Ni^{2+} in the water sample, Jalali and Aliakbar, (2015) modified the mercapto functionalized MCM-41 mesoporous silica with 4-nitrophenol and the resulting material was employed as the adsorbent phase in the D-μSPE system. The combination of silver-nanoparticle (Ag-NP) as solid adsorbent and D-μSPE for determination of Hg^{2+} in water sample was reported by Krawczyk and Stanisz (2015).

In spite of the popularity gain by the application of D-µSPE technique in the pre-concentration process, however, the laborious and time-consuming procedure such as centrifugation and filtration is always required in retrieving adsorbents after extraction (Wierucka and Biziuk, 2014). Hence, the application of magnetic nanoparticle (MNP) as the adsorbent phase for D-µSPE has drawn attention by many researchers (Giakisikli and Anthemidis, 2013). With magnetic property, MNP can be retrieved from the water by using external magnetic field without any instrumentation.

2.5.4 MNP as adsorbent phase in D-μSPE

Magnetic nanoparticle (MNP) has the special characteristic such as large surface area, easy to isolate by applying the external magnetic force and simplicity in preparation. When MNP are used adsorbents, their superparamagnetic properties allow it to be separated from water by an external magnetic field. As a result, the duration of sample preparation can be significantly shortened. Iron oxide (Fe_3O_4) is the most common MNP (Lee et al., 2015). Pure Fe_3O_4 is an inorganic nanoparticle which tends to form large

aggregates which may alter its surface area. Fe_3O_4 is also not selective to any compounds, and this may lead to its unsuitability to be used as the adsorbent phase for D-μSPE. Thus, coating and modification of the surface of Fe_3O_4 with appropriate method and materials are necessary to overcome this limitation. The coating material for Fe_3O_4 can consist of carbon (Baig et al., 2014), chitosan (Jiang et al., 2015), polymers (Muliwa et al., 2016), silica gel (Kunzmann et al., 2011; Lien and Wu, 2008), silver-nanoparticle (López-Garcia et al., 2015) and surfactants (Asgharinezhad and Ebrahimzadeh, 2016).

2.5.5 Silica coated iron oxide magnetic nanoparticle (Fe_3O_4-SiO_2)

Silica gel is the most common used material that has been used to modified iron oxide due to its chemical stability, low-cost, simple preparation step, versatile and modifiable properties (Bumb et al., 2008; Kunzmann et al., 2011; Lien and Wu, 2008). Moreover, the silica gel can be modified with various chemicals to improve its property for metal ions adsorption (Khor et al., 2017). Hence, the silica gel coated iron oxide magnetic nanoparticle (Fe_3O_4-SiO_2) that modified with various metal capturing ligand have been frequently applied as adsorbent phase for D-µSPE (Adlnasab et al., 2014; Abolhasani et al., 2015; Alonso et al., 2016; Cui et al., 2015; Es'haghi et al., 2016; Sobhi et al., 2017; Zhang et al., 2014).

2.5.6 Ligand modified Fe_3O_4-SiO_2 and its application in the pre-concentration of Hg^{2+} in water sample

Various ligands have been used to modify the Fe_3O_4-SiO_2 to produce adsorbent phase that selective towards the adsorption of Hg^{2+} in water. By using the ligand modified Fe_3O_4-SiO_2 as the adsorbent in the extraction process, various analytical methods has been developed for the determination of traces Hg^{2+} in the water sample. For example, as reported in many literatures (Mudasir et al., 2016; Zhang et al., 2014), dithizone (Figure 2.25a) was one of the effective adsorbents for Hg^{2+}. Adlnasab et al. (2014) modified the

chloro-functionalized Fe_3O_4-SiO_2 with dithizone, and this material was successfully applied for the determination of trace Hg^{2+} in the environmental sample by using D-μSPE technique coupling with Continuous-Flow Cold Vapor Atomic Absorption Spectrometry method (CF-CVAAS). The limit of detection (LOD) achieved by this method was 50 ng/L. Cui et al. (2015) introduced a selective magnetic adsorbent for Hg^{2+} in environmental samples. They grafted the *N*-(2-acetylaminoethyl)-N'-(3-triethoxysilylpropyl)thiourea (AMPTs) (Figure 2.25b) onto the Fe_3O_4-SiO_2. The Hg^{2+} extracted by Fe_3O_4-SiO_2-AMPTs was examined using mercury analyser and the detection limit obtained was 17 ng/L (Cui et al., 2015). To improve the analytical performance of MNP, the silica was also modified with L-cysteine (Figure 2.25c) (Xiang et al., 2013). This thiol modified Fe_3O_4-SiO_2 was employed as the effective adsorbent for Hg^{2+} and the reported method of the detection limit of 60 ng/L (Xiang et al., 2013). In Beiraghi et al. (2014), a sulphur-rich ligand named thiodiethanethiol (Figure 2.25d) was used as the modifier to generate the adsorbent for separation and pre-concentration of various heavy metals which include Hg^{2+} in an environmental sample. The extracted Hg^{2+} was determined using CV-AAS and the LOD recorded by this proposed method was 4.0 ng/L. In another study, an effective and selective adsorbent for Hg^{2+} was synthesized through a series of reaction which includes the functionalization of Fe_3O_4-SiO_2 with APTS and modification of this amine functionalized Fe_3O_4-SiO_2 with a synthetic ligand named 1-(p-acetyl phenyl)-3-(o-ethoxy phenyl)triazene (Figure 2.25e) (Rofouei et al., 2012). The Hg^{2+} extracted by this adsorbent via D-μSPE was analysed by Inductively Coupled Plasma Optical Emission Spectrometry (ICP-OES) and the LOD achieved by this proposed method was 40 ng/L (Rofouei et al., 2012). 1,5-diphenylcarbazide (DPC) (Figure 2.25f) with its favourable coordination capacity and selectively toward Hg^{2+} was chosen as the doping material for the preparation of functionalized magnetic particle (Zhai et al., 2010). Fe_3O_4-SiO_2-DPC was used as an adsorbent in D-μSPE for the

determination of Hg^{2+} in aqueous solution. In this study, Hg^{2+} was analysed using CV-AAS, and the reported LOD was 160.0 ng/L. (Zhai et al., 2010).

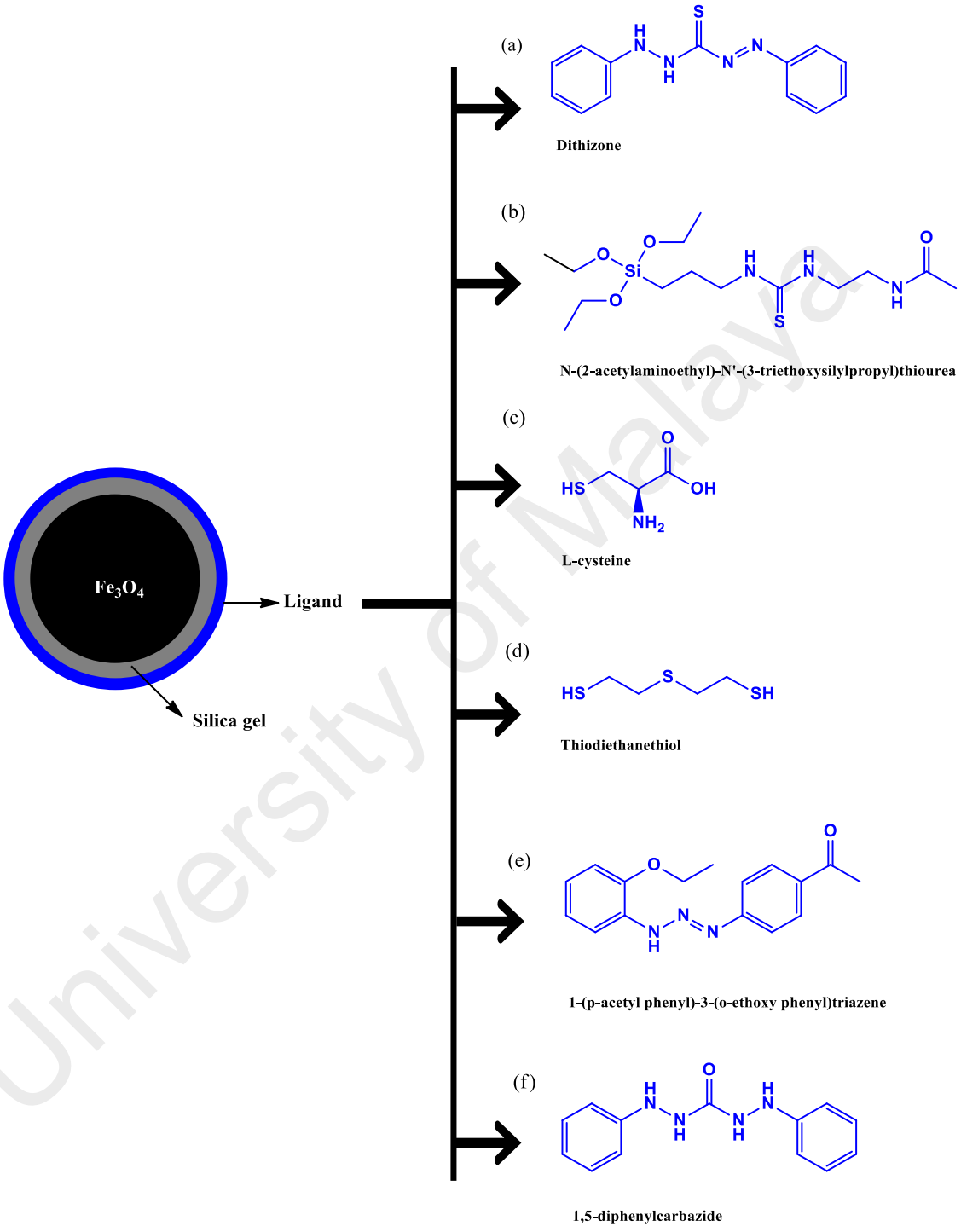

Figure 2.25: A variety of metal capturing ligand used to modify Fe_3O_4-SiO_2.

2.5.7 Ligand incorporated Fe_3O_4-SiO_2 in pre-concentration of Hg^{2+} from water sample

Generally, the reactions involved in the preparation of adsorbents with magnetic property are such as (i) synthesis of Fe_3O_4, (ii) coating of Fe_3O_4 with silica layer, (iii) functionalization Fe_3O_4-SiO_2 and (iv) bonding of selected ligand onto the functionalized Fe_3O_4-SiO_2 which may also involve several steps (Alonso et al., 2016; Cui et al., 2015; Sobhi et al., 2017). Some of this reactions involved higher temperature reflux and also time-consuming. Hence, this study demonstrated a simple preparation route for the preparation of ligand modified Fe_3O_4-SiO_2. This study demonstrated the coating of silica gel doped with metal capturing ligand onto Fe_3O_4 to produce an adsorbent for pre-concentration of Hg^{2+}. This method simplifies the preparation of adsorbent by incorporating the ligand during the coating of Fe_3O_4 with silica layer which was performed in single step (Figure 2.26).

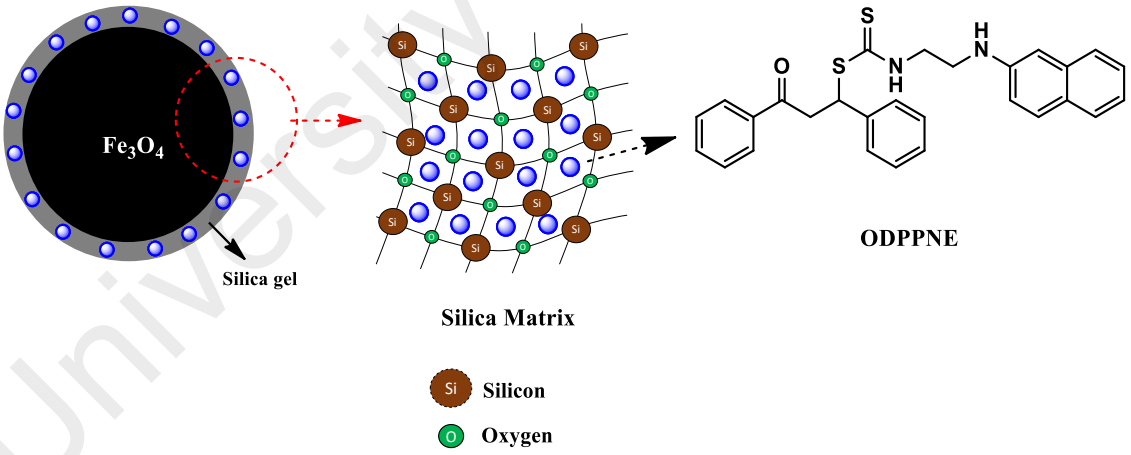

Figure 2.26: ODPPNE incorporated silica coated magnetic nanoparticle (ODPPNE@MNP).

CHAPTER 3: MATERIALS AND METHODS

3.1 Materials and Chemicals

N-(1-Naphthyl)ethylenediamine hydrochloride (98.5%) was purchased from BDH (England). Chalcone (97%) and tetraethoxysilane (99.999%) (TEOS) were obtained from Sigma (USA). Carbon disulfide (≥99.90%) (CS_2), mercury (II) nitrate ($Hg(NO_3)_2$), iron (II) chloride tetrahydrate (≥98.0%) ($FeCl_2.4H_2O$), iron (III) chloride hexahydrate (99.0-102.0%) ($FeCl_3.6H_2O$), ammonia hydroxide solution (25%) (NH_4OH), concentrated hydrochloric acid (37%) (HCl), concentrated sulphuric acid (98%) (H_2SO_4), concentrated phosphoric acid (85%) (H_3PO_4), ethanol (≥99.9%) (EtOH), methanol (≥99.8%) (MeOH), isopropanol (≥99.8%) (iPrOH) and dichloromethane (≥99.9%) (DCM) were obtained from Merck (Germany). The standard solutions of Cr^{3+}, Cd^{2+}, Cu^{2+}, Ni^{2+}, Pb^{2+}, and Zn^{2+} with the concentration of 1000 mg/L were obtained from Merck (Germany). Ultra-pure deionized water was produced by Elga (UK) water purification system.

3.2 Instrumental Analysis

FTIR spectra were recorded using Perkin Elmer Spectrum 400 ATR/FTIR spectrophotometer. NMR spectrum was recorded by using Nuclear Magnetic Resonance spectroscopy FT-NMR ECA 400. Hitachi Energy Dispersive X-ray spectroscopy (EDX) and Field Emission Scanning Electron Microscopy (FESEM) SU8200 was used for elemental analysis and SEM imaging. The thermogravimetric analysis (TGA) and differential thermal analysis (DTA) were carried out using Perkin Elmer Simultaneous Thermal Analyzer STA-6000. The concentration of Hg^{2+} ion was monitored using NIC Mercury Analyser RA-3 whereas the concentration of other metal ions was determined using Agilent Inductively Coupled Plasma Mass Spectrometry ICPMS 7500 Single Turbo

System. UV-Visible spectra were recorded using Thermo Fisher Scientific GENESYS 10S UV-Vis Spectrophotometer.

3.3 Preparation of ODPPNE

ODPPNE was synthesized by reacting *N*-(1-Naphthyl)ethylenediamine hydrochloride, chalcone and CS_2 in methanol as described by Behalo and Aly (2010). Briefly, 1 mmol of *N*-(1-Naphthyl)ethylenediamine hydrochloride and CS_2 (9 mmol) were first dissolved in 30 mL methanol. The mixture was stirred for 60 min at room temperature. Then, 1 mmol of chalcone was then added, and the mixture was refluxed for 24 h. The obtained product in solid form was washed with dichloromethane to remove the unreacted chalcone followed by acidified water to separate *N*-(1-Naphthyl)ethylenediamine hydrochloride residue from the pure product. The NMR spectra of ODPPNE are presented in Appendix A (^{1}H-NMR) and Appendix B (^{13}C-NMR).

Yield: 78%; Melting point. 171-173°C. (IR, cm^{-1}) 3388 (N-H), 1675 (C=O), 1596-1510 (N-C=S), 1080-979 (S-C=S), 820 (C=S). ^{1}H-NMR DMSO-d_6, δ ppm = 3.12 (t, 2H, CH_2N), 3.49 (t, 2H, CH_2N), 3.80 (dd, 1H, CH_2CO), 4.02 (dd, 1H, CH_2CO), 5.36 (t, 1H, CHS), 6.57 (d,1H, Ar), 7.10 (t, 1H, Ar), 7.22 (t, 2H, Ar), 7.35-7.53 (m, 8H, Ar), 7.63 (t, 1H, Ar), 8.02 (d, 2H, Ar), 8.10 (d, 1H, Ar), 8.28 (d, 1H, Ar), 8.32 (brs, 2H, NH) . ^{13}C-NMR DMSO-d_6, δ ppm = 37.96, 40.90, 41.10, 44.95, 103.36, 123.11, 124.20, 124.29, 124.40, 125.18, 126.32, 127.91, 128.31, 128.51, 128.67, 129.19, 132.41, 133.66, 137.29, 142.72, 145.77, 198.70.

3.4 Preparation of Chalcone and ODPPNE incorporated sol-gel

Chalcone and ODPPNE incorporated sol-gel (SG-C and SG-ODPPNE) were prepared as reported by previous studies (Ali et al., 2012; Saad et al., 2006; Turanov et al., 2016; Yost et al., 2000). Briefly, a mixture of TEOS, ethanol, and water in the molar ratio of 1:4:16 was first acidified with concentrated hydrochloric acid to form a sol solution (Buckley and Greenblatt, 1994). Then, the pre-dissolved chalcone and ODPPNE was added to the sol solution, and the molar ratio of TEOS to chalcone and ODPPNE was kept at 30:1 (Esmaeili Bidhendi et al., 2014; Tadayon et al., 2012; Yost et al., 2000). The resulting solution was stirred vigorously for 2 h in a capped vial to allow the gelation to occur. The synthesized sol-gel was dried in the oven for 24 h at 60 °C. The gel was then ground to the size of 0.06 and 2.00 mm in diameter. For conditioning, the sol-gel was soaked in deionized water for 24 h and then dried at 60 °C for 24 h.

3.5 Metal ion adsorption by SG-C and SG-ODPPNE

3.5.1 Determination of the selectivity of SG-C and SG-ODPPNE

The selectivity of SG-C and SG-ODPPNE towards the adsorption of metal ions was evaluated by adding 50 mg of the prepared adsorbents to 10 mL of aqueous solution containing 1 mg/L of Cr^{3+}, Ni^{2+}, Cu^{2+}, Zn^{2+}, Cd^{2+}, Hg^{2+} and Pb^{2+} in a plastic vial. The mixture was shaken using an orbital shaker at 150 rpm for 24 h. The remaining concentration of the metal ions in the solution was analysed using ICP-MS.

3.5.2 Batch adsorption of aqueous Hg^{2+} by SG-ODPPNE

In this study, 50 mg of SG-ODPPNE was first added to the 10 mL of 1 mg/L Hg^{2+} solution in a plastic vial. The mixture was then shaken with an orbital shaker at the defined time interval, and the remaining Hg^{2+} in solution was analysed using portable NIC Mercury Analyser model RA-3 (Tokyo, Japan). Several operation conditions which can influence the adsorption process such as pH of the solution (pH 6-9), the initial concentration of Hg^{2+} (1-100 mg/L), contact time (5-360 min), dosage (0.01-0.10 g) and size of SG-ODPPNE (0.06 mm and 2.00 mm) were evaluated. Removal percentage (%R) of Hg^{2+} in aqueous solution by SG-ODPPNE and the adsorption capacity Q_e (mg/g) of SG-ODPPNE at equilibrium were determined using the following equations (Equation 3.1 and Equation 3.2):

$$\%R = \frac{C_o - C_e}{C_o} \times 100\% \qquad \text{Equation 3.1}$$

$$Q_e = \frac{C_o - C_e}{m} \times V \qquad \text{Equation 3.2}$$

where C_o (mg/L) represents the initial concentration of Hg^{2+}, C_e (mg/L) is the concentration of Hg^{2+} at equilibrium, m (g) is the amount of adsorbent and V (L) is the volume of aqueous solution.

3.5.3 Hg^{2+} removal by SG-ODPPNE adsorbent in real water samples

The ability of SG-ODPPNE to remove Hg^{2+} in real environment water samples was also investigated. In this study, lake water (from Tasik Varsity, University of Malaya, Kuala Lumpur, Malaysia), drinking water, and deionized water were spiked with 1 mg/L of Hg^{2+}. Then, 50 mg of SG-ODPPNE was added to each 10 mL of this spiked real water sample in the plastic vial. The mixture was shaken using an orbital shaker for 6 h, and the concentration of the remaining Hg^{2+} was determined with Mercury Analyser.

3.6 Pre-concentration and determination of Hg^{2+} in water

3.6.1 Synthesis of magnetic nanoparticle (MNP)

MNP was synthesized as reported by Karaagac et al. (2010). Briefly, $FeCl_3.6H_2O$ and $FeCl_2.4H_2O$ was first dissolved in 50 mL of deionized water with the molar ratio Fe^{3+}:Fe^{2+} of 3:2. Then, 50 mL of 25% ammonium hydroxide was added, and the mixture was stirred for 30 min. The MNP was precipitated using the external magnetic field. The synthesized MNP was washed with deionized water and dried using freeze dryer.

3.6.2 Synthesis of ODPPNE-silica coated magnetic nanoparticle (ODPPNE@MNP)

0.1 g of ODPPNE was first dissolved in 20 mL of methanol. Then, 0.3 g of MNP was dispersed in the mixture of isopropanol (50 mL) and deionized water (4 mL). The ODPPNE solution was then added into the dispersed MNP followed by the addition of 2 mL of TEOS and 5 mL of 25% ammonium hydroxide solution. The mixture solution was stirred for 24 h. The obtained ODPPNE@MNP was precipitated using an external magnet field. ODPPNE@MNP was washed with deionized water and ethanol. Then, the ODPPNE@MNP was dried under vacuum. Besides ODPPNE@MNP, the silica coated MNP (SiO_2@MNP) was obtained through same procedure but without the addition of ODPPNE.

3.6.3 Pre-concentration of Hg^{2+} using ODPPNE@MNP as solid phase for dispersive micro solid phase extraction (D-µSPE)

The pre-concentration and determination of Hg^{2+} in water were carried out using ODPPNE@MNP as the solid phase for the D-µSPE method. In this experiment, the operation parameters of D-µSPE such as pH of the solution (pH 5-9), the initial concentration of Hg^{2+} (0.5-100 mg/L), adsorption time (5-30 min), selectivity, dosage of ODPPNE@MNP (5-30 mg), type of desorption reagent (HCl, H_2SO_4 and H_3PO_4), the

volume of desorption reagent (0.25-25 mL), and desorption time (1-10 min) were optimized to obtain the optimal condition for Hg^{2+} analysis. These parameters were found to influence the performance of heavy metals pre-concentration process (Abolhasani et al., 2015; Adlnasab et al., 2014; Sobhi et al., 2017). This experiment was started by the addition of ODPPNE@MNP to the 25 mL of 1 mg/L Hg^{2+} solution. The mixture was then sonicated using an ultrasonic agitator for the defined time interval. After sonication, the ODPPNE@MNP was isolated by using a magnet, and the solution was decanted. The isolated ODPPNE@MNP was rinsed with deionized water for three times before Hg^{2+} desorption process. For the Hg^{2+} desorption process, the isolated ODPPNE@MNP was dispersed in HCl solution. The amount of Hg^{2+} in HCl was analysed using Mercury Analyser. Recovery efficiency (%E) of Hg^{2+} in aqueous solution by ODPPNE@MNP was determined using the following equation:

$$\%E = \frac{C_r}{C_o} \times 100\% \quad \text{Equation 3.3}$$

where C_o (mg/L) represents the initial concentration of Hg^{2+}, C_r (mg/L) is the concentration of extracted Hg^{2+}.

3.6.4 Pre-concentration of Hg^{2+} in real water samples

The developed D-μSPE method was applied in the real water samples analysis to verify its applicability. In this study, 25 mL of the selected drinking, tap and surface water (lake water) sample were spiked with known concentration of Hg^{2+} varying from 0.05 μg/L to 2 μg/L and the pH of this water sample was adjusted to pH 7. 15 mg of ODPNNE@MNP was dispersed in the water sample by the aid of ultra-sonication for 10 min. After the sonication process, the ODPPNE@MNP was isolated from the water sample by using magnet. The isolated ODPPNE@MNP was washed with the deionized water three times to eliminate the unabsorbed Hg^{2+} before the desorption process. For the Hg^{2+} desorption

process, isolated ODPPNE@MNP was dispersed in 0.25 mL of 1.5 M HCl for 5 min. The HCl solution was separated from ODPPNE@MNP and the amount of desorbed Hg^{2+} in HCl was analysed.

CHAPTER 4: RESULTS AND DISCUSSIONS

4.1 Characterization of SG-C, SG-ODPPNE and ODPPNE@MNP

4.1.1 FTIR Analysis

In this study, the three-component one-pot reaction was used to produced ODPPNE as metal capturing ligand. The three components that involved were CS_2, *N*-(1-Naphthyl)ethylenediamine hydrochloride and chalcone. During the reaction, CS_2 was first reacted with *N*-(1-Naphthyl)ethylenediamine hydrochloride to produce (2-(naphthalen-2-ylamino)ethyl)carbamodithioate (*I*). Then, (2-(naphthalen-2-ylamino)ethyl)carbamodithioate was then reacted with chalcone to produce ODPPNE (Figure 2.24). For chalcone, the main characteristic peaks in FTIR were found to appear in the region of 1589-1400 cm^{-1} (Figure 4.1a). These peaks were attributed to aliphatic and aromatic C=C stretching of chalcone (Prasadarao and Mohan, 2012). Besides that, the C-H stretching bands of the =C-H group of chalcone were observed at 3050-3028 cm^{-1} (Aksöz and Ertan, 2012). The characteristic peak of C=O for chalcone appeared at 1663 cm^{-1}. For ODPPNE, the peak at 3401 cm^{-1} was attributed to N-H stretching (Figure 4.1b) and the peak at 2918 and 2907 was corresponded to the sp3 C-H stretch (Behalo and Aly, 2010). The presence of S-C=S group was characterized by the peaks at 1060 and 940 cm^{-1} (Onwudiwe and Ajibade, 2011). The peak at 820 cm^{-1} confirmed the presence of C=S (Tiwari et al., 2015). The peaks at 1580 -1450 cm^{-1} represents the C-N stretching in N-C=S group of ODPPNE (Onwudiwe and Ajibade, 2011).

IR spectra for SG (blank silica gel, Figure 4.2a), SG-C (Figure 4.2b) and, SG-ODPPNE (Figure 4.2c) showed a strong peak around 1080 cm^{-1} corresponded to asymmetric stretching of Si-O-Si (Bari et al., 2009). SG-ODPPNE showed the characteristic peaks of free ODPPNE suggesting ODPPNE was incorporated into the sol-gel matrix (Figure 4.2c). These characteristic peaks appeared at 3372, 2920, 2912, 1673,

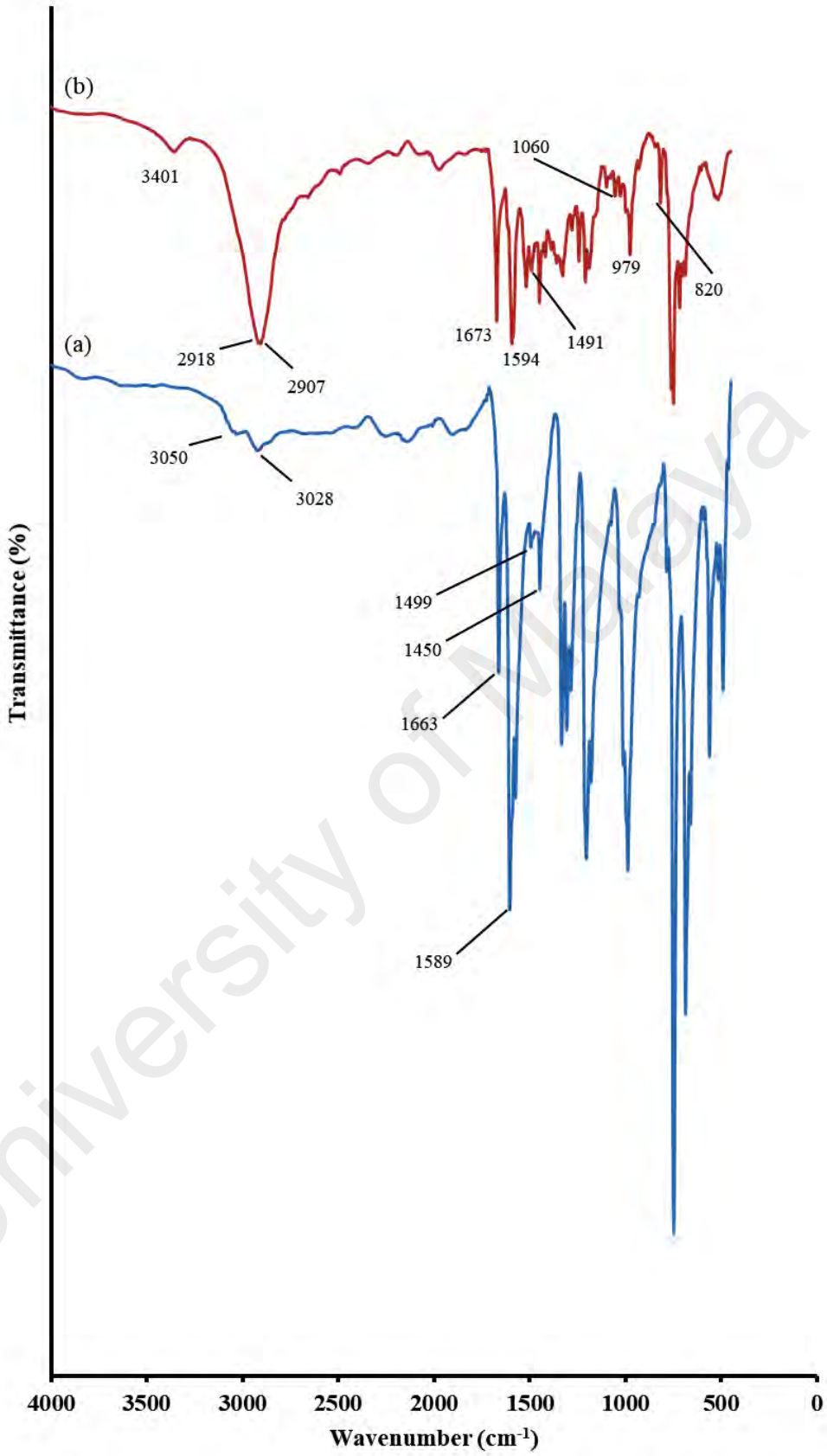

Figure 4.1: IR spectrum of (a) Chalcone and (b) ODPPNE.

1587 and 1497 cm^{-1}. On the other hand, the peaks that appeared around 1500-1400 cm^{-1} for SG-C indicates the presence of chalcone in the sol-gel matrix (Figure 4.2b). To understand the mechanism of the interaction between Hg^{2+} and the ODPPNE that containing in the sol-gel matrix, SG-ODPPNE was isolated from the solution after Hg^{2+} adsorption process. The SG-ODPPNE was then characterized using FTIR. The result showed that the characteristic peak of N-C=S group of ODPPNE was shifted from 1497-1466 cm^{-1} (Figure 4.2c) to 1488-1397 cm^{-1} (Figure 4.2d). This downward shift showed the involvement of N-C=S group in the complexation between ODPPNE with Hg^{2+}.

In order to prove the presence of ODPPNE on the ODPPNE@MNP, the IR spectrum of MNP (Fe_3O_4), SiO_2@MNP and ODPPNE@MNP (Figure 4.3) were recorded. For MNP (Figure 4.3a), the presence of a strong band at around 568 cm^{-1} was attributed to Fe–O stretching vibration (Karaagac and Kockar, 2016; Li et al., 2015). This peak was also observed in the IR spectrum of SiO_2@MNP (Figure 4.3b) and ODPPNE@MNP (Figure 4.3c). For SiO_2@MNP and ODPPNE@MNP, the appearances of strong absorption peak around 1080 cm^{-1} indicated the presence of Si-O bonding (Bari et al., 2009). This observation indicated that silica gel was successfully coated on MNP. On the other hand, the characteristic peak of free ODPPNE ligand at 3352, 2918, 2890, 1673, 1594, 1492 and 1467 cm^{-1} was found to appear in the IR spectrum of ODPPNE@MNP. Hence, this is a strong evidence that ODPPNE was incorporated into the silica gel matric which is coated on MNP. To prove the adsorption of Hg^{2+} by ODPPNE@MNP, ODPPNE@MNP was isolated from the Hg^{2+} solution after adsorption process. The characteristic peaks of ODPPNE which indicates the N-C=S group was found to be shifted from 1492-1467 cm^{-1} to 1497-1472 cm^{-1} (Figure 4.3d). This result further proves the interaction between ODPPNE and Hg^{2+} in the silica gel matrix.

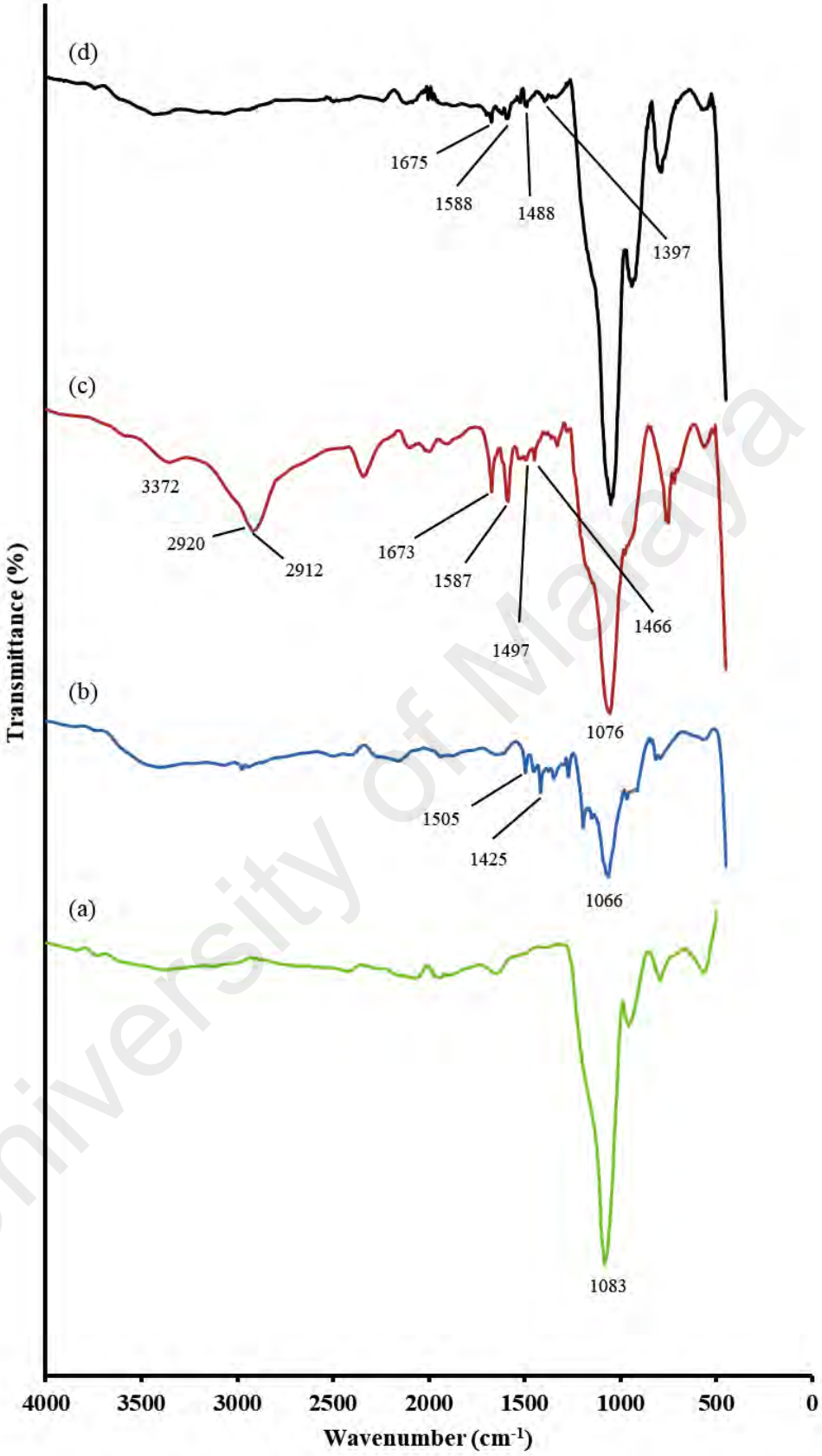

Figure 4.2: IR spectrum of (a) SG, (b) SG-C and (c) SG-ODPPNE and (d) isolated SG-ODPPNE after Hg^{2+} adsorption.

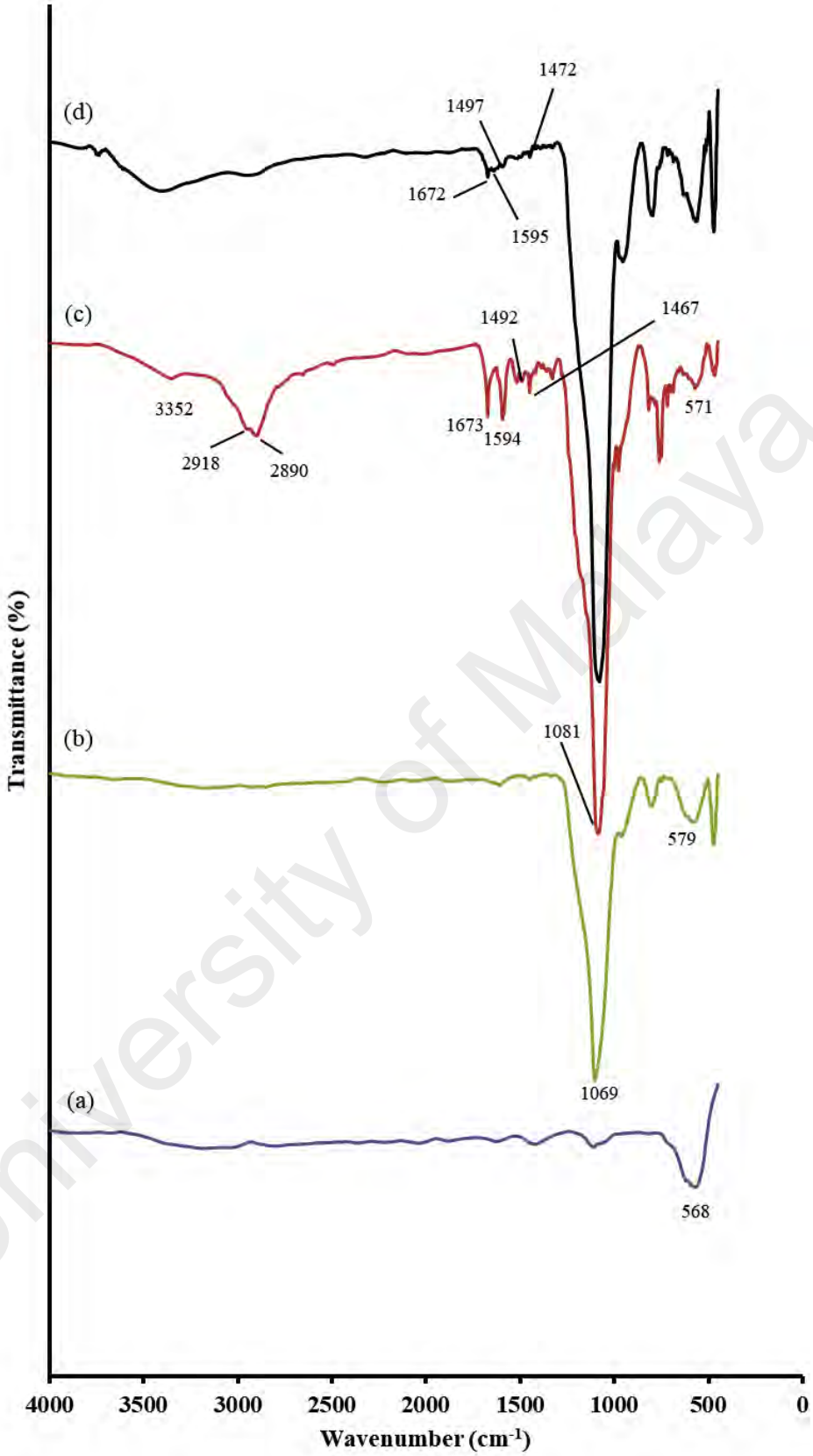

Figure 4.3: IR spectrum of (a) MNP (Fe_3O_4), (b) SiO_2@MNP, (c) ODPPNE@MNP and (d) isolated ODPPNE@MNP after Hg^{2+} adsorption.

4.1.2 Elemental Analysis

SG-ODPPNE, SG-C, and SG were analysed using EDX to confirm the presence of ODPPNE and chalcone in the sol-gel matrix. The result in Table 4.1 indicated that the nitrogen and sulphur were detected in SG-ODPPNE as compared to SG and SG-C. This result further indicates the presence of ODPPNE in the silica gel matrix. For SG-C, the percentage of carbon was detected at the level of 9.73% showing the presence of chalcone in SG-C. To further confirm the adsorption of Hg^{2+} by the SG-ODPPNE, after adsorption of Hg^{2+}, SG-ODPPNE, SG-C and SG were isolated and analysed using EDX. The result showed that Hg^{2+} was detected in both SG-C and SG-ODPPNE only. Therefore, it can be concluded that both SG-C and SG-ODPPNE have the ability to adsorb Hg^{2+}.

Table 4.1: Elemental composition of SG, SG-C and SG-ODPPNE.

Element	Composition of element (%)				
	SG	SG-C*	SG-C**	SG-ODPPNE*	SG-ODPPNE**
Silica (Si)	29.62	39.06	29.14	49.32	26.94
Oxygen (O)	70.38	51.21	47.60	34.64	34.20
Carbon (C)	-	9.73	22.82	11.70	28.51
Nitrogen (N)	-	-	-	4.22	7.73
Sulphur (S)	-	-	-	0.12	1.71
Hg^{2+}	-	-	0.44	-	0.91

* Determined before adsorption process
**Determined after adsorption process
#Not detected

In order to verify the presence of ODPPNE in ODPPNE@MNP, MNP, SiO_2@MNP, and ODPPNE@MNP were also analysed using EDX. The presence of nitrogen and sulphur in ODPPNE@MNP indicated that ODPPNE was successfully incorporated on SiO_2@MNP (Figure 4.2). To further confirm the adsorption of Hg^{2+} by SiO_2@MNP and ODPPNE@MNP, both adsorbents were isolated from the Hg^{2+} solution after adsorption process, and the isolated adsorbents were then subjected to EDX analysis.

According to the result obtained (Table 4.2), Hg^{2+} was only detected on the isolated ODPPNE@MNP. This observation further indicates the role of ODPPNE in the adsorption of Hg^{2+}.

Table 4.2: Elemental composition of MNP, SiO_2@MNP and ODPPNE@MNP.

Element	Composition of element (%)				
	MNP	SiO_2@MNP*	SiO_2@MNP**	ODPPNE @MNP*	ODPPNE @MNP**
Iron (Fe)	74.63	23.85	17.18	15.58	9.73
Oxygen (O)	25.37	43.25	52.79	45.55	37.49
Silica (Si)	-	32.90	30.03	19.07	12.98
Carbon (C)	-	-	-	12.65	11.11
Nitrogen (N)	-	-	-	5.93	1.83
Sulphur (S)	-	-	-	1.22	1.53
Hg^{2+}	-	-	#ND	-	25.34

* Determined before adsorption process
**Determined after adsorption process
#Not detected

4.1.3 SEM analysis

Scanning electron microscopy was performed to observe the morphology of SG, SG-C, SG-ODPPNE, MNP, SiO_2@MNP, and ODPPNE@MNP. The SEM image of SG (Figure 4.4a), SG-C (Figure 4.4b) and SG-ODPPNE (Figure 4.4c) showed that the morphology of these three materials was almost similar. For MNP, the agglomeration of this nano-size material was observed in the SEM image (Figure 4.5a). Both SiO_2@MNP (Figure 4.5b) and ODPPNE@MNP (Figure 4.5c) exhibited the spherical shape with the diameter ranging from around 600 – 700 nm. There are no significant differences in morphology between SiO_2@MNP and ODPPNE@MNP.

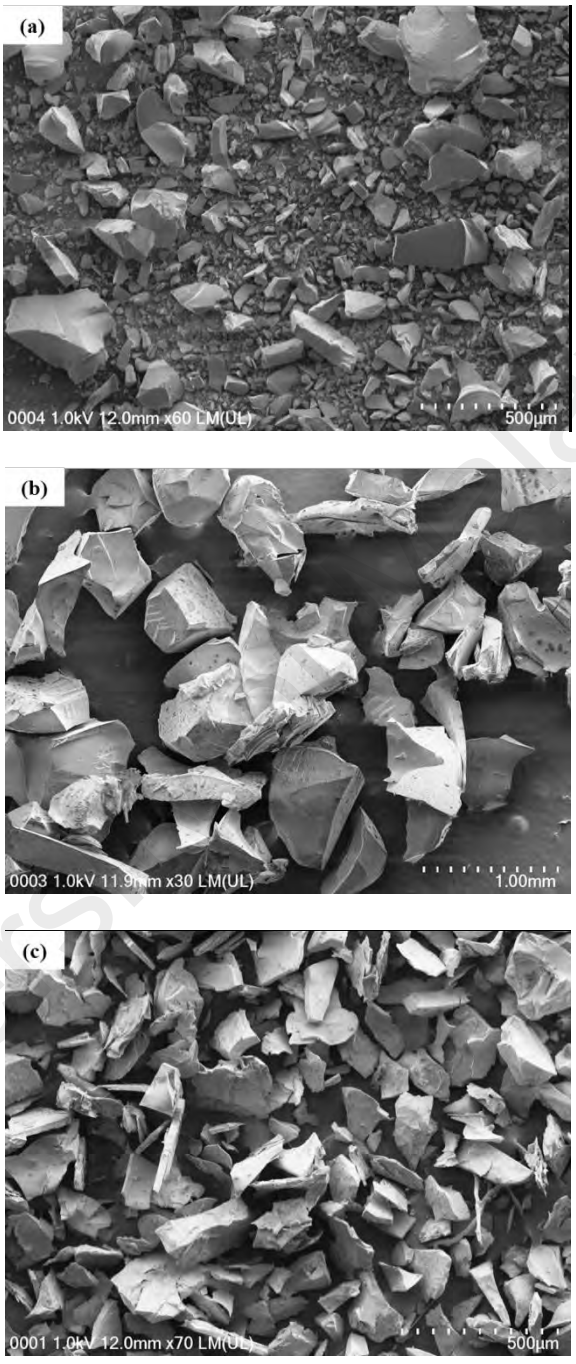

Figure 4.4: SEM images of (a) SG, (b) SG-C and (c) SG-ODPPNE.

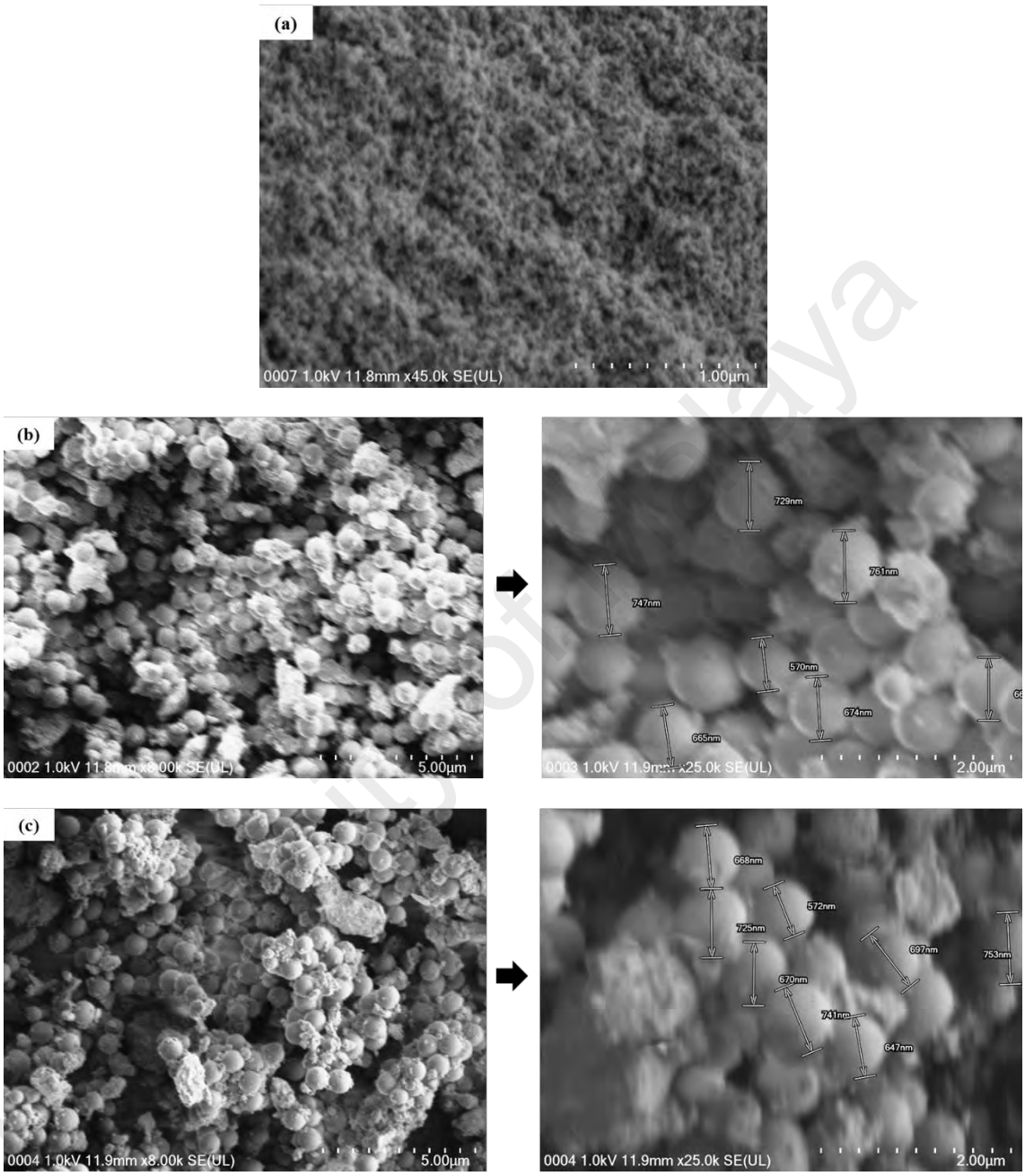

Figure 4.5: SEM images of (a) MNP, (b) SiO_2@MNP and (c) ODPPNE@MNP.

4.1.4 TGA and DTA Analysis

TGA and DTA analysis were performed to further characterize the synthesized adsorbents. The TGA (Figure 4.6a) and DTA (Figure 4.6b) profiles showed that SG-ODPPNE, SG-C, and SG exhibit the first weight loss at around 150 °C corresponded to the removal of physically adsorbed water. SG-ODPPNE and SG-C experienced the second weight loss that occurred at 160 – 400 °C. The maximum weight loss for SG-ODPPNE and SG-C was found to occur at 241 and 344 °C, respectively. These weight losses indicate the decomposition of ODPPNE and chalcone that containing in the silica gel matrix. Based on the weight loss data, the loading of chalcone and ODPPNE in SG-C and SG-ODPPNE was 50 and 90 mg/g, respectively.

The TGA and DTA profile of MNP, SiO_2@MNP, and ODPPNE@MNP are presented in Figure 4.7. All synthesized materials showed a sharp weight loss at the temperature around 100 °C which corresponded to the loss of absorbed water. The ODPPNE@MNP experienced a second weight loss at around 400 to 600 °C, which corresponded to the decomposition of ODPPNE that incorporated in the silica gel matrix of ODPPNE@MNP. Based on the weight loss of ODPPNE, the concentration of ODPPNE in ODPPNE@MNP was 26 mg/g.

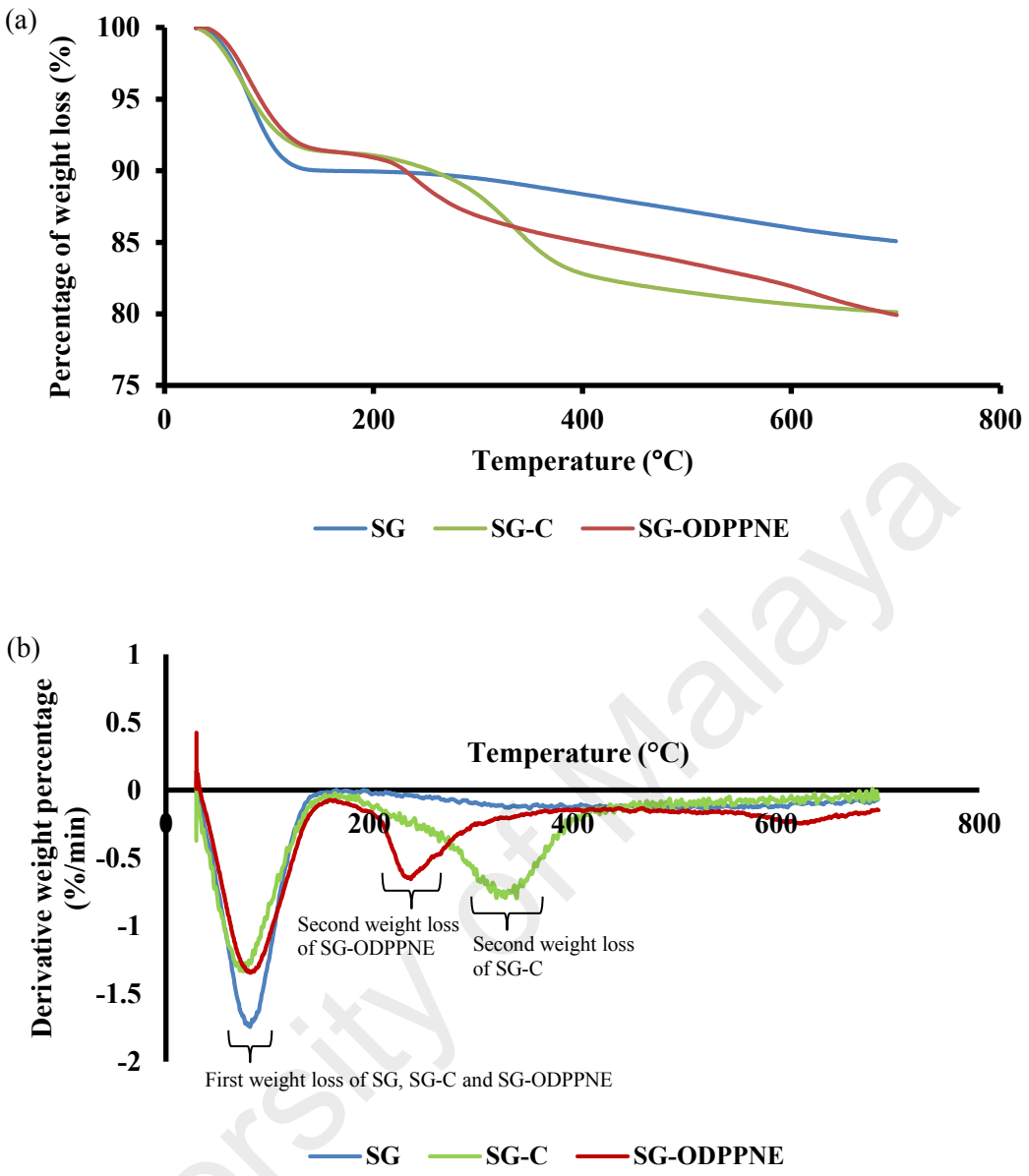

Figure 4.6: (a) TGA and (b) DTA profile of SG, SG-C and SG-ODPPNE.

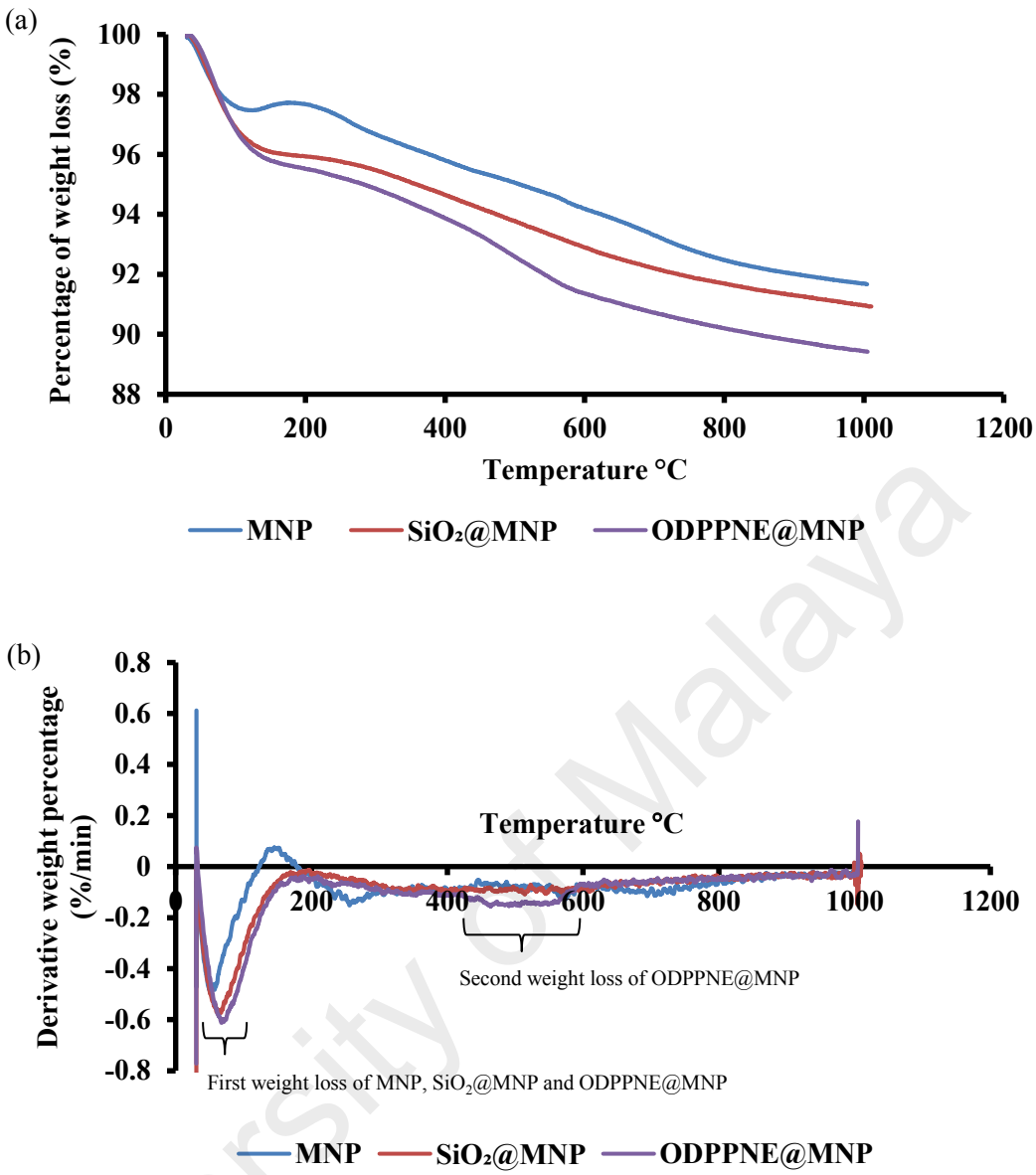

Figure 4.7: (a) TGA and (b) DTA profile of MNP, SiO_2@MNP and ODPPNE@MNP.

4.1.5 Leaching Test

To investigate the stability of embedded ODPPNE in the silica gel matrix, the SG-ODPPNE and ODPPNE@MNP were shaken in water at different pHs for 24 h. The water was then analysed using a UV-Visible spectrometer to detect the ODPPNE. The UV-Visible spectrum of free ODPPNE at pH 5, 7 and 8 showed two λ_{max} at 248 and 322 nm (Figure 4.8). The result indicated ODPPNE was not detected in water and therefore it was concluded that ODPPNE was not leached into the water during the adsorption process. Also, to ensure the stability of the adsorbed Hg^{2+} on SG-ODPPNE and ODPPNE@MNP, the isolated adsorbent was exposed to water with different pHs for 24 h. Then, the presence of Hg^{2+} was determined using Mercury Analyser. The results showed that the Hg^{2+} was not detected in all cases.

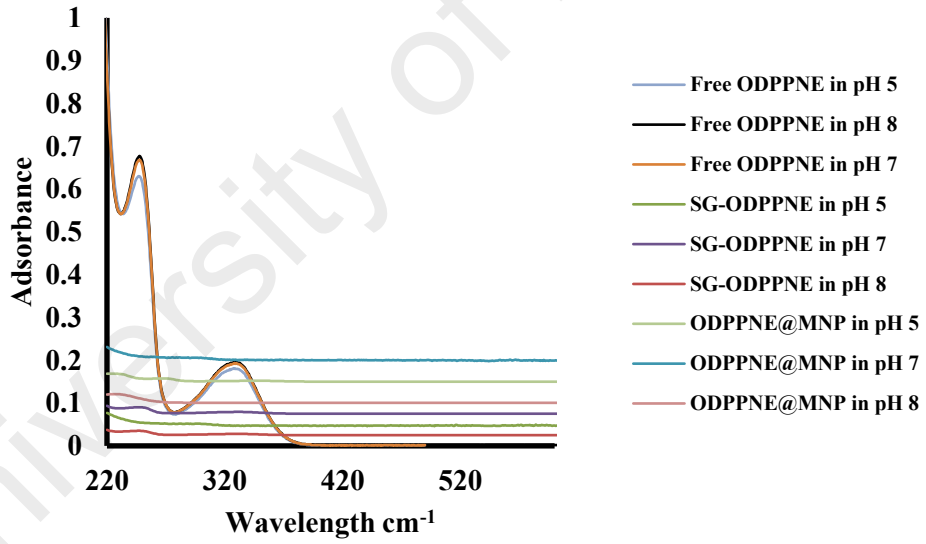

Figure 4.8: The comparison of UV spectra for free ODPPNE, SG-ODPPNE and ODPPNE@MNP in water with different pH. (The overlapped UV spectra of SG-ODPPNE and ODPPNE@MNP was separated by cumulatively adding 0.025 to the UV spectra in a sequence order SG-ODPPNE (pH 8, 5 and 7) and ODPPNE@MNP (pH 8, 5 and 7).)

4.2 Selectivity of SG-C, SG-ODPPNE, SiO_2@MNP, and ODPPNE@MNP in the removal of heavy metals

The ability of SG-C, SG-ODPPNE, and SG to remove metals ion was evaluated using a solution containing 1 mg/L of Cr^{3+}, Ni^{2+}, Cu^{2+}, Zn^{2+}, Cd^{2+}, Pb^{2+} and Hg^{2+} (Figure 4.9). The removal percentage of the selected metal ions by SG was ranged from 10.4 to 16.6%. When SG-C was used as an adsorbent, removal percentage of Cu^{2+} and Hg^{2+} were clearly increased to 38.4 and 45.4%, respectively. The removal of Hg^{2+} was increased to 65.3% when SG-ODPPNE was used as an adsorbent. Also, the removal percentage of Cr^{3+} and Pb^{2+} was also found to increase to 34.2, and 23.9%, respectively.

The adsorption performance of SiO_2@MNP and ODPPNE@MNP toward Hg^{2+} in the presence of various metal ions such as Cr^{3+}, Ni^{2+}, Cu^{2+}, Zn^{2+}, Cd^{2+}, and Pb^{2+} was also investigated. As shown in Figure 4.10, the SiO_2@MNP showed no selectivity and low removal percentages (3.3-20.8%) towards all selected metal ions. For ODPPNE@MNP, 81.4% of Hg^{2+} was successfully removed as compared to the other metal ions where the removal efficiency was ranged from, 9.6 to 44.0%. In general, it can be concluded that the metal ions adsorption efficiency of the silica gel particularly for Cr^{3+}, Cu^{2+}, Hg^{2+}, and Pb^{2+} could be enhanced by incorporating the chalcone. The selectivity of silica gel as well as the silica gel coated MNP in the adsorption of Hg^{2+}, could be further enhanced by incorporating the ODPPNE with dithiocarbamate moiety as metal capturing ligand.

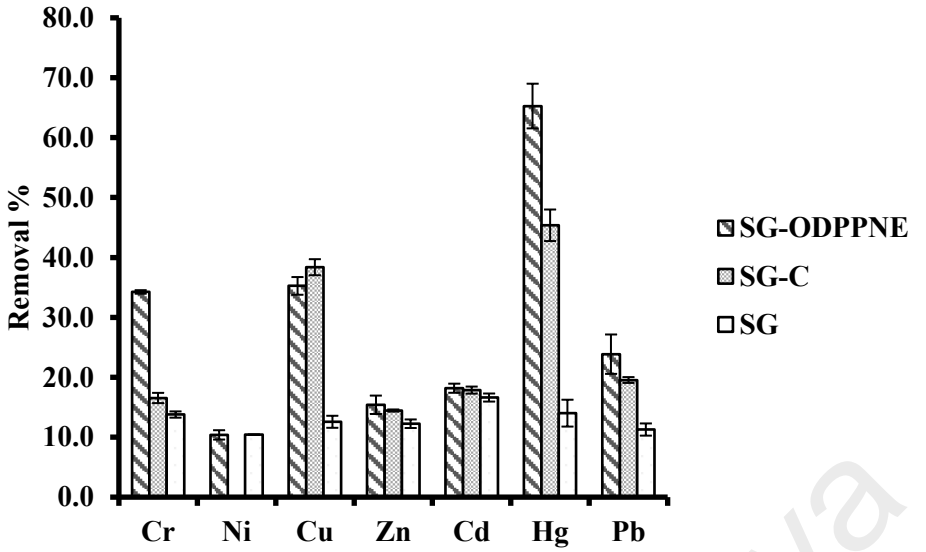

Figure 4.9: The removal percentage of Cr^{3+}, Ni^{2+}, Cu^{2+}, Zn^{2+}, Cd^{2+}, Hg^{2+} and Pb^{2+} by SG-ODPPNE, SG-C and SG in aqueous sample. (Amount of adsorbent = 50 mg, [Metal ion] = 1 mg/L, volume of aqueous solution = 10 mL, pH of aqueous solution = 7.5 and contact time = 24 h).

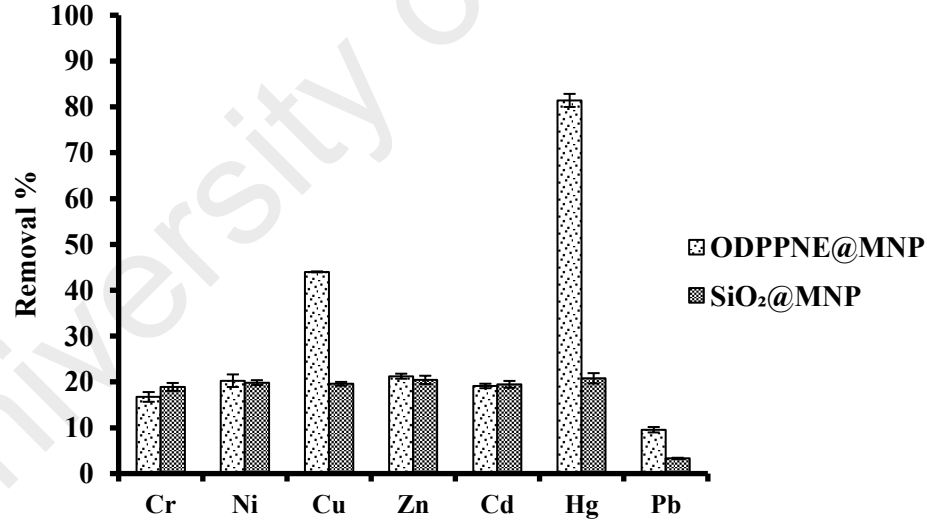

Figure 4.10: The removal percentage of Cr^{3+}, Ni^{2+}, Cu^{2+}, Zn^{2+}, Cd^{2+}, Hg^{2+} and Pb^{2+} by ODPPNE@MNP and SiO_2@MNP in aqueous sample. (Amount of adsorbents = 15 mg, [Metal ion] = 1 mg/L, volume of aqueous solution = 25 mL, pH of aqueous solution = 8 and contact time = 30 min).

4.3 Hg^{2+} removal in aqueous by SG-ODPPNE

Effect of several important parameters toward the removal of aqueous Hg^{2+} by SG-ODPPNE was studied in detail in order to obtain the optimum condition for removal Hg^{2+} in water. By using the obtained conditions, the isotherm and kinetics of the adsorption of Hg^{2+} by SG-ODPPNE were then determined. The performance of the developed method in the real water treatment was also evaluated.

4.3.1 Effect of adsorbent size

To study the effect of the size of SG-ODPPNE on the removal of Hg^{2+}, SG-ODPPNE was ground into the size of 0.06 and 2 mm. 54.1% of Hg^{2+} was removed by SG-ODPPNE with the size of 2 mm whereas SG-ODPPNE with the size of 0.06 mm managed to improve the Hg^{2+} removal efficiency to 77.4% (Figure 4.11). This result indicated that SG-ODPPNE with the larger surface area (smaller particle size) (Rahman and Padavettan, 2012) provides more binding sites to adsorb Hg^{2+}. Therefore, adsorbent with the size of 0.06 mm was selected for further study.

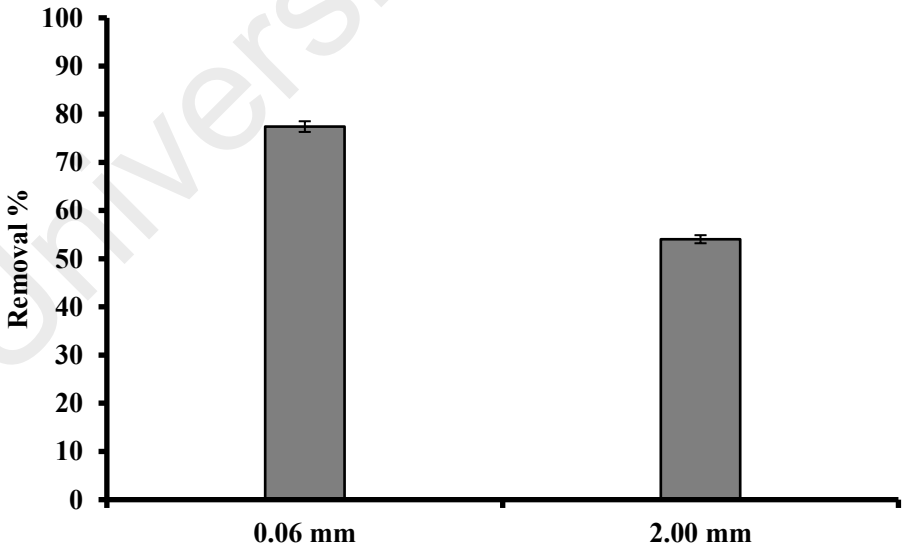

Figure 4.11: Effect of 0.06 mm and 2.00 mm SG-ODPPNE on removal percentage of Hg^{2+} in aqueous sample. (Amount of SG-ODPPNE = 50 mg, [Hg^{2+}] = 1 mg/L, volume of Hg^{2+} solution = 10 mL, pH of Hg^{2+} solution = 7.5 and contact time = 24 h).

4.3.2 Effect of pH of aqueous solution

In this study, the effect of pH on the efficiency of Hg^{2+} removal was determined by varying the pH of the Hg^{2+} solution from 6 to 9 (Figure 4.12). The removal efficiency of Hg^{2+} was found to increase when the pH was increased from 6 to 8. The efficiency of Hg^{2+} removal was found to reduce when the pH was exceeded 8. This result indicated that the adsorption process in aqueous solution is a pH-dependent process. Due to the presence of secondary amine groups, ODPPNE can present in the form of neutral, deprotonated and protonated species (Figure 4.13a). In this study, the pKa of ODPPNE was calculated using MarvinSketch software (Version 17.2.6). The calculated pKa of ODPPNE was 4.21 and 7.32. Based on the calculated pKa, ODPPNE appeared dominantly in neutral and deprotonated forms at the selected pH range (Figure 4.13b). Therefore, the lower efficiency of SG-ODPPNE in Hg^{2+} removal at acidic condition was mainly due to the presence of the higher fraction of neutral ODPPNE (Figure 4.13a) which has the lower capability to complex with Hg^{2+}. When the pH increases, the higher amount of ODPPNE appeared in the deprotonated form. Deprotonated ODPPNE could interact favorably with Hg^{2+} due to the presence of negative charge. At pH 9, the decreased in the adsorption efficiency might due to the formation of $Hg(OH)_2$ which is neutral and less likely to complex with ODPPNE as compared to Hg^{2+} (Shen et al., 2014).

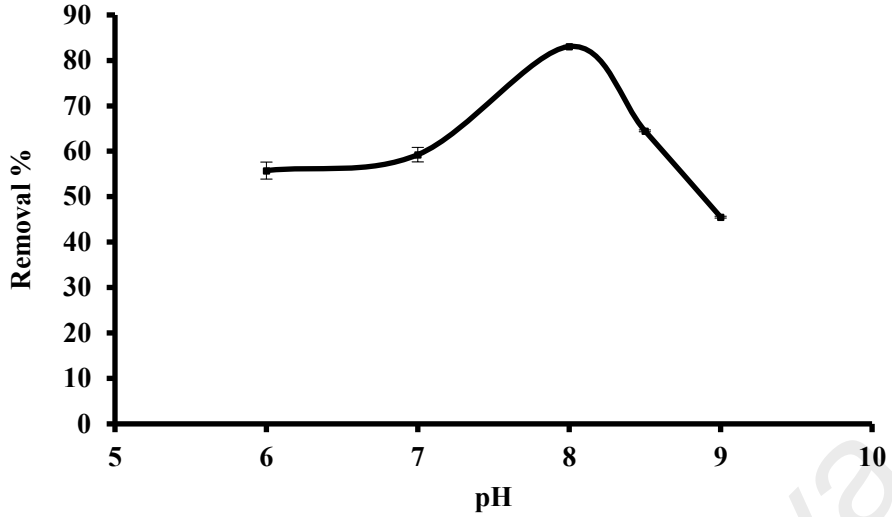

Figure 4.12: Effect of pH on the removal efficiency of Hg^{2+} in aqueous sample by SG-ODPPNE. (Amount of SG-ODPPNE = 50 mg, [Hg^{2+}] = 1 mg/L, volume of Hg^{2+} solution = 10 mL and contact time = 24 h).

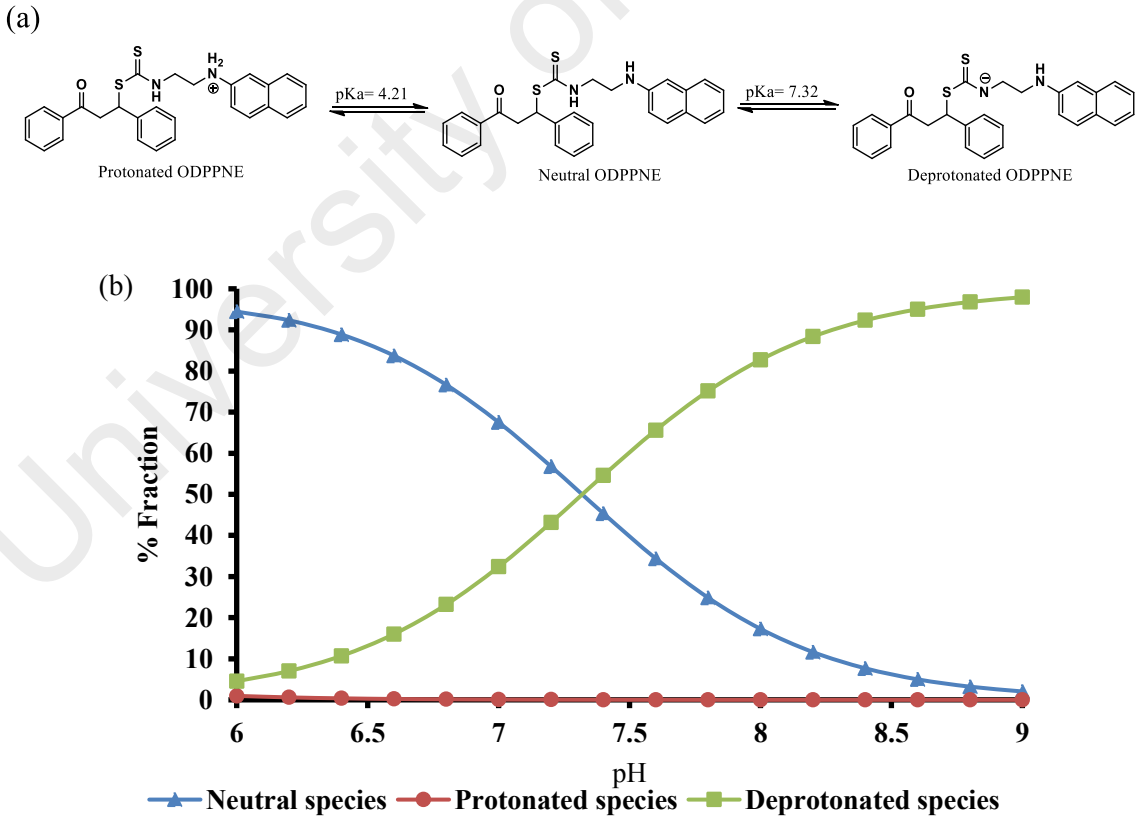

Figure 4.13: (a) The structure of neutral, protonated and deprotonated ODPPNE, and (b) The variation of fraction of neutral, protonated and deprotonated ODPPNE in the pH range of 6 to 8.

4.3.3 Effect of contact time

The contact time for the adsorption process is important for the determination of the kinetic of Hg^{2+} removal. In this experiment, the removal of Hg^{2+} by SG-ODPPNE was evaluated from 5 to 360 min. The result showed that the percentage removal of Hg^{2+} increased rapidly to 58.9% for the first 60 min (Figure 4.14). After 60 min, the percentage removal of Hg^{2+} was found to increase slowly to 82.1% at 240 min. No significant enhancement in Hg^{2+} removal was observed after 240 min. This may due to the available site of adsorbent for adsorption of Hg^{2+}decrease with time and finally saturated after 240 min (Zewail and Yousef, 2015).

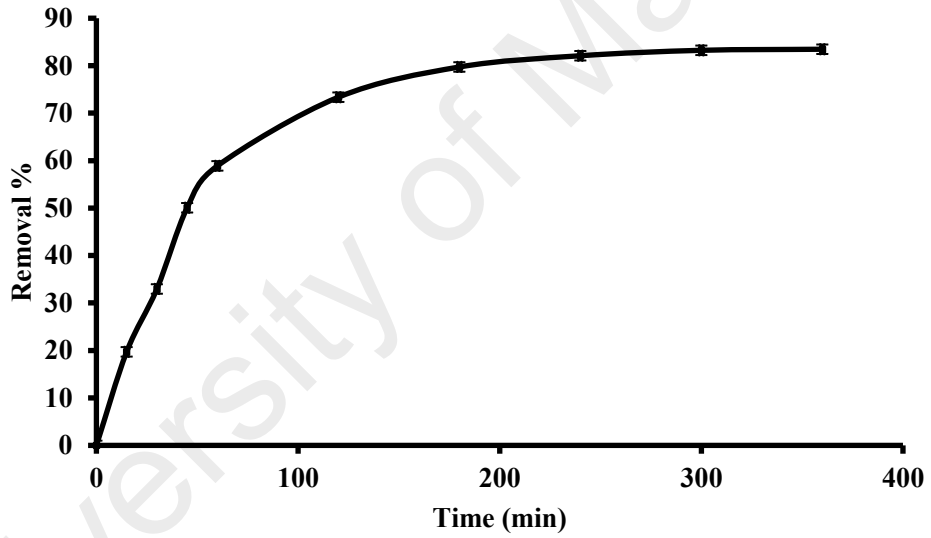

Figure 4.14: Effect of contact time on the removal percentage of Hg^{2+} in aqueous sample by SG-ODPPNE. (Amount of SG-ODPPNE = 50 mg, $[Hg^{2+}]$ = 1 mg/L, volume of Hg^{2+} solution = 10 mL and pH of Hg^{2+} solution = 8).

4.3.4 Effect of Hg^{2+} initial concentration

The effect of initial Hg^{2+} concentration was studied by varying the initial concentration of Hg^{2+} from 1 to 100 mg/L. The result showed that the removal percentage decreased with increasing initial concentration of the Hg^{2+} solution (Figure 4.15). This could be explained by the fact that the amount of Hg^{2+} increases with increasing concentration of the Hg^{2+} solution. However, the number of adsorption sites remained constant and subsequently higher amount of Hg^{2+} was not absorbed and remained in the solution when the higher concentration of the Hg^{2+} solution was used.

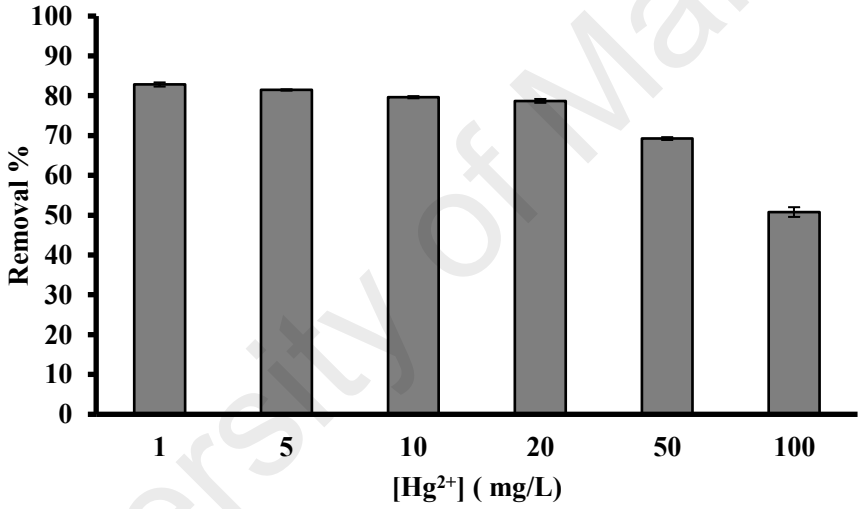

Figure 4.15: Effect of Hg^{2+} concentration on removal percentage of Hg^{2+} in aqueous sample. (Amount of SG-ODPPNE = 50 mg, volume of Hg^{2+} solution = 10 mL, pH of Hg^{2+} solution = 8 and contact time = 6 h).

4.3.5 Effect of SG-ODPPNE dosage

The dosage of SG-ODPPNE is an important parameter to obtain quantitative Hg^{2+} removal. The removal of Hg^{2+} was found to increase from 58.2 to 78.7% when the amount of SG-ODPPNE increased from 10 to 50 mg (Figure 4.16). No significant improvement on Hg^{2+} removal was observed when 100 mg of SG-ODPPNE was used. The increased of the removal percentage of Hg^{2+} with increasing dosage was due to the presence of higher amount of adsorption site which is accessible for Hg^{2+}. At the higher amount of SG-ODPPNE, the saturation of Hg^{2+} removal percentage was due to the overlapping of adsorption site that reduced the effective surface area (Mandal et al., 2013).

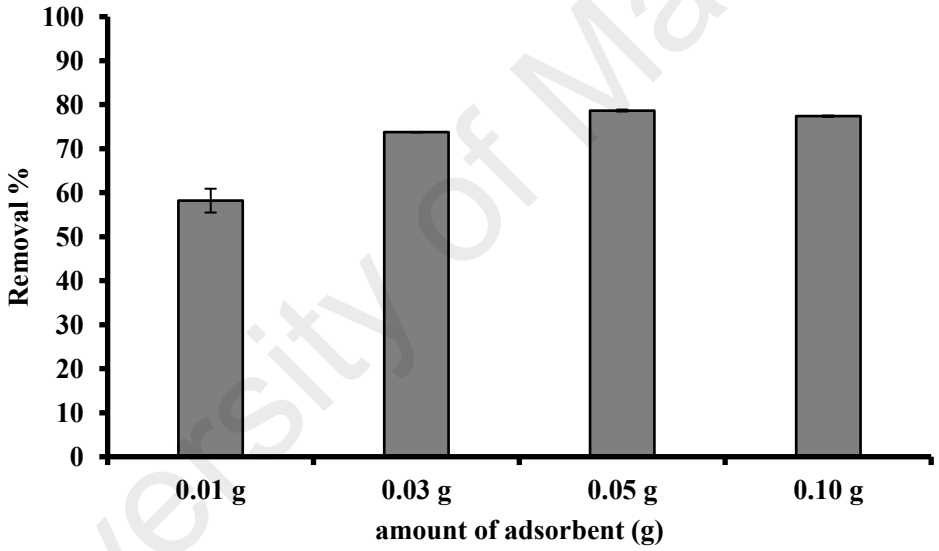

Figure 4.16: Effect of SG-ODPPNE amount on removal percentage of Hg^{2+} in aqueous sample. ([Hg^{2+}] = 1 mg/L, volume of Hg^{2+} solution = 10 mL, pH of Hg^{2+} solution = 8 and contact time = 6 h).

4.3.6 Application of SG-ODPPNE in the removal of Hg^{2+} in real water samples

Adsorption experiment was carried out in drinking water and lake water to evaluate the performance of SG-ODPPNE in the removal of Hg^{2+} in real water samples. These two water samples have different water matrices. The selected water samples were found to be free from Hg^{2+}. Therefore, the selected water samples were spiked with Hg^{2+} at the level of 1 mg/L. As compared to the deionized water, no significant reduction in the Hg^{2+} removal efficiency was observed when the adsorption was performed in the selected water samples. This result indicated that the selected water matrices were not significantly influenced the adsorption of Hg^{2+} by SG-ODPPNE (Figure 4.17).

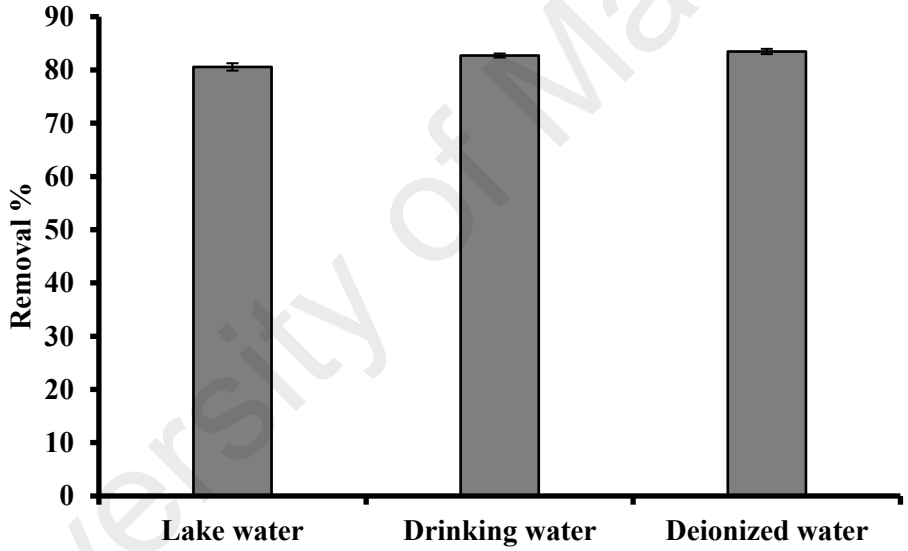

Figure 4.17: Removal percentage of Hg^{2+} by SG-ODPPNE in real water samples. (Amount of SG-ODPPNE = 50 mg, spiked [Hg^{2+}] = 1 mg/L, volume of water samples = 10 mL, pH of water samples = 8 and contact time = 6 h).

The adsorption capacity of SG-ODPPNE on Hg^{2+} was compared with previously reported dithiocarbamate-based adsorbents (Table 4.3). These adsorbents were prepared by anchoring the 3-aminopropyltriethoxysilane onto the surface of silica gel (Mahmoud, 1999; Venkatesan et al., 2002), mesoporous silica gel (Venkatesan et al., 2003), and magnetite coated siliceous hybrid shells (Tavares et al., 2013) followed by the addition

of CS_2 to yield dithiocarbamate functional group. The adsorption capacity of SG-ODPPNE was found to be lower than the dithiocarbamate anchored silica gel and mesoporous silica gel. This might due to the ODPPNE that located in the sol-gel matrix and less accessible by Hg^{2+}. For dithiocarbamate anchored silica gel and mesoporous silica gel with higher adsorption capacity, the dithiocarbamate is located at the surface of adsorbents and more accessible by Hg^{2+}. In term of selectivity, the performance of SG-ODPPNE was found to be comparable with dithiocarbamate anchored silica gel (Mahmoud, 1999).

Table 4.3: Comparison of the adsorption capacity and selectivity of SG-ODPPNE with other reported dithiocarbamate-based absorbents.

Adsorbent	**Maximum Adsorption Capacity (mg/g)**	**Selectivity [Metal ion (normalized Q_e)]**
Dithiocarbamate anchored silica gel[1]	[#]NR	**Hg^{2+}(1)**, Mg^{2+}(0.02), Ca^{2+}(0.06), Cr^{3+}(0.12), Mn^{2+}(0.12), Co^{2+}(0.09), Cu^{2+}(0.32), Zn^{2+}(0.10), Cd^{2+}(0.16), Ba^{2+}(0.30), Pb^{2+}(0.45)
Dithiocarbamate anchored silica gel[2]	~61	[#]NR
Dithiocarbamate grafted on mesoporous silica[3]	40	[#]NR
Magnetite coated with siliceous hybrid shells[4]	20	[#]NR
Chalcone based dithiocarbamate derivative incorporated sol-gel[5]	13.5	**Hg^{2+}(1)**, Cr^{3+}(0.52), Ni^{2+}(0.16), Cu^{2+}(0.54), Zn^{2+}(0.24), Cd^{2+}(0.28), and Pb^{2+}(0.37)

[#]NR: Not reported

[1]Mahmoud, 1999, [2]Venkatesan et al., 2002, [3]Venkatesan et al., 2003, [4]Tavares et al., 2013 and [5]This work.

4.4 Pre-concentration of Hg^{2+} in aqueous sample by ODPPNE@MNP

So far, most of the ligand incorporated silica gels are frequently used as adsorbents for the metal ions removal. In this study, SG-ODPPNE was coated onto the magnetic particles for the preparation of adsorbent (ODPPNE@MNP) for the pre-concentration of Hg^{2+}. This study demonstrated the application of ligand incorporated silica gel in trace Hg^{2+} analysis. The selected method for pre-concentration was D-μSPE (Figure 4.18). In D-μSPE, ODPPNE@MNP as the solid adsorbent was dispersed in water through sonication to allow the adsorption of Hg^{2+}. After adsorption, ODPPNE@MNP was separated from water using an external magnet. In this case, the magnetic property was added to the ODPPNE@MNP to ease the separation of adsorbent after the pre-concentration process. Then the water sample was decanted leaving the ODPPNE@MNP in the vials. The Hg^{2+} that adsorbed by ODPPNE@MNP was desorbed using desorption reagent, and the Hg^{2+} was analysed using mercury analyser. In this study, the operating parameters (such as the amount of adsorbent, adsorption time, pH and concentration of Hg^{2+}) of D-μSPE were optimized to develop an efficient pre-concentration technique.

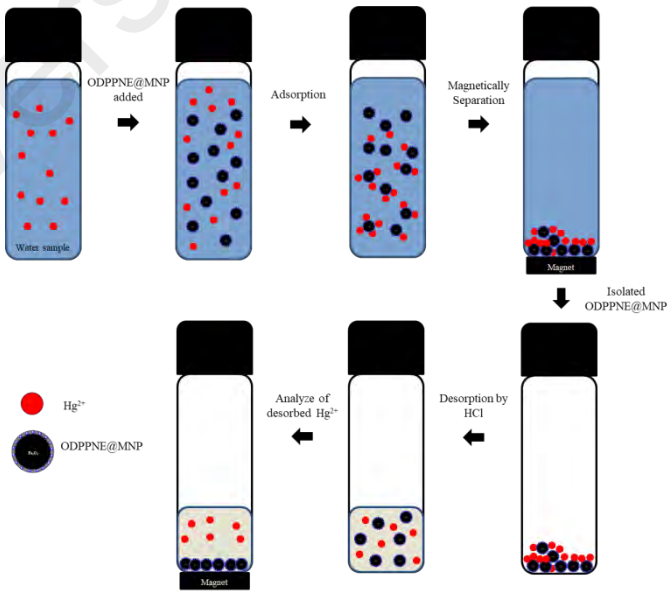

Figure 4.18: D-μSPE process.

4.4.1 Amount of ODPPNE@MNP

The adsorption process was carried out by varying the amount of ODPPNE@MNP from 5 to 30 mg to determine the optimum amount of ODPPNE@MNP required to achieve the optimum adsorption of Hg^{2+}. The percent removal of Hg^{2+} was found to increase from 88.7 to 93.6% when the amount of ODPPNE@MNP was increased from 5 to 15 mg. This result was mainly due to the increased of metal adsorption site when the amount of ODPPNE@MNP was increased. However, there was no significant increase in the percent removal of Hg^{2+} when the amount of ODPPNE@MNP was increased to 20, and 30 mg (Figure 4.19). This result indicates that 15 mg of ODPPNE@MNP was sufficient to achieve the highest Hg^{2+} removal efficiency. Thus, the dosage of ODPPNE@MNP used for subsequent adsorption process was 15 mg.

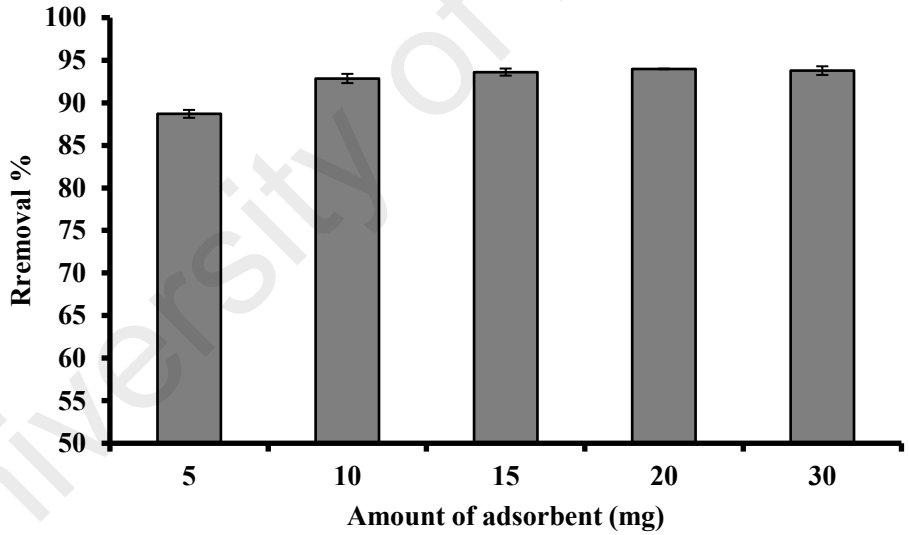

Figure 4.19: Effect of the amount of ODPPNE@MNP on removal percentage of Hg^{2+} in water. ([Hg^{2+}] = 1 mg/L, volume of Hg^{2+} solution = 25 mL, pH of aqueous solution = 8 and adsorption time = 30 min).

4.4.2 Adsorption time

In D-μSPE, ODPPNE@MNP was dispersed in the water with the aid of sonication. Hence, the sonication time was investigated to ensure the ODPPNE@MNP was completely and evenly dispersed in the Hg^{2+} solution to acquire the optimal removal efficiency. According to the result obtained (Figure. 4.20), the removal efficiency achieved increased significantly to 91.6% for the first 5 min of sonication. At 10 min, the obtained percent removal was 93.6%, and it remained constant after 10 min of sonication time. Therefore, the adsorption time for D-μSPE was fixed to 10 min in this study.

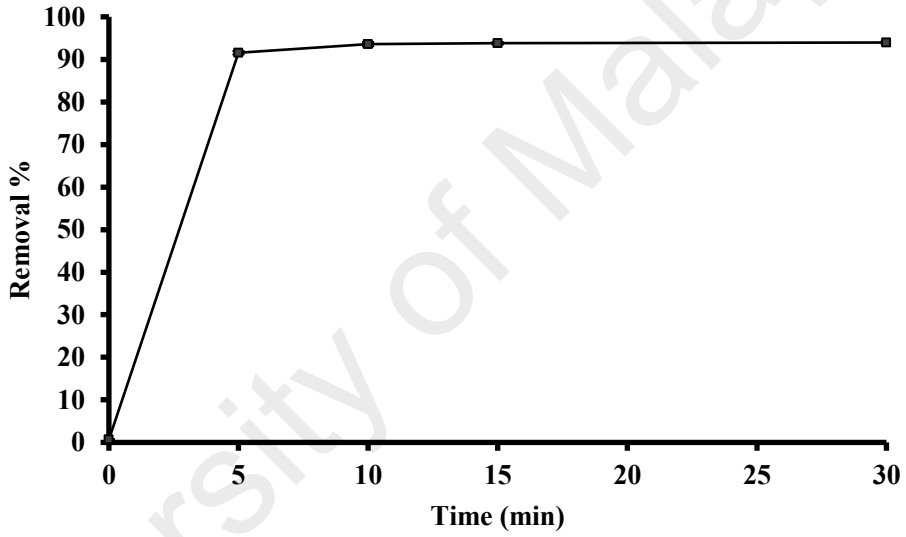

Figure 4.20: Effect of adsorption time on removal percentage of Hg^{2+} in aqueous solution. (Amount of ODPPNE@MNP = 15 mg, $[Hg^{2+}]$ = 1 mg/L, pH of aqueous solution = 8 and volume of Hg^{2+} solution = 25 mL.

4.4.3 pH of aqueous solution

The effect of pH on the performance of ODPPNE@MNP for Hg^{2+} adsorption was studied by varying the pH of the solution from 5 to 9. The result (Figure 4.21) showed that the adsorption of Hg^{2+} by ODPPNE@MNP was found to increase from 51.1 to around 90% when the pH of the solution was increased from 5 to 8. This result is in agreement with SG-ODPPNE which also achieved it highest adsorption efficiency at pH 8. As shown in

Section 4.3.2, the calculated pKa of ODPPNE was 4.21 and 7.32. Therefore, ODPPNE also appeared dominantly in neutral and deprotonated forms at this selected pH range. The lower efficiency of ODPPNE@MNP in Hg^{2+} removal at acidic condition was mainly due to the presence of the higher fraction of neutral ODPPNE which has the lower capability to complex with Hg^{2+}. When the pH increases to 8, the higher amount of ODPPNE appeared in the deprotonated form. Deprotonated ODPPNE could interact favorably with Hg^{2+} due to the presence of negative charge. When the pH of the aqueous solution was high, the formation of $Hg(OH)_2$ which is neutral and less favorable (Shen et al., 2014) to interact with ODPPNE as compared with Hg^{2+}. Since ODPPNE@MNP showed slightly higher efficiency in adsorbing Hg^{2+} at pH 7, this pH condition was selected for the following experiment.

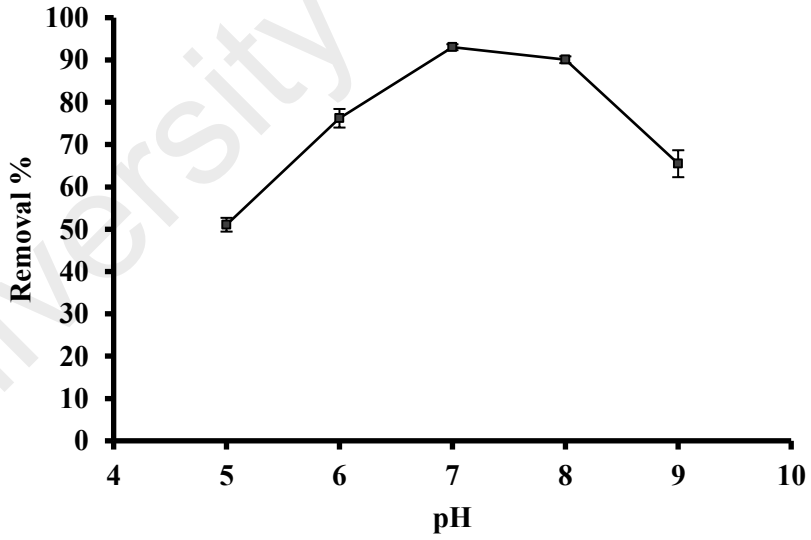

Figure 4.21: Effect of pH on removal percentage of Hg^{2+} in aqueous solution. (Amount of ODPPNE@MNP = 15 mg, $[Hg^{2+}]$ = 1 mg/L, volume of aqueous solution = 25 mL and adsorption time = 10 min).

4.4.4 Concentration of Hg^{2+} in aqueous solution

The effect of initial concentration of Hg^{2+} in the aqueous sample on the adsorption performance of ODPPNE@MNP was studied by varying the initial concentration of Hg^{2+} from 0.5 to 100 mg/L. The result (Figure 4.22) indicated that the adsorption efficiency of Hg^{2+} by ODPPNE@MNP was excellent when the concentration of Hg^{2+} was increased from 0.5 to 10 mg/L, and 97% of Hg^{2+} was removed. However, the efficiency of ODPPNE@MNP was found to reduce when the concentration of Hg^{2+} was further increased to 50 and 100 mg/L. This observation was due to the increasing amount of Hg^{2+} when the concentration was increased, but the available active site at ODPPNE@MNP remained unchanged and saturated with Hg^{2+} (Denizli et al., 2000).

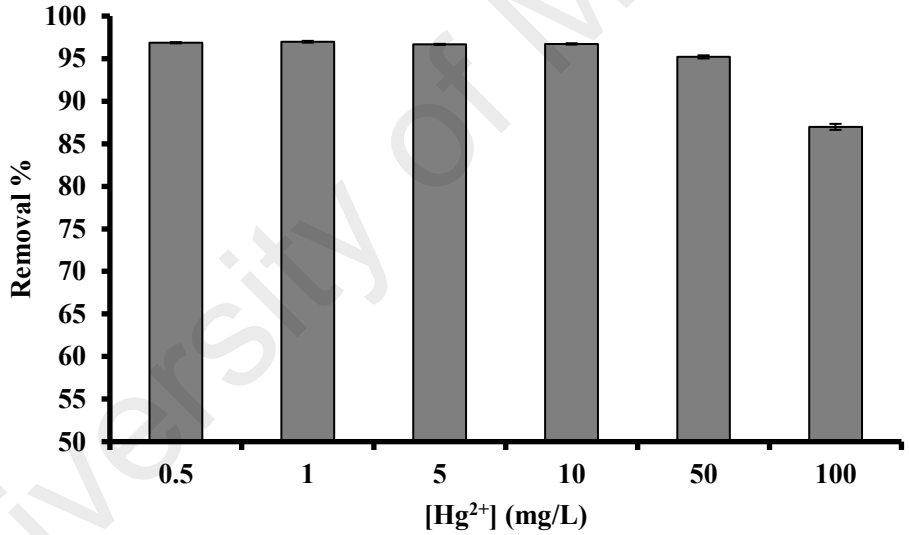

Figure 4.22: Effect of Hg^{2+} concentration on removal percentage of Hg^{2+} in aqueous sample. (Amount of ODPPNE@MNP = 15 mg, volume of aqueous solution = 25 mL, adsorption time = 10 min and pH of aqueous solution = 7).

4.4.5 Desorption reagent for Hg^{2+}

In order to determine the most suitable desorption reagent to desorb the adsorbed Hg^{2+} from ODPPNE@MNP, several types of acids which included hydrochloric acid (HCl), sulphuric acid (H_2SO_4) and phosphoric acid (H_3PO_4) with different concentration were used in the desorption process. Acid was selected because it can dissolve metal ions. Desorption process was also carry out using sonication. According to Figure 4.23, the highest percentage recovery of Hg^{2+} was achieved using HCl as desorption reagent as compared to H_2SO_4 and H_3PO_4. This result might be due to the favorable reaction between Hg^{2+} with HCl to form chloro complexes of Hg^{2+} (Bhattacharyya et al., 2013). The effect of concentration of acid on the desorption of Hg^{2+} was evaluated in this experiment. Figure 4.23 showed that the percent recovery of Hg^{2+} was increased with increasing concentration of acid ranging from 0.5 to 1.5 M. No significant changes in the percent recovery when the concentration of acid was further increased to 2.0 M. Therefore, HCl with the concentration of 1.5 M was selected as desorption reagent in the D-μSPE. The recovery process was performed under by varying the volume of HCl from 0.25 to 25 mL to determine the effect of volume of 1.5 M HCl toward the Hg^{2+} recovery efficiency. The result showed that the recovery efficiency of Hg^{2+} was unaffected by the volume of HCl (Figure 4.24). Therefore, 0.25 mL of 1.5 M HCl was selected as desorption reagent to reduce the chemical consumption of the developed D-μSPE.

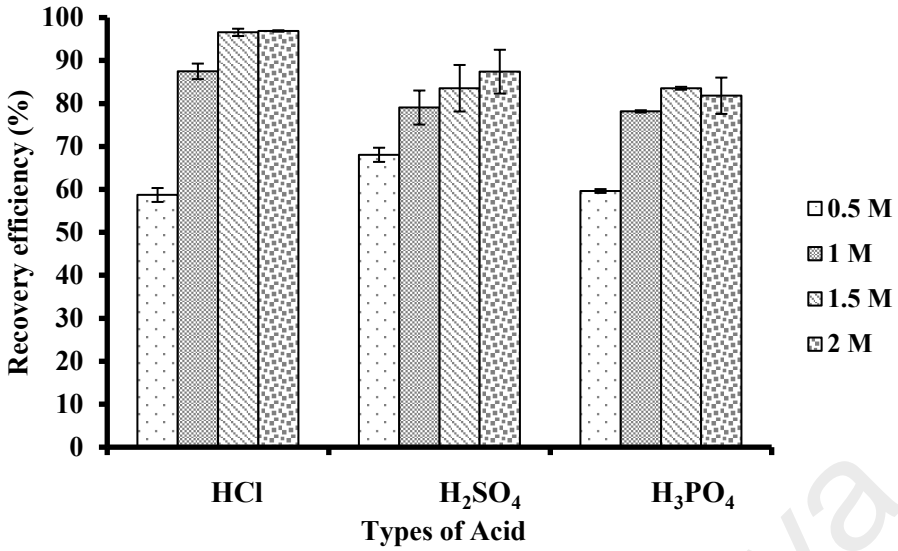

Figure 4.23: Effect of the type of eluent used and it's concentration on recovery efficiency of Hg^{2+} in aqueous solution. (Amount of ODPPNE@MNP = 15 mg, volume of aqueous solution = 25 mL, adsorption time = 10 min, pH of aqueous solution = 7, desorption time = 30 min and volume of acid = 25 mL).

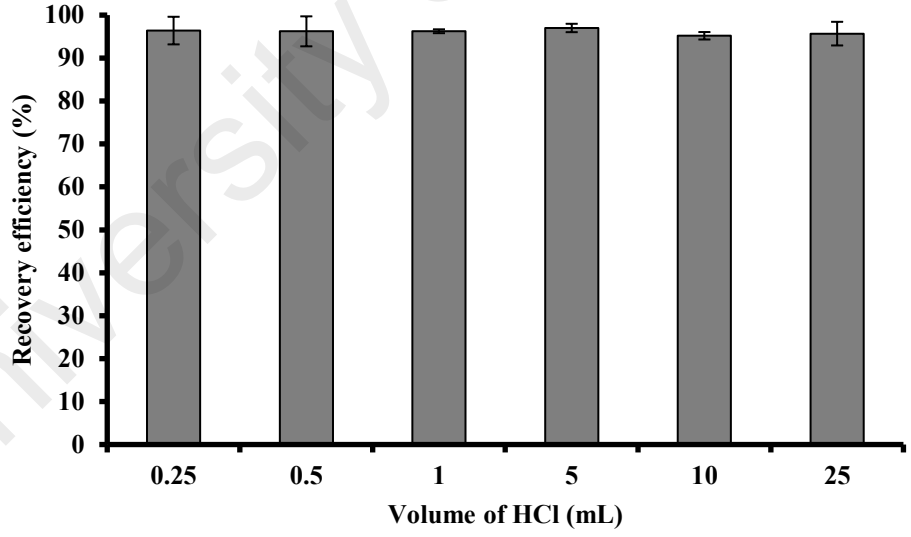

Figure 4.24: Effect of the volume of HCl on recovery efficiency of Hg^{2+} in aqueous solution. (Amount of ODPPNE@MNP = 15 mg, volume of aqueous solution = 25 mL, adsorption time = 10 min, pH of aqueous solution = 7, desorption time = 30 min and and [HCl] = 1.5 M).

4.4.6 Desorption Time

Desorption time was studied in detail to obtain a fast and efficient D-μSPE technique for Hg^{2+} analysis. In this study, the desorption proses were carried out with the aid of sonication to enhance desorption process. The recovery of Hg^{2+} was examined within 1 to 10 min of sonication. The result showed that (Figure 4.25), the percent recovery of Hg^{2+} was increased significantly to 98.7% within first 5 min. The recovery of Hg^{2+} was remained unchanged after 5 min of sonication. Therefore, desorption process by sonication was performed at 5 min for the following experiment.

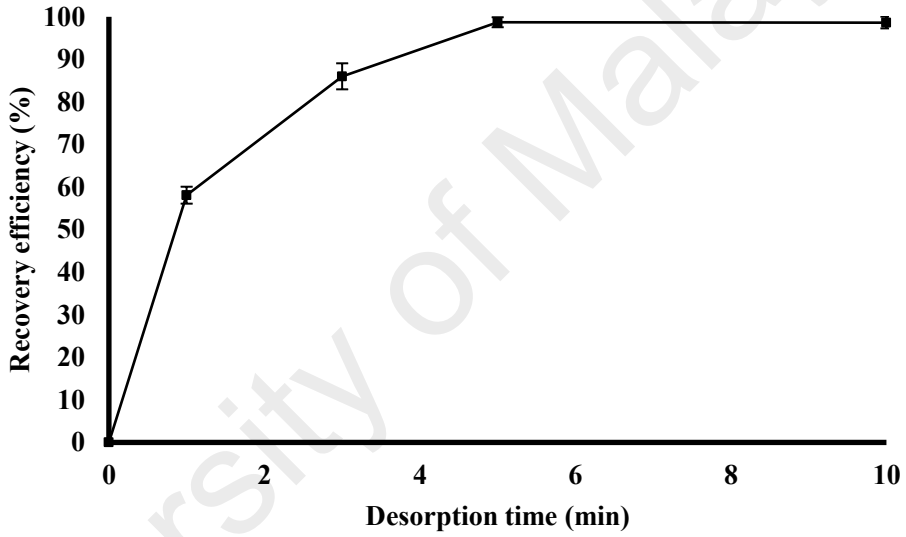

Figure 4.25: Effect of the desorption time recovery efficiency of Hg^{2+} in aqueous solution. (Amount of ODPPNE@MNP = 15 mg, volume of aqueous solution = 25 mL, adsorption time = 10 min, pH of aqueous solution = 7, volume of HCl = 0.25 mL and [HCl] = 1.5 M).

4.4.7 Reusability of ODPPNE@MNP in D-μSPE process

Reusability is an important feature for the adsorbents in the green chemical analysis. Reusable adsorbents can reduce the chemical consumption during its production. In this experiment, the used ODPPNE@MNP was washed with 1.5 M of HCl and deionized water for three times before the following pre-concentration process was performed to ensure the ODPPNE@MNP was completely free from Hg^{2+}. Each pre-concentration process was performed under identical conditions as the first process, and the percent recovery of Hg^{2+} was monitored. As shown in Figure 4.26, the percent recovery remained constant (> 95%) within the first four pre-concentration. However, the percent recovery of Hg^{2+} was found to decrease to 91.4% and 84.4% for the fifth and sixth time of the pre-concentration process. The degradation in the Hg^{2+} pre-concentration efficiency might occur due to the dissolution of the silica gel coating by acid which causes the ODPPNE to leak from ODPPNE@MNP and consequently reduced the efficiency of ODPPNE@MNP in the pre-concentration process. As a conclusion, the ODPPNE@MNP can be reused up to four times of pre-concentration.

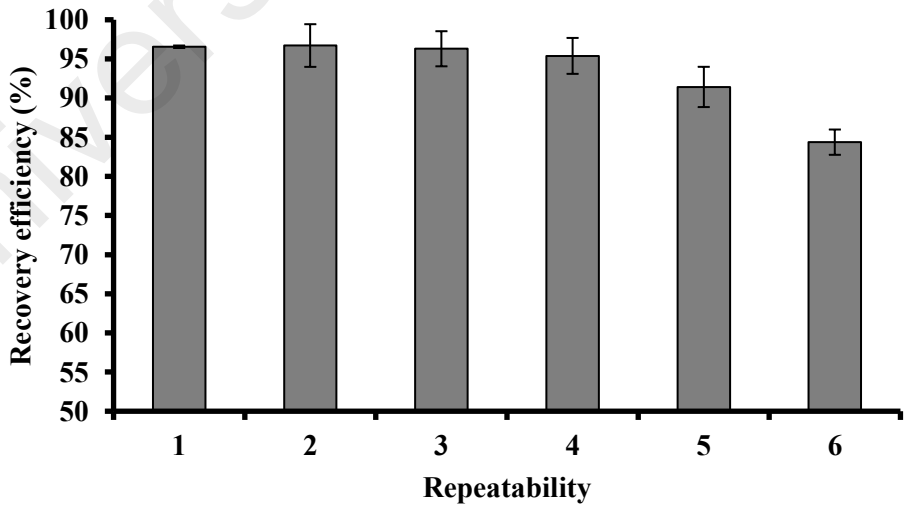

Figure 4.26: Reusability of ODPPNE@MNP. (Amount of ODPPNE@MNP = 15 mg, volume of aqueous solution = 25 mL, adsorption time = 10 min, pH of aqueous solution = 7, volume of HCl = 0.25 mL, [HCl] = 1.5 M, and desorption time = 10 min).

4.4.8 Application of ODPPNE@MNP as solid adsorbent in the pre-concentration of Hg^{2+} in real water sample

According to the Section 4.4.1-4.47, the optimized condition for the pre-concentration of Hg^{2+} was 15 mg of ODPPNE@MNP, adsorption time of 10 min, pH 7, 1.5 M of HCl as desorption reagent, and 5 min of desorption time. The pre-concentration factor for the optimized method was calculated using Equation 4.1:

$$\text{Pre} - \text{concentration Factor } = \frac{V_0}{V_f} \qquad \text{Equation 4.1}$$

where V_0 and V_f are the initial volumes of the water sample and volume of desorption agent. In this experiment, Hg^{2+} in 25 mL of water sample was adsorbed by ODPPNE@MNP, and 0.25 mL of 1.5 M HCl was used to desorb the adsorbed Hg^{2+}. Therefore, he pre-concentration factor for Hg^{2+} in this study was 100.

The analytical performance and validation of the optimized pre-concentration method were evaluated using linearity, the method of detection limit (MDL) or limit of detection (LOD), limit of quantitation (LOQ), inter-day and intra-day precision. The optimized method showed good regression coefficient (R^2) of 0.9985 for the linear range of 50 to 5000 ng/L. The MDL and LOQ were determined through seven replicates of deionized water spiked with Hg^{2+} at the concentration that equal to signal to noise ratio of five (Ripp, 1996). MDL and LOQ were determined using the following equations (Equation 4.2 and Equation 3):

$$MDL = s \times (t - value) \qquad \text{Equation 4.2}$$

$$LOQ = s \times 10 \qquad \text{Equation 4.3}$$

where s is the standard deviation of the concentration of Hg^{2+} obtained from the seven replicates and t-value is the t-student value based on six degrees of freedom which is

equal to 3.143. The obtained MDL and LOQ for the optimized method were 4.0 and 12.9 ng/L, respectively. These values were far below the maximum contaminant level goal (MCLG) of inorganic mercury, which is 2 µg/L (U.S. EPA, 2009). The intra-day and inter-day reproducibility of the proposed method was expressed in relative standard deviation (%RSD) by analysing five replicates of 0.05 μg/L Hg^{2+}. %RSD obtained for intra-day and inter-day analyses were 6.9 and 3.7%, respectively.

For validation, drinking water, tap water, and surface water that spiked with Hg^{2+} at the concentration of 50, 500 and, 2000 ng/L were analysed using the optimized method. The intraday and interday precision of the optimized method are presented in Table 4.4. The obtained recovery for Hg^{2+} was ranged from 90.1 to 99.0 % with relative standard deviation of 0.7 - 8.8 and 1.1 - 7.7% for the intra-day and inter-day precision. These results showed that the matrices of the selected water samples have no significant effect on the performance of the developed method. A typical comparison with other methods reported by previous studies is presented in Table 4.5. The analytical characteristics such as MDL or LOD, LOQ, and linearity range obtained from the optimized method are more sensitive than other previous methods. Therefore, it can be concluded that the proposed method was an effective and robust method for the pre-concentration of Hg^{2+} in water.

Table 4.4: Intra and inter day analysis result for real water samples.

Sample	Spiked [Hg^{2+}] (ng/L)	Intra-day (n=5)		Inter-day (n=5)	
		Recovery efficiency (%)	RSD (%)	Recovery efficiency (%)	RSD (%)
Drinking water	50	96.2	8.8	95.1	1.1
	500	97.5	1.9	96.9	2.3
	2000	98.1	8.7	98.1	4.0
Tap Water	50	99.0	0.7	92.3	4.7
	500	98.2	6.6	98.1	5.9
	2000	90.1	3.1	96.6	7.7
Surface Water	50	90.7	6.5	91.4	5.2
	500	90.8	3.6	90.3	3.4
	2000	91.8	5.2	91.2	1.2

Table 4.5: Comparison with previous reported analytical methods for pre-concentration or determination of Hg^{2+} in aqueous sample.

Adsorbent	Analytical Method	Detection Limit (ng/L)	LOQ (ng/L)	Linearity (μg/L)
Fe_3O_4 magnetic nanoparticles functionalized with dithizone[1]	D-μSPE/CV-AAS	50*	200	0.2-100
Fe_3O_4 nanoparticles covered with a shell of silica and modified with the N-(2 acetylaminoethyl)-N-(3-triethoxysilylpropyl)thiourea[2]	D-μSPE /DMA	17*	#NR	#NR
Thiol-modified magnetic silica sorbent[3]	D-μSPE /CV-AAS	60*	#NR	0.2-5
Thiodiethanethiol grafted tetraethyl orthosilicate modified nanoparticles[4]	D-μSPE /CV-AAS	4*	#NR	0.01-750
Fe_3O_4 magnetite nanoparticles modified with 1-(p-acetyl phenyl)-3-(o-ethoxy phenyl) triazene[5]	D-μSPE /ICP-OES	40*	130	0.2-200
Magnetic nanoparticles functionalized with 1,5-bis(di-2- pyridil)methylene thiocarbohydrazide[6]	FI-MSPME/CV-ETAAS	7.4*	#NR	0.099-10/10-50
Rattle-type Fe_3O_4@SnO_2 core-shell nanoparticles[7]	D-μSPE /CV-AAS	28*	#NR	0.1-40
ODPPNE@MNP[8]	D-μSPE /MA	4.0**	12.9	0.05-5.0

*LOD, **MDL, #NR: Not reported

[1]Adlnasab et al., 2014, [2]Cui et al., 2015, [3]Xiang et al., 2013, [4]Beiraghi et al., 2014, [5]Rofouei et al., 2012, [6]Alonso et al., 2016, [7]Mehdinia et al., 2017 and [8]This work.

4.5 Adsorption isotherm

Adsorption isotherm describes the phenomenon that is governing the retention, release, and mobility of a substance from the aqueous to a solid-phase at a constant temperature and pH (Foo and Hameed, 2010). In this study, the adsorption isotherm was determined to understand the mechanism of adsorption of Hg^{2+} by SG-ODPPNE and MNP@ODPPNE. The obtained adsorption data were fitted to Langmuir and Freundlich models to obtain the best model that described the adsorption Hg^{2+} process by both SG-ODPPNE and MNP@ODPPNE (Abas et al., 2013). Langmuir model assumes the adsorption occurs at monolayer or so-called unilayer adsorption (Sadeek et al., 2015). According to this model, sorbates are adsorbed by equivalent active site with identical energy. These active sites were located on the surface of adsorbent and consequently formed a saturated monolayer. The Langmuir model can be expressed by Equation 4.4 (Foo and Hameed, 2010):

$$\frac{C_e}{Q_e} = \frac{1}{Q_m B_L} + \frac{C_e}{Q_m} \qquad \text{Equation 4.4}$$

where C_e is referring to the concentration of sorbate which is Hg^{2+} at equilibrium, Q_e and Q_m represent the adsorption capacity of adsorbent at equilibrium and maximum adsorption capacity (mg/g), and B_L is the Langmuir constant (L/mg) related to the energy of adsorption. By plotting the curve of C_e/Q_e versus C_e, Q_m and B_L can be determined from slope and intercept of the graph. The dimensionless constant or separation factor R_L can be determined to show the favorability of adsorption. R_L can be calculated using the following Equation 4.5 (Ramos-Ramírez et al., 2009):

$$R_L = \frac{1}{1 + (B_L \times C_o)} \qquad \text{Equation 4.5}$$

where C_o represents the initial concentration of Hg^{2+} as adsorbate. The adsorption process

is described as favorable if $0 < R_L < 1$, unfavorable if $R_L > 1$ and linear when $R_L = 0$ (Ramos-Ramírez et al., 2009). For SG-ODPPNE, the C_e/Q_e versus C_e plot (Figure 4.27a) was linear with the correlation coefficients (R^2) of 0.9993. The Q_m obtained from the curve was 13.5 mg/g, and the R_L value was in the range of 0.1428 to 0.9434. The results obtained from the R_L value indicates the adsorption of Hg^{2+} is a favorable process. The C_e/Q_e versus C_e plot (Figure 4.27b) for ODPPNE@MNP was also linear with the R^2 value of 0.9988. The Q_m obtained for ODPPNE@MNP was 185.2 mg/g.

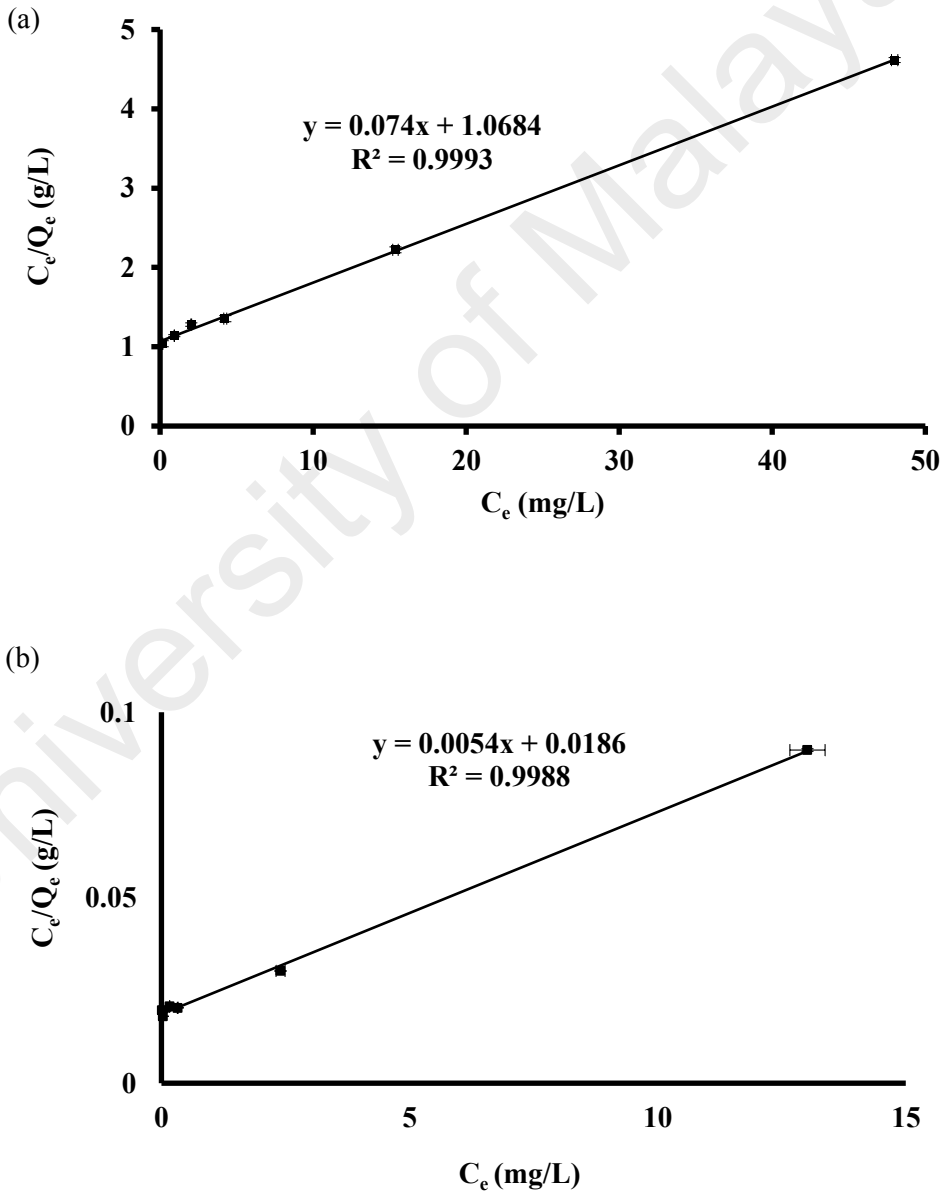

Figure 4.27: Linearized adsorption isotherm Langmuir Model for Hg^{2+} adsorption on (a) SG-ODPPNE and (b) ODPPNE@MNP.

ODPPNE@MNP also showed favorable adsorption process towards Hg^{2+} with the R_L value ranging from 0.0333 to 0.8732. The Q_m value obtained for ODPPNE@MNP was 13.7 times higher than SG-ODPPNE. ODPPNE@MNP with smaller particle (~600 nm) with the larger surface area could adsorb higher amount of Hg^{2+} as compared to SG-ODPPNE with the size of 0.06 mm.

Freundlich isotherm is an empirical equation that describes the adsorption process on the heterogeneous surface with the non-uniform active site, which also refers to multilayer adsorption process (Sadeek et al., 2015; Yan et al., 2015). The Freundlich model can be described by Equation 4.6 (Mushtaq et al., 2016):

$$\log Q_e = \log B_f + \frac{1}{n}\log C_e \qquad \text{Equation 4.6}$$

where B_f represents the Freundlich constant that related to adsorption capacity, and n is the adsorption intensity constant. The R^2 values obtained from log Q_e versus log C_e curve (Figure 4.28) for SG-ODPPNE and MNP@ODPPNE were 0.9713 and 0.9800, respectively.

The best-fitted model for this adsorption process was determined by the R^2 and Chi-square values (χ^2) obtained from Figure 4.27 and Figure 4.28 (Mandal et al., 2013). The result showed that the R^2 value of Langmuir model was significantly higher than Freundlich model for both SG-ODPPNE and MNP@ODPPNE (Table 4.6). In addition, the χ^2 of Langmuir model for SG-ODPPNE and MNP@ODPPNE adsorption was found to be lower than Freundlich model. This observation suggested that the adsorption process of Hg^{2+} on SG-ODPPNE and ODPPNE@MNP follows Langmuir isotherm model which indicates the unilayer adsorption. In addition, this result also indicated that ODPPNE trapped in the silica gel matrix are equivalent active site with identical energy for Hg^{2+} adsorption.

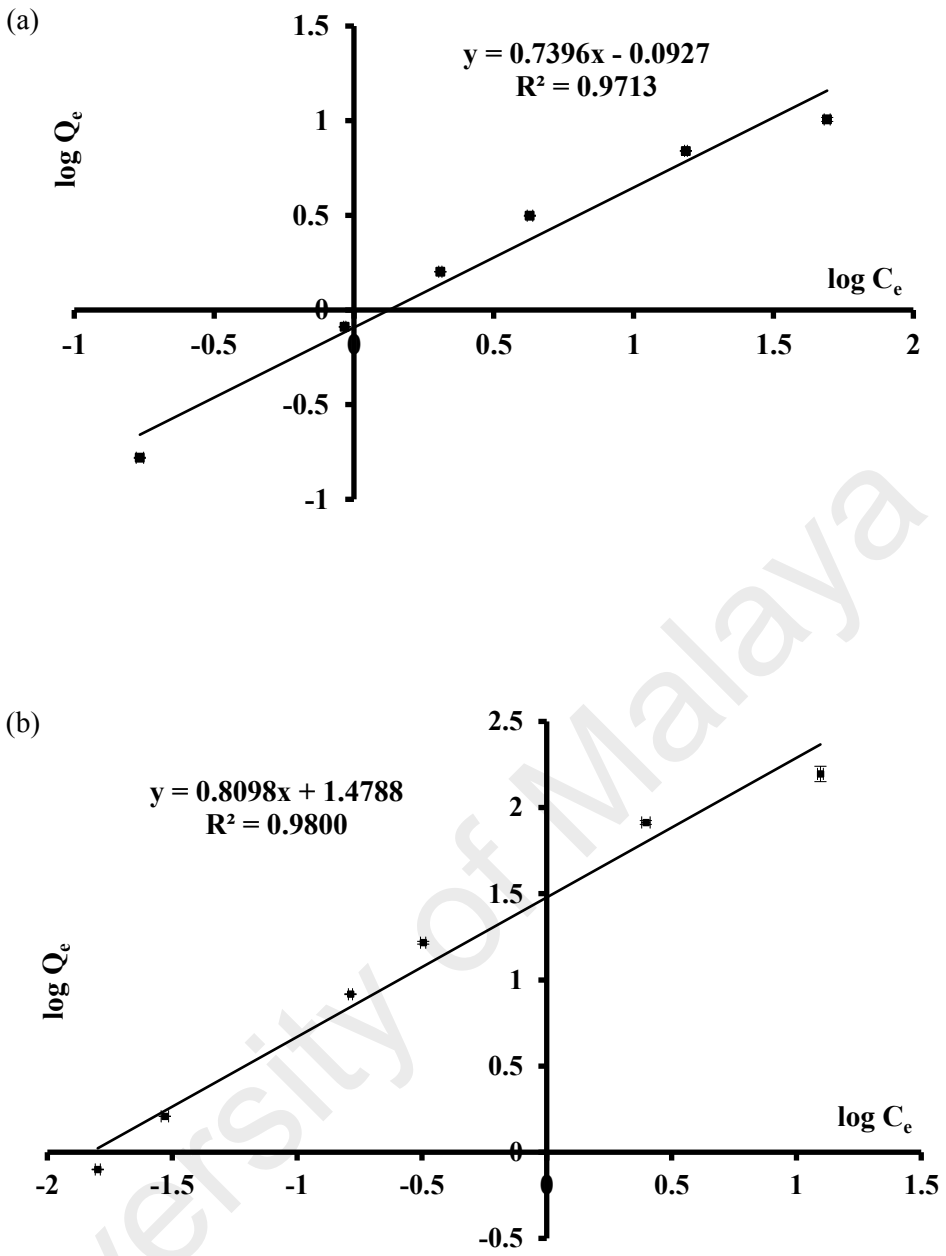

Figure 4.28: Linearized adsorption isotherm Freundlich Model for Hg^{2+} adsorption on (a) SG-ODPPNE and (b) ODPPNE@MNP.

Table 4.6: Adsorption isotherm parameter of (a) Langmuir and (b) Freundlich model.

(a)

Parameter	Langmuir model	
	SG-ODPPNE	**ODPPNE@MNP**
Q_m (mg/g)	13.5135	185.1852
B_L (L/mg)	0.06926	0.2903
R_L	0.14-0.94	0.033-0.87
R^2	0.9993	0.9988
χ^2	0.0139	0.1891

(b)

Parameter	Freundlich model	
	SG-ODPPNE	**ODPPNE@MNP**
B_F (L/mg)	0.8078	30.1162
$1/n$	0.7396	0.8098
n	1.3521	1.2349
R^2	0.9713	0.9800
χ^2	1.6830	33.9432

4.6 Kinetics study

Adsorption kinetics study was carried out to further determine the mechanism of the adsorption of Hg^{2+} by SG-ODPPNE and MNP@ODPPNE. This study was performed by fitting the obtained data to several kinetic models (Wu et al., 2014). In this study, the data were fitted into pseudo-first order, pseudo-second order and intra particle diffusion models.

4.6.1 Pseudo-first order and Pseudo-second order Model

In the past four decades, Pseudo-first order model has been widely used to study the kinetics of the adsorption of pollutants from aqueous solution by various adsorbents such as peat, organobentonite, chitosan, etc. (Cheung et al., 2007; Ho, 2006; Yan et al., 2015). This model describes the adsorption process in the absent of sorbate-sorbate interaction (Kumar, 2006). In this study the sorbate is referring to Hg^{2+}. The linearized equation of pseudo-first order is presented as follows (Equation 4.7) (Ho, 2006):

$$\log(Q_e - Q_t) = \log Q_e - \frac{k_1}{2.303} t \qquad \text{Equation 4.7}$$

where Q_t (mg/g) is the amount of adsorbed adsorbate at time t and k_1 represents the pseudo-first order rate constant.

The data from adsorption of Hg^{2+} by SG-ODPPNE were found to be well fitted at the early stages of the adsorption process (Figure 4.29a) due to the absent of sorbate-sorbate interaction on SG-ODPPNE (Kumar, 2006). However, the linear slope was deviated after 60 min of adsorption time and suggested that pseudo-first order model was inapplicable to describe the entire adsorption process due to the sorbate-sorbate interaction that occurred after 60 min (Ho and MacKay, 1998). On the other hand, the data obtained from adsorption of Hg^{2+} by ODPPNE@MNP was not fitted well to this

model where the poor value of R^2 (0.5275) was obtained (Figure 4.29b). This result further indicates the presence of strong sorbate-sorbate interaction.

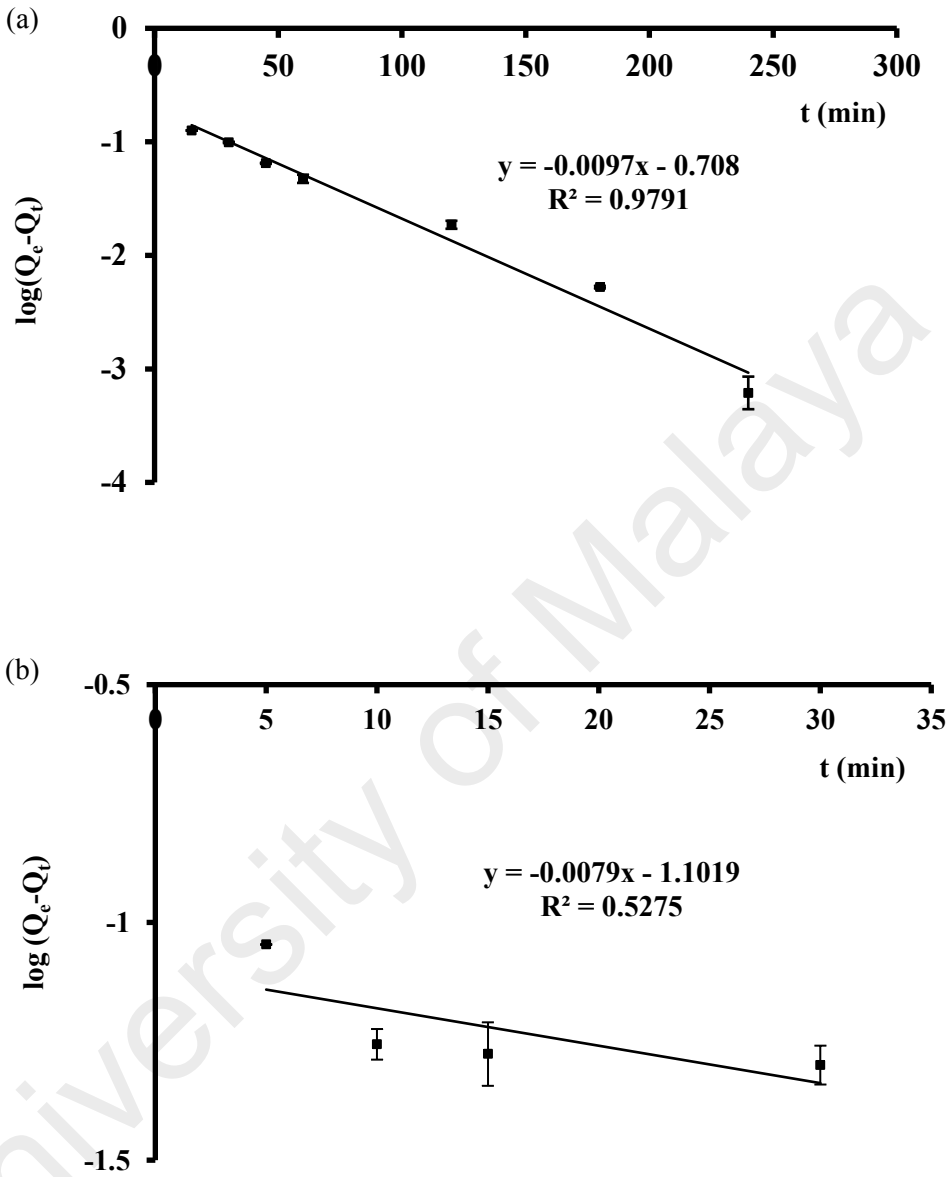

Figure 4.29: Pseudo-first order model for the adsorption of Hg^{2+} on (a) SG-ODPPNE and (b) ODPPNE@MNP.

To further evaluate the kinetics of adsorption process, the experiment data were fitted into pseudo-second order model. Pseudo-second order model describes the chemisorption between sorbate and adsorbent, which involved sharing or transfer of valence electron (Ho, 2006). The pseudo-second order equation is described by equation 4.8:

$$\frac{t}{Q_t} = \frac{t}{Q_e} + \frac{1}{k_2 {Q_e}^2} \qquad \text{Equation 4.8}$$

where Q_t (mg/g) is the amount of adsorbed adsorbate at time t and k_2 is the pseudo-second order rate constant which can be determined from the intercept of graph t/Q_t versus t.

According to Table 4.7 and Figure 4.30, the R^2 values (0.9953 and 1) obtained from pseudo-second order plot of SG-ODPPNE and ODPPNE@MNP was found to be higher than that of pseudo-first order. This result suggested that the pseudo-second order model was the better model to describe the kinetics of the sorption process in this study. Therefore, it can be concluded that the adsorption of Hg^{2+} by SG-ODPPNE and ODPPNE@MNP was a chemisorption process which involved complexation reaction between ODPPNE and Hg^{2+}.

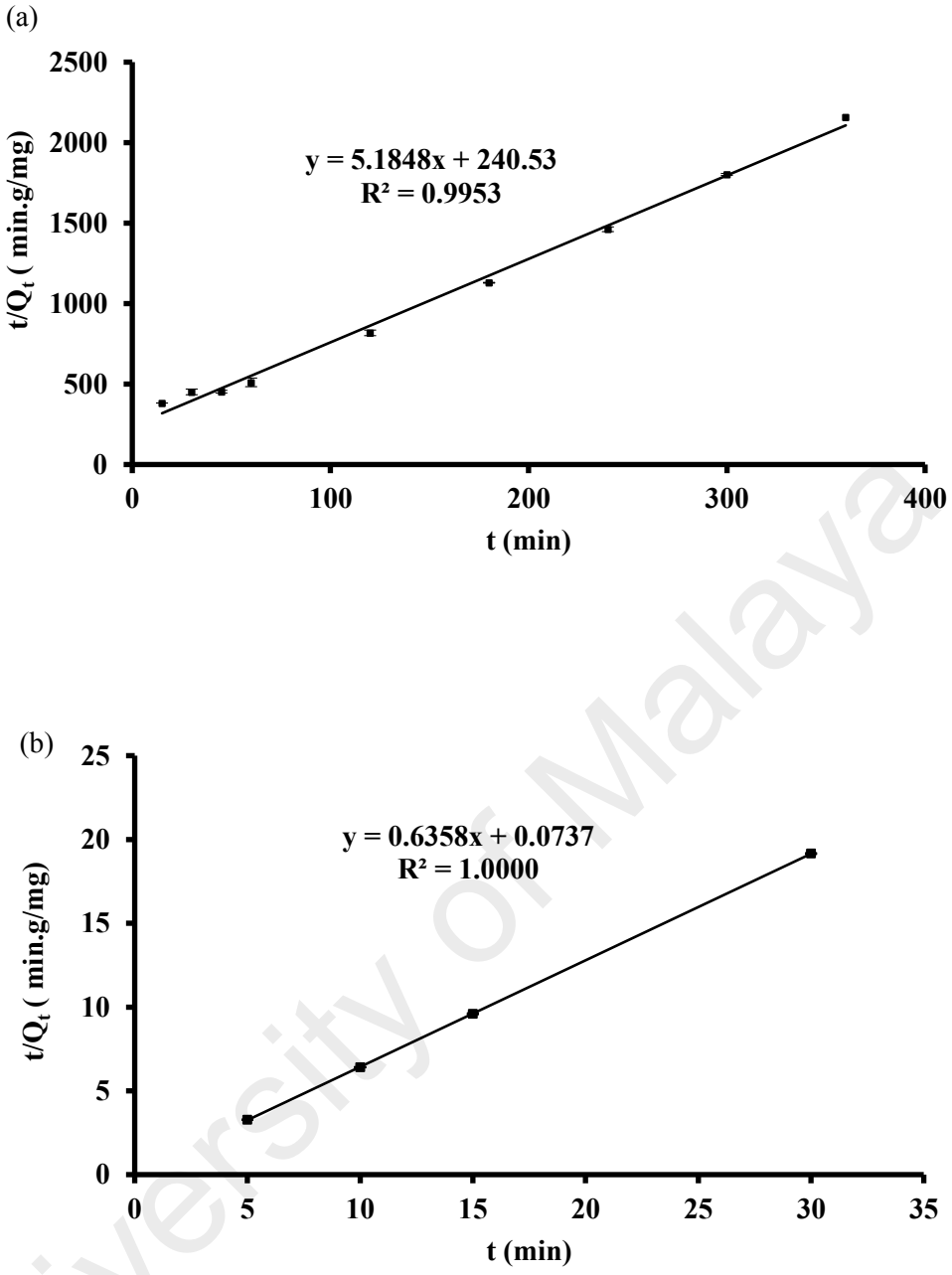

Figure 4.30: Pseudo-second order model for the adsorption of Hg^{2+} on (a) SG-ODPPNE and (b) ODPPNE@MNP.

Table 4.7: Kinetic study parameter of (a) Pseudo-first order and (b) Pseudo-second order.

(a)

Parameter	Pseudo-first order model	
	SG-ODPPNE	**ODPPNE@MNP**
$Q_{e,cal}$ *(mg/g)*	0.1653	1.6163
$Q_{e,exp}$ *(mg/g)*	0.1959	0.0791
k_1 *(min^{-1})*	0.0244	0.0182
R^2	0.9791	0.5275

(b)

Parameter	Pseudo-second order model	
	SG-ODPPNE	**ODPPNE@MNP**
$Q_{e,cal}$ *(mg/g)*	0.1653	1.6163
$Q_{e,exp}$ *(mg/g)*	0.1929	1.5728
k_2 *(min.g)/mg*	0.1118	5.4850
R^2	0.9953	1.0000

4.6.2 Intra-particle diffusion and Boyd model

In general, solid-liquid adsorption process involves three stages (Wen et al., 2015). The first stage is the film diffusion of sorbate through the bulk phase to the surface of the adsorbent. The second step involves the gradual adsorption or intra-particle diffusion of sorbate. The final stage is related to the equilibrium stage. In this study, the Weber and Morris intra-particle diffusion model was used to predict the rate of determining step of the adsorption process (Wen et al., 2015). This model can be described by Equation 4.9:

$$Q_t = k_{id}\sqrt{t} + C_{id} \qquad \text{Equation 4.9}$$

where k_{id} is the intra-particle diffusion rate constant, and C_{id} is a constant related to the thickness of the boundary layer. If the graph of Q_t versus $\sqrt{(t)}$ is linear and pass through the origin, it indicates the intra-particle diffusion step is the only rate-determining step for entire adsorption process. Otherwise, multi-linear slope indicates that transportation stage and equilibrium stage may also control the adsorption process (Cheung et al., 2007).

According to Figure 4.31a, three linear portions were observed for Q_t versus $\sqrt{(t)}$ curve of SG-ODPPNE. The first slope represents the mechanism where Hg^{2+} was transported from aqueous solution to the external surface of the adsorbent. The second slope denotes the gradual adsorption of Hg^{2+} onto SG-ODPPNE. The final part of the linear slope represents the equilibrium stage. At this final stage, diffusion rate was slow down due to the low concentration of Hg^{2+}. For the adsorption of Hg^{2+} by ODPPNE@MNP, the intra-particle diffusion curve (Figure 4.31b) showed two linear portions only. This observation also has been reported by other studies (Mahmound, 2015; Nethaji et al., 2013). The first slope in this graph was corresponded to the external mass transport of Hg^{2+} to external surface of ODPPNE@MNP. The second portion of the slope represented the gradual adsorption of Hg^{2+} onto ODPPNE@MNP via intra-particle diffusion.

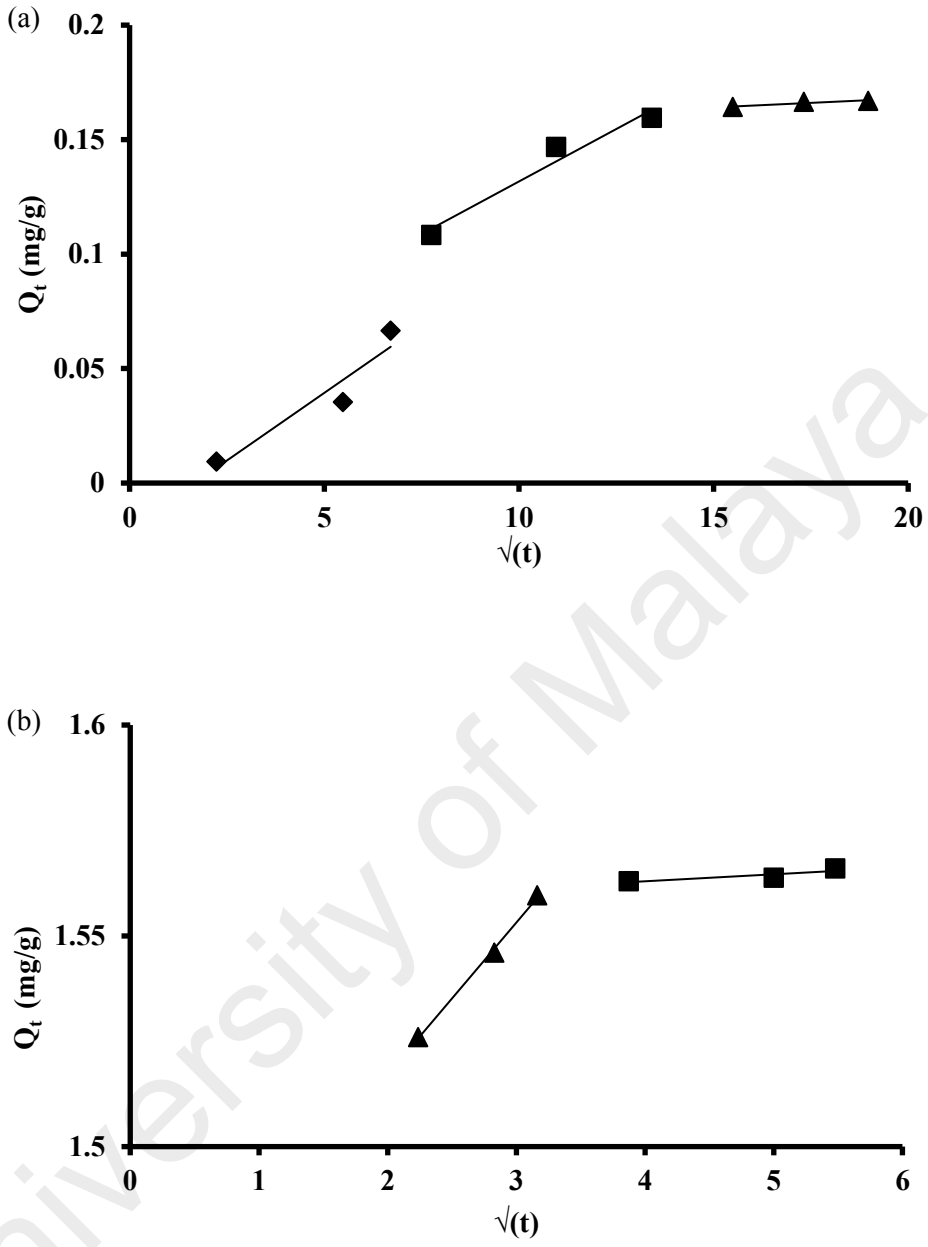

Figure 4.31: The intra-particle diffusion model for the adsorption of Hg^{2+} on (a) SG-ODPPNE and (b) ODPPNE@MNP.

The multi-linear slope obtained from this kinetic study indicated that the entire adsorption process of Hg^{2+} onto SG-ODPPNE and ODPPNE@MNP was controlled by two or more mechanisms involved. However, there was only one rate-determining step that exists in the particular time range as described by Cheung et al. (2007). Since the equilibrium stages are fast and it can consider as not the determining step (Karthikeyan et al., 2010). Therefore, the kinetic data were further analysed with Boyd model to distinguished either film diffusion or intra-particle diffusion stages was the main rate-determining step of this adsorption process, (Gusain et al., 2014). The Boyd model can be described by the Equation 4.10 (Kumar et al., 2005):

$$F = 1 - \left(\frac{6}{\pi^2}\right)\exp[-Bt] \qquad \text{Equation 4.10}$$

$$F = \frac{Q_t}{Q_e} \qquad \text{Equation 4.11}$$

where F is the fraction of Hg^{2+} adsorbed at different time t and Bt is a mathematical function of F. By substituting Equation 4.10 into Equation 4.11, the kinetic expression can be written as:

$$Bt = -0.4977 - \ln(1 - F) \qquad \text{Equation 4.12}$$

Therefore, the Bt value was calculated from Equation 4.12, and the Boyd plot was obtained by plotting the graph Bt against t. If the slope of this graph is a straight line that passes through the origin, the intraparticle diffusion stages were the rate-determining step otherwise the reaction was governed by film diffusion stage (Mohan and Singh, 2002). According to Boyd plot presented in Figure 4.32, the slope obtained was not pass through the origin for both SG-ODPPNE and ODPPNE@MNP. This result indicated that film diffusion stage was the rate-determining step in both adsorption processes.

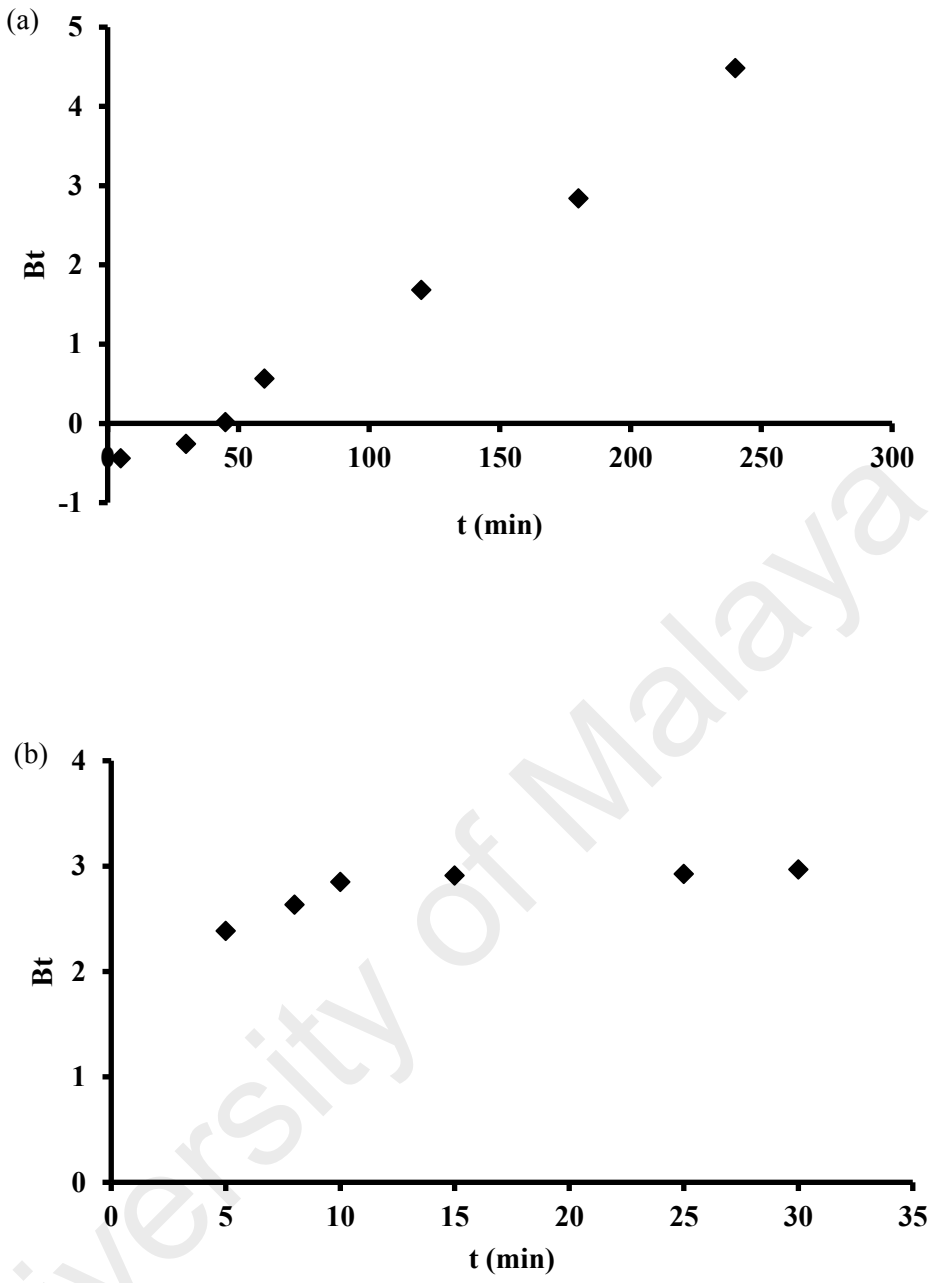

Figure 4.32: Boyd plot for the adsorption of Hg^{2+} on (a) SG-ODPPNE and (b) ODPPNE@MNP.

CHAPTER 5: CONCLUSIONS AND FUTURE WORK

5.1 Conclusions

In this study, the chalcone was chemically modified to obtain dithiocarbamate derivative (ODPPNE). The synthesized ODPPNE was incorporated into the sol-gel matrix to form SG-ODPPNE as the adsorbent. The result showed that the efficiency and selectivity of Hg^{2+} removal were largely enhanced by modifying the chalcone into dithiocarbamate derivative. The adsorption of Hg^{2+} was studied in batch mode under different experimental conditions. The result showed that the efficiency of the Hg^{2+} adsorption process depends on the size of adsorbent, pH of the solution, contact time, the concentration of Hg^{2+} and the SG-ODPPNE dosage. By applying the optimized condition, 80% of Hg^{2+} was successfully removed from aqueous solution by using SG-ODPPNE as the adsorbent. The removal efficiency of Hg^{2+} by SG-ODPPNE was not significantly influenced by the matrices effect of the real water samples.

ODPPNE incorporated silica gel was also coated on the surface of the magnetic nanoparticle (MNP) to demonstrate the application of this hybrid material, ODPPNE@MNP, in the pre-concentration of Hg^{2+} in water. By using this method of preparation, the synthesize route of ligand modified adsorbent was simplified, and the chemical usage was minimized. The ODPPNE@MNP was used as the adsorbent for the pre-concentration process to determine the trace amount of Hg^{2+} in the water sample. Under optimize condition, an effective method was developed by employing ODPPNE@MNP as the solid adsorbent for aqueous Hg^{2+} in D-μSPE process. This D-μSPE method with low method detection limit (4 ng/L), wide linearity (50-5000 ng/L), high pre-concentration factor (100) and good repeatability (4.5-6.5 %) was successfully demonstrated. The applicability of the developed method in the analysis of Hg^{2+} was evaluated by using three real water samples (drinking water, tap water, and surface water). The determination of Hg^{2+} in drinking water, tap water and surface water by the

developed method achieved the recovery efficiency of 90.1 to 99.0 % with the intraday and interday relative standard deviation of 0.7-8.8 % and 1.1-7.7 %, respectively.

The adsorption of Hg^{2+} by SG-ODPPNE and ODPPNE@MNP was found to obey the Langmuir model which suggested the presence of monolayer adsorption. The kinetics study showed that the adsorption of Hg^{2+} by SG-ODPPNE and ODPPNE@MNP was found to follow the pseudo-second-order model which implies the presence of chemisorption process. The mechanisms involved in adsorption process were film diffusion, intra-particle diffusion, and equilibrium stage. It was also found that the intra-particle diffusion step was not the only rate-determining step in this adsorption process. The kinetic data were further analysed by Boyd model to distinguish either film diffusion, or intra-particle diffusion was governing the overall adsorption reaction. The Boyd plot indicated that overall adsorption process of Hg^{2+} by SG-ODPPNE and ODPPNE@MNP was governed by the film diffusion stage.

5.2 Future works

In future, several research works, which are the extension of the current study, can be carried out. First, the natural product with metal capturing ability such as curcumin, quercetin, rutin, and morin can be incorporated into silica gel matrix to generate the effective adsorbent for metal ions. Secondly, some of these natural products with similar structure with chalcone such as curcumin can be further modified into dithiocarbamate derivative to produce the selective and effective adsorbent for Hg^{2+} removal and pre-concentration of trace Hg^{2+} in the water sample.

REFERENCES

Abas, S. N. A., Ismail, M. H. S., Kamal, M. L., & Izhar, S. (2013). Adsorption process of heavy metals by low cost adsorbent: A review. *World Applied Sciences Journal, 28*, 1518-1530.

Abbaspour, N., Hurrell, R., & Kelishadi, R. (2014). Review on iron and its importance for human health. *Journal of Research in Medical Sciences: The Official Journal of Isfahan University of Medical Sciences, 19*, 164-174

Abdolmohammad-Zadeh, H., & Talleb, Z. (2012). Dispersive solid phase micro-extraction of dopamine from human serum using a nano-structured Ni-Al layered double hydroxide, and its direct determination by spectrofluorometry. *Microchimica Acta, 179*, 25-32.

Abolhasani, J., Khanmiri, R. H., Babazadeh, M., Ghorbani-Kalhor, E., Edjlali, L., & Hassanpour, A. (2015). Determination of Hg (II) ions in sea food samples after extraction and preconcentration by novel Fe_3O_4@ SiO_2@ polythiophene magnetic nanocomposite. *Environmental Monitoring and Assessment, 187*, 554.

Abu-Eishah, S. I. (2008). Removal of Zn, Cd, and Pb ions from water by Sarooj clay. *Applied Clay Science, 42*, 201-205.

Adjei-Kyereme, Y., Donkor, A. K., Golow, A. A., Yeboah, P. O., & Pwamang, J. (2015). Mercury concentrations in water and sediments in rivers impacted by artisanal gold mining in the Asutifi district, Ghana. *Research Journal of Chemical and Environmental Sciences, 3*, 40-48.

Adlnasab, L., Ebrahimzadeh, H., Asgharinezhad, A. A., Aghdam, M. N., Dehghani, A., & Esmaeilpour, S. (2014). A preconcentration procedure for determination of ultra-trace mercury (II) in environmental samples employing continuous-flow cold vapor atomic absorption spectrometry. *Food Analytical Methods, 7*, 616-628.

Aguado, J., Arsuaga, J. M., & Arencibia, A. (2005). Adsorption of aqueous mercury (II) on propylthiol-functionalized mesoporous silica obtained by cocondensation. *Industrial & Engineering Chemistry Research, 44*, 3665-3671.

Aksöz, B. E., & Ertan, R. (2012). Spectral properties of chalcones II. *Fabad Journal of Pharmaceutical Sciences, 37*, 205-216.

Ali, A. S. M., Razak, N. A., & Ab Rahman, I. (2012). Study on the preparation of a sol-gel sorbent based thiosemicarbazone for selective removal of heavy metal ions. *World Applied Sciences Journal, 16*, 1040-1047.

Alonso, E. V., Guerrero, M. L., Cueto, P. C., Benítez, J. B., Pavón, J. M. C., & de Torres, A. G. (2016). Development of an on-line solid phase extraction method based on new functionalized magnetic nanoparticles. Use in the determination of mercury in biological and sea-water samples. *Talanta, 153*, 228-239.

Ambu, S., Yong, S. F. Y., Lim, Y. A. L., Wah, M. J., Chen, D. K. F., Ooi, S. S., ... & Nyanachendram, D. (2014). The chemical, heavy metal and microbial quality of well water in an urbanised village in the Klang Valley. *International e-Journal of Science, Medicine & Education, 8*, 28-44.

Amuda, O. S., & Amoo, I. A. (2007). Coagulation/flocculation process and sludge conditioning in beverage industrial wastewater treatment. *Journal of Hazardous Materials, 141*, 778-783.

Anand, P., Kunnumakkara, A. B., Newman, R. A., & Aggarwal, B. B. (2007). Bioavailability of curcumin: problems and promises. *Molecular Pharmaceutics, 4*, 807-818.

Anastassiades, M., Lehotay, S. J., Štajnbaher, D., & Schenck, F. J. (2003). Fast and easy multiresidue method employing acetonitrile extraction/partitioning and "dispersive solid-phase extraction" for the determination of pesticide residues in produce. *Journal of AOAC International, 86*, 412-431.

Antochshuk, V., Olkhovyk, O., Jaroniec, M., Park, I. S., & Ryoo, R. (2003). Benzoylthiourea-modified mesoporous silica for mercury (II) removal. *Langmuir*, *19,* 3031-3034.

Arbabi, M., & Golshani, N. (2016). Removal of copper ions Cu (II) from industrial wastewater. *International Journal of Epidemiologic Research, 3*, 283-293.

Arcibar-Orozco, J. A., Rangel-Mendez, J. R., & Diaz-Flores, P. E. (2015). Simultaneous adsorption of Pb (II)-Cd (II), Pb (II)-phenol, and Cd (II)-phenol by activated carbon cloth in aqueous solution. *Water, Air, & Soil Pollution, 226*, 2197.

Asghari, A., Arghavani-Beydokhti, S., & Rajabi, M. (2016). Solid phase extraction of heavy metal ions in environmental samples on chemically bonded single-walled carbon nanotubes with 2-((3-silylpropylimino) methyl) phenol. *Journal of Applied Chemistry, 10*, 107-120.

Asgharinezhad, A. A., & Ebrahimzadeh, H. (2016). A simple and fast method based on mixed hemimicelles coated magnetite nanoparticles for simultaneous extraction of acidic and basic pollutants. *Analytical and Bioanalytical Chemistry, 408*, 473-486.

Asgharinezhad, A. A., Ebrahimzadeh, H., Mirbabaei, F., Mollazadeh, N., & Shekari, N. (2014). Dispersive micro-solid-phase extraction of benzodiazepines from biological fluids based on polyaniline/magnetic nanoparticles composite. *Analytica Chimica Acta, 844*, 80-89.

Avigliano, E., Schenone, N. F., Volpedo, A. V., Goessler, W., & Cirelli, A. F. (2015). Heavy metals and trace elements in muscle of silverside (Odontesthes bonariensis) and water from different environments (Argentina): aquatic pollution and consumption effect approach. *Science of the Total Environment, 506*, 102-108.

Bahadir, Z., Bulut, V. N., Hidalgo, M., Soylak, M., & Marguí, E. (2015). Determination of trace amounts of hexavalent chromium in drinking waters by dispersive microsolid-phase extraction using modified multiwalled carbon nanotubes combined with total reflection X-ray fluorescence spectrometry. *Spectrochimica Acta Part B: Atomic Spectroscopy, 107*, 170-177.

Bai, L., Hu, H., Fu, W., Wan, J., Cheng, X., Zhuge, L., ... & Chen, Q. (2011). Synthesis of a novel silica-supported dithiocarbamate adsorbent and its properties for the removal of heavy metal ions. *Journal of Hazardous Materials, 195*, 261-275.

Baig, R. N., Nadagouda, M. N., & Varma, R. S. (2014). Carbon-coated magnetic palladium: applications in partial oxidation of alcohols and coupling reactions. *Green Chemistry, 16*, 4333-4338.

Banaei, A., Vojoudi, H., Karimi, S., Bahar, S., & Pourbasheer, E. (2015). Synthesis and characterization of new modified silica coated magnetite nanoparticles with bisaldehyde as selective adsorbents of Ag (I) from aqueous samples. *RSC Advances, 5*, 83304-83313.

Barakat, M. A. (2011). New trends in removing heavy metals from industrial wastewater. *Arabian Journal of Chemistry, 4*, 361-377.

Bari, F., Begum, N., Jamaludin, S. B., & Hussin, K. (2009). Extraction and separation of Cu (II), Ni (II) and Zn (II) by sol–gel silica immobilized with Cyanex 272. *Hydrometallurgy, 96*, 140-147.

Bazrafshan, E., Moein, H., Kord Mostafapour, F., & Nakhaie, S. (2012). Application of electrocoagulation process for dairy wastewater treatment. *Journal of Chemistry, 2013*, 1-8.

Behalo, M. S., & Aly, A. A. (2010). Facile, Three-Component Synthesis of Dithiocarbamate Derivatives with Potent Antimicrobial Activity. *Phosphorus, Sulfur, and Silicon and The Related Elements, 185*, 2194-2200.

Beiraghi, A., Pourghazi, K., & Amoli-Diva, M. (2014). Thiodiethanethiol modified silica coated magnetic nanoparticles for preconcentration and determination of ultratrace amounts of mercury, lead, and cadmium in environmental and food samples. *Analytical Letters, 47*, 1210-1223.

Bessbousse, H., Rhlalou, T., Verchère, J. F., & Lebrun, L. (2010). Mercury removal from wastewater using a poly (vinylalcohol)/poly (vinylimidazole) complexing membrane. *Chemical Engineering Journal, 164*, 37-48.

Bhattacharyya, A., Basu, S., & Dutta, S. (2013). Reclamation of wastes for mercury removal-A review. In Grohens, Y., Kumar, S. K., Boudenne, A., & Weimin, Y. (Eds.), *Recycling and Reuse of Materials and Their Products* (pp. 155-178). Oakville, Ontario: Apple Academic Press.

Blue, L. Y., Van Aelstyn, M. A., Matlock, M., & Atwood, D. A. (2008). Low-level mercury removal from groundwater using a synthetic chelating ligand. *Water Research, 42*, 2025-2028.

Bost, M., Houdart, S., Oberli, M., Kalonji, E., Huneau, J. F., & Margaritis, I. (2016). Dietary copper and human health: Current evidence and unresolved issues. *Journal of Trace Elements in Medicine and Biology, 35*, 107-115.

Bridges, C. C., & Zalups, R. K. (2010). Transport of inorganic mercury and methylmercury in target tissues and organs. *Journal of Toxicology and Environmental Health, Part B, 13*, 385-410.

Brinker, C. J., & Scherer, G. W. (2013). *Sol-gel science: the physics and chemistry of sol-gel processing*. San Diego, California: Academic Press Inc.

Bumb, A., Brechbiel, M. W., Choyke, P. L., Fugger, L., Eggeman, A., Prabhakaran, D., ... & Dobson, P. J. (2008). Synthesis and characterization of ultra-small superparamagnetic iron oxide nanoparticles thinly coated with silica. *Nanotechnology, 19*, 335601.

Cestari, A. R., & Airoldi, C. (1997). Chemisorption on thiol–silicas: divalent cations as a function of pH and primary amines on thiol–mercury adsorbed. *Journal of Colloid and Interface Science, 195*, 338-342.

Chandra, V., & Kim, K. S. (2011). Highly selective adsorption of Hg^{2+} by a polypyrrole–reduced graphene oxide composite. *Chemical Communications, 47*, 3942-3944.

Cheung, W. H., Szeto, Y. S., & McKay, G. (2007). Intraparticle diffusion processes during acid dye adsorption onto chitosan. *Bioresource Technology, 98*, 2897-2904.

Ciriminna, R., Fidalgo, A., Pandarus, V., Béland, F., Ilharco, L. M., & Pagliaro, M. (2013). The sol–gel route to advanced silica-based materials and recent applications. *Chemical Reviews, 113*, 6592-6620.

Costa, C. C., Melo, D. M. A., Melo, M. A. F., Mendoza, M. E., Nascimento, J. C., Andrade, J. M., & Barros, J. M. F. (2014). Effects of different structure-directing agents (SDA) in MCM-41 on the adsorption of CO_2. *Journal of Porous Materials, 21*, 1069-1077.

Cui, Y., Liu, S., Wei, K., Liu, Y., & Hu, Z. (2015). Magnetic solid-phase extraction of trace-level mercury (II) ions using magnetic core-shell nanoparticles modified with thiourea-derived chelating agents. *Microchimica Acta, 182*, 1337-1344.

Da'na, E., & Sayari, A. (2011). Adsorption of copper on amine-functionalized SBA-15 prepared by co-condensation: equilibrium properties. *Chemical Engineering Journal, 166*, 445-453.

Dag, Ö., Yoshina-Ishii, C., Asefa, T., MacLachlan, M. J., Grondey, H., Coombs, N., & Ozin, G. A. (2001). Oriented periodic mesoporous organosilica (PMO) film with organic functionality inside the channel walls. *Advanced Functional Materials, 11*, 213-217.

Daniel, R., & Kawasaki, N. (2016). The distribution of heavy metals and nutrients along Selangor River and its adjacent mining ponds, Malaysia. *International Journal of Advances in Agricultural & Environmental Engineering, 3*, 241-244

Danks, A. E., Hall, S. R., & Schnepp, Z. (2016). The evolution of 'sol–gel'chemistry as a technique for materials synthesis. *Materials Horizons, 3*, 91-112.

Denizli, A., Kesenci, K., Arica, Y., & Pişkin, E. (2000). Dithiocarbamate-incorporated monosize polystyrene microspheres for selective removal of mercury ions. *Reactive and Functional Polymers, 44*, 235-243.

Dimitriev, Y., Ivanova, Y., & Iordanova, R. (2008). History of sol-gel science and technology. *Journal of the University of Chemical technology and Metallurgy, 43*, 181-192.

Ding, Y., Ding, C., Ye, N., Liu, Z., Wold, E. A., Chen, H., ... & Zhou, J. (2016). Discovery and development of natural product oridonin-inspired anticancer agents. *European Journal of Medicinal Chemistry, 122*, 102-117.

Dolatabadi, J. E. N., Mokhtarzadeh, A., Ghareghoran, S. M., & Dehghan, G. (2014). Synthesis, characterization and antioxidant property of quercetin-Tb (III) complex. *Advanced Pharmaceutical Bulletin, 4*, 101-104.

Dong, C., Zhang, F., Pang, Z., & Yang, G. (2016). Efficient and selective adsorption of multi-metal ions using sulfonated cellulose as adsorbent. *Carbohydrate Polymers, 151*, 230-236.

Ebadian, M. A. (2001). *Mercury contaminated material decontamination methods: investigation and assessment* (HCET-2000-D053-002-04). Pittsburgh, PA: National Energy Technology Lab.

Es' haghi, Z., Bardajee, G. R., & Azimi, S. (2016). Magnetic dispersive micro solid-phase extraction for trace mercury pre-concentration and determination in water, hemodialysis solution and fish samples. *Microchemical Journal, 127*, 170-177.

Esmaeili Bidhendi, M., Nabi Bidhendi, G. R., Mehrdadi, N., & Rashedi, H. (2014). Modified Mesoporous Silica (SBA–15) with Trithiane as a new effective adsorbent for mercury ions removal from aqueous environment. *Journal of Environmental Health Science and Engineering, 12*, 100.

Evangelista, S. M., DeOliveira, E., Castro, G. R., Zara, L. F., & Prado, A. G. (2007). Hexagonal mesoporous silica modified with 2-mercaptothiazoline for removing mercury from water solution. *Surface Science, 601*, 2194-2202.

Fan, H. T., Sun, W., Jiang, B., Wang, Q. J., Li, D. W., Huang, C. C., ... & Li, W. X. (2016). Adsorption of antimony (III) from aqueous solution by mercapto-functionalized silica-supported organic–inorganic hybrid sorbent: Mechanism insights. *Chemical Engineering Journal, 286*, 128-138.

Feist, B. (2016). Selective dispersive micro solid-phase extraction using oxidized multiwalled carbon nanotubes modified with 1, 10-phenanthroline for preconcentration of lead ions. *Food Chemistry, 209*, 37-42.

Fenech, M. (2001). The role of folic acid and Vitamin B12 in genomic stability of human cells. *Mutation Research/Fundamental and Molecular Mechanisms of Mutagenesis, 475*, 57-67.

Ferniza-García, F., Amaya-Chávez, A., Roa-Morales, G., & Barrera-Díaz, C. E. (2017). Removal of Pb, Cu, Cd, and Zn Present in Aqueous Solution Using Coupled Electrocoagulation-Phytoremediation Treatment. *International Journal of Electrochemistry, 2017*, 7681451.

Figueira, P., Lopes, C. B., Daniel-da-Silva, A. L., Pereira, E., Duarte, A. C., & Trindade, T. (2011). Removal of mercury (II) by dithiocarbamate surface functionalized magnetite particles: application to synthetic and natural spiked waters. *Water Research, 45*, 5773-5784.

Folens, K., Huysman, S., Van Hulle, S., & Du Laing, G. (2017). Chemical and economic optimization of the coagulation-flocculation process for silver removal and recovery from industrial wastewater. *Separation and Purification Technology, 179*, 145-151.

Foo, K., & Hameed, B. H. (2010). Insights into the modeling of adsorption isotherm systems. *Chemical Engineering Journal, 156*, 2-10.

Fu, F., & Wang, Q. (2011). Removal of heavy metal ions from wastewaters: A review. *Journal of Environmental Management, 92*, 407-418.

Furia, E., Marino, T., & Russo, N. (2014). Insights into the coordination mode of quercetin with the Al (III) ion from a combined experimental and theoretical study. *Dalton Transactions, 43*, 7269-7274.

Ghazaghi, M., Mousavi, H. Z., Rashidi, A. M., Shirkhanloo, H., & Rahighi, R. (2016). Innovative separation and preconcentration technique of coagulating homogenous dispersive micro solid phase extraction exploiting graphene oxide nanosheets. *Analytica Chimica Acta, 902*, 33-42.

Ghorbani, M., Lashkenari, M. S., & Eisazadeh, H. (2011). Application of polyaniline nanocomposite coated on rice husk ash for removal of Hg(II) from aqueous media. *Synthetic Metals, 161*, 1430-1433.

Ghouila, H., Meksi, N., Haddar, W., Mhenni, M. F., & Jannet, H. B. (2012). Extraction, identification and dyeing studies of Isosalipurposide, a natural chalcone dye from Acacia cyanophylla flowers on wool. *Industrial Crops and Products, 35*, 31-36.

Giakisikli, G., & Anthemidis, A. N. (2013). Magnetic materials as sorbents for metal/metalloid preconcentration and/or separation. A review. *Analytica Chimica Acta, 789*, 1-16.

Gilmour, C. C., Podar, M., Bullock, A. L., Graham, A. M., Brown, S. D., Somenahally, A. C., ... & Elias, D. A. (2013). Mercury methylation by novel microorganisms from new environments. *Environmental Science & Technology, 47*, 11810-11820.

Girginova, P. I., Daniel-da-Silva, A. L., Lopes, C. B., Figueira, P., Otero, M., Amaral, V. S., ... & Trindade, T. (2010). Silica coated magnetite particles for magnetic removal of Hg^{2+} from water. *Journal of Colloid and Interface Science, 345*, 234-240.

Goher, M. E., Hassan, A. M., Abdel-Moniem, I. A., Fahmy, A. H., & El-sayed, S. M. (2014). Evaluation of surface water quality and heavy metal indices of Ismailia Canal, Nile River, Egypt. *The Egyptian Journal of Aquatic Research, 40*, 225-233.

Guo, X., Feng, Y., Ma, L., Gao, D., Jing, J., Yu, J., ... & Zhang, Y. (2017). Phosphoryl functionalized mesoporous silica for uranium adsorption. *Applied Surface Science, 402*, 53-60.

Gusain, D., Bux, F., & Sharma, Y. C. (2014). Abatement of chromium by adsorption on nanocrystalline zirconia using response surface methodology. *Journal of Molecular Liquids, 197*, 131-141.

Gutierrez, F. A., Gonzalez-Dominguez, J. M., Ansón-Casaos, A., Hernández-Ferrer, J., Rubianes, M. D., Martínez, M. T., & Rivas, G. (2017). Single-walled carbon nanotubes covalently functionalized with cysteine: A new alternative for the highly sensitive and selective Cd (II) quantification. *Sensors and Actuators B: Chemical, 249*, 506-514.

Habila, M., Yilmaz, E., ALOthman, Z. A., & Soylak, M. (2014). Flame atomic absorption spectrometric determination of Cd, Pb, and Cu in food samples after pre-concentration using 4-(2-thiazolylazo) resorcinol-modified activated carbon. *Journal of Industrial and Engineering Chemistry, 20*, 3989-3993.

Haitzer, M., Aiken, G. R., & Ryan, J. N. (2002). Binding of mercury (II) to dissolved organic matter: the role of the mercury-to-DOM concentration ratio. *Environmental Science & Technology, 36*, 3564-3570.

Hakizimana, J. N., Gourich, B., Chafi, M., Stiriba, Y., Vial, C., Drogui, P., & Naja, J. (2017). Electrocoagulation process in water treatment: A review of electrocoagulation modeling approaches. *Desalination, 404*, 1-21.

Hashim, N., Muda, Z., Hussein, M. Z., Isa, I. M., Mohamed, A., Kamari, A., ... & Jaafar, A. (2016). A brief review on recent graphene oxide-based material nanocomposites: Synthesis and applications. *Journal of Materials and Environmental Science, 7*, 3225-3243.

He, S., Zhao, C., Yao, P., & Yang, S. (2015). Synthesis of silica-supported multidentate ligands adsorbents for the removal of heavy metal ions. *Environmental Engineering Science, 32*, 593-601

He, S., Zhao, C., Yao, P., & Yang, S. (2016). Chemical modification of silica gel with multidentate ligands for heavy metals removal. *Desalination and Water Treatment, 57*, 1722-1732.

Heard, P. J. (2005). Main group dithiocarbamate complexes. In Karlin, K. D. (Ed), *Progress in Inorganic Chemistry* (pp. 1-69). Hoboken, New Jersey: John Wiley & Sons, Inc.

Heidari, A., Younesi, H., & Mehraban, Z. (2009). Removal of Ni (II), Cd (II), and Pb (II) from a ternary aqueous solution by amino functionalized mesoporous and nano mesoporous silica. *Chemical Engineering Journal, 153*, 70-79.

Hench, L. L., & West, J. K. (1990). The sol-gel process. *Chemical Reviews*, *9*, 33-72.

Henneberry, Y. K., Kraus, T. E., Fleck, J. A., Krabbenhoft, D. P., Bachand, P. M., & Horwath, W. R. (2011). Removal of inorganic mercury and methylmercury from surface waters following coagulation of dissolved organic matter with metal-based salts. *Science of the Total Environment, 409*, 631-637.

Ho, Y. S. (2006). Review of second-order models for adsorption systems. *Journal of Hazardous Materials, 136*, 681-689.

Ho, Y. S., & McKay, G. (1998). The kinetics of sorption of basic dyes from aqueous solution by sphagnum moss peat. *The Canadian Journal of Chemical Engineering, 76*, 822-827.

Hoffmann, F., Cornelius, M., Morell, J., & Fröba, M. (2006). Silica-based mesoporous organic–inorganic hybrid materials. *Angewandte Chemie International Edition, 45*, 3216-3251.

Hong, Y. S., Kim, Y. M., & Lee, K. E. (2012). Methylmercury exposure and health effects. *Journal of Preventive Medicine and Public Health, 45*, 353-363.

Hsieh, C. T., Hsieh, T. J., El-Shazly, M., Chuang, D. W., Tsai, Y. H., Yen, C. T., ... & Chang, F. R. (2012). Synthesis of chalcone derivatives as potential anti-diabetic agents. *Bioorganic & Medicinal Chemistry Letters, 22*, 3912-3915.

Hu, B., He, M., & Chen, B. (2015). Nanometer-sized materials for solid-phase extraction of trace elements. *Analytical and Bioanalytical Chemistry, 407*, 2685-2710.

Huang, X., Chang, X., He, Q., Cui, Y., Zhai, Y., & Jiang, N. (2008). Tris (2-aminoethyl) amine functionalized silica gel for solid-phase extraction and preconcentration of Cr (III), Cd (II) and Pb (II) from waters. *Journal of Hazardous Materials, 157*, 154-160.

Huang, Y., Du, J. R., Zhang, Y., Lawless, D., & Feng, X. (2015). Removal of mercury (II) from wastewater by polyvinylamine-enhanced ultrafiltration. *Separation and Purification Technology, 154*, 1-10.

Huang, Y., Du, J., Zhang, Y., Lawless, D., & Feng, X. (2016). Batch process of polymer-enhanced ultrafiltration to recover mercury (II) from wastewater. *Journal of Membrane Science, 514*, 229-240.

Ikeda, N. E. A., Novak, E. M., Maria, D. A., Velosa, A. S., & Pereira, R. M. S. (2015). Synthesis, characterization and biological evaluation of Rutin–zinc (II) flavonoid-metal complex. *Chemico-biological Interactions, 239*, 184-191.

Islam, M. S., Ahmed, M. K., Raknuzzaman, M., Habibullah-Al-Mamun, M., & Islam, M. K. (2015). Heavy metal pollution in surface water and sediment: a preliminary assessment of an urban river in a developing country. *Ecological Indicators, 48*, 282-291.

Jal, P. K., Patel, S., & Mishra, B. K. (2004). Chemical modification of silica surface by immobilization of functional groups for extractive concentration of metal ions. *Talanta, 62*, 1005-1028.

Jalali, M., & Aliakbar, A. (2015). Synthesis, characterisation and application of mercapto- and polyaminophenol-bifunctionalised MCM-41 for dispersive micro solid phase extraction of Ni (II) prio to inductively coupled plasma-optical emission spectrometry (DMSPE-ICP-OES). *International Journal of Environmental Analytical Chemistry, 95*, 542-555.

Jana, S., Saikia, A., Purkait, M. K., & Mohanty, K. (2011). Chitosan based ceramic ultrafiltration membrane: preparation, characterization and application to remove Hg (II) and As (III) using polymer enhanced ultrafiltration. *Chemical Engineering Journal, 170*, 209-219.

Jiang, X., Cheng, J., Zhou, H., Li, F., Wu, W., & Ding, K. (2015). Polyaniline-coated chitosan-functionalized magnetic nanoparticles: preparation for the extraction and analysis of endocrine-disrupting phenols in environmental water and juice samples. *Talanta, 141*, 239-246.

Johari, K., Saman, N., & Mat, H. (2014). A comparative evaluation of mercury (II) adsorption equilibrium and kinetics onto silica gel and sulfur-functionalised silica gels adsorbents. *The Canadian Journal of Chemical Engineering, 92*, 1048-1058.

Kabay, N., and Bryjak, M. (2013). Hybrid Processes Combining Sorption and Membrane Filtration. In Hoek, E. M. V., & Tarabara V. V. (Eds), *Encyclopedia of Membrane Science and Technology* (pp. 1–21). Hoboken, New Jersey: John Wiley & Sons, Inc.

Kanchi, S., Singh, P., & Bisetty, K. (2014). Dithiocarbamates as hazardous remediation agent: A critical review on progress in environmental chemistry for inorganic species studies of 20 th century. *Arabian Journal of Chemistry, 7*, 11-25.

Karaagac, O., & Kockar, H. (2016). A simple way to obtain high saturation magnetization for superparamagnetic iron oxide nanoparticles synthesized in air atmosphere: Optimization by experimental design. *Journal of Magnetism and Magnetic Materials, 409*, 116-123.

Karaagac, O., Kockar, H., Beyaz, S., & Tanrisever, T. (2010). A simple way to synthesize superparamagnetic iron oxide nanoparticles in air atmosphere: Iron ion concentration effect. *IEEE Transactions on Magnetics, 46*, 3978-3983.

Karri, V. V. S. R., Gowthamarajan, K., Satish Kumar, M., & Rajkumar, M. (2015). Multiple biological actions of curcumin in the management of diabetic foot ulcer complications: A systematic review. *Tropical Medicine & Surgery, 3*, 1000179.

Karthiga, D., Rajeshwari, A., Chakravarty, S., Chandrasekaran, N., & Mukherjee, A. (2016). Determination of mercury (II) ions in aqueous solution using silver nanorods as a probe. *Analytical Methods, 8*, 3756-3762.

Karthikeyan, S., Sivakumar, B., & Sivakumar, N. (2010). Film and pore diffusion modeling for adsorption of Reactive Red 2 from aqueous solution on to activated carbon prepared from bio-diesel industrial waste. *Journal of Chemistry, 7*, S175-S184.

Kavand, M., Kaghazchi, T., & Soleimani, M. (2014). Optimization of parameters for competitive adsorption of heavy metal ions (Pb, Ni, Cd) onto activated carbon. *Korean Journal of Chemical Engineering, 31*, 692-700.

Khan, A., Mahmood, F., Khokhar, M. Y., & Ahmed, S. (2006). Functionalized sol–gel material for extraction of mercury (II). *Reactive and Functional Polymers, 66*, 1014-1020.

Khezeli, T., & Daneshfar, A. (2017). Development of dispersive micro-solid phase extraction based on micro and nano sorbents. *TrAC Trends in Analytical Chemistry, 89*, 99-118.

Khor, S. W., Lee, Y. K., Abas, M. R. B., & Tay, K. S. (2017). Application of chalcone-based dithiocarbamate derivative incorporated sol–gel for the removal of Hg (II) ion from water. *Journal of Sol-Gel Science and Technology, 82*, 834-845.

Khoramzadeh, B., Nasernejad, B., & Halladj. (2013). Mercury biosorption from aqueous solution by Sugarcane Bagasse. *Journal of the Taiwan Institute of Chemical Engineers, 44*, 266-269.

Kocot, K., & Sitko, R. (2014). Trace and ultratrace determination of heavy metal ions by energy-dispersive X-ray fluorescence spectrometry using graphene as solid sorbent in dispersive micro solid-phase extraction. *Spectrochimica Acta Part B: Atomic Spectroscopy, 94*, 7-13.

Kocot, K., Zawisza, B., Marguí, E., Queralt, I., Hidalgo, M., & Sitko, R. (2013). Dispersive micro solid-phase extraction using multiwalled carbon nanotubes combined with portable total-reflection X-ray fluorescence spectrometry for the determination of trace amounts of Pb and Cd in water samples. *Journal of Analytical Atomic Spectrometry, 28*, 736-742.

Krawczyk, M., & Jeszka-Skowron, M. (2016). Multiwalled carbon nanotubes as solid sorbent in dispersive micro solid-phase extraction for the sequential determination of cadmium and lead in water samples. *Microchemical Journal, 126*, 296-301.

Krawczyk, M., & Stanisz, E. (2015). Silver nanoparticles as a solid sorbent in ultrasound-assisted dispersive micro solid-phase extraction for the atomic absorption spectrometric determination of mercury in water samples. *Journal of Analytical Atomic Spectrometry, 30*, 2353-2358.

Krawczyk, M., Akbari, S., Jeszka-Skowron, M., Pajootan, E., & Fard, F. S. (2016). Application of dendrimer modified halloysite nanotubes as a new sorbent for ultrasound-assisted dispersive micro-solid phase extraction and sequential determination of cadmium and lead in water samples. *Journal of Analytical Atomic Spectrometry, 31*, 1505-1514.

Kumar, D., Wu, X., Fu, Q., Ho, J. W. C., Kanhere, P. D., Li, L., & Chen, Z. (2015). Development of durable self-cleaning coatings using organic–inorganic hybrid sol–gel method. *Applied Surface Science, 344*, 205-212.

Kumar, K. V. (2006). Linear and non-linear regression analysis for the sorption kinetics of methylene blue onto activated carbon. *Journal of Hazardous Materials, 137*, 1538-1544.

Kumar, K. V., Ramamurthi, V., & Sivanesan, S. (2005). Modeling the mechanism involved during the sorption of methylene blue onto fly ash. *Journal of Colloid and Interface Science, 284*, 14-21.

Kunzmann, A., Andersson, B., Vogt, C., Feliu, N., Ye, F., Gabrielsson, S., ... & Krug, H. (2011). Efficient internalization of silica-coated iron oxide nanoparticles of different sizes by primary human macrophages and dendritic cells. *Toxicology and Applied Pharmacology, 253*, 81-93.

Kurniawan, T. A., Chan, G. Y., Lo, W. H., & Babel, S. (2006). Physico–chemical treatment techniques for wastewater laden with heavy metals. *Chemical Engineering Journal, 118*, 83-98.

Lambertsson, L. (2005). *Mercury species transformations in marine and biological systems studied by isotope dilution mass spectrometry and stable isotope tracers* (Doctoral dissertation, Umeå University, Sweden). Retrieved from http://www.diva-portal.org/smash/record.jsf?pid=diva2%3A143518&dswid=8036

Lamborg, C. H., Fitzgerald, W. F., Damman, A. W. H., Benoit, J. M., Balcom, P. H., & Engstrom, D. R. (2002). Modern and historic atmospheric mercury fluxes in both hemispheres: global and regional mercury cycling implications. *Global Biogeochemical Cycles, 16*, 51-1-51-11.

Lanciné, G. D., Bamory, K., Raymond, L., Jean-Luc, S., Christelle, B., & Jean, B. (2008). Coagulation-Flocculation treatment of a tropical surface water with alum for dissolved organic matter (DOM) removal: Influence of alum dose and pH adjustment. *Journal of International Environmental Application & Science, 3*, 247-257.

Langford, N. J., & Ferner, R. E. (1999). Toxicity of mercury. *Journal of Human Hypertension, 13*, 651-656.

Lee, S. H., Lee, D. H., Jung, H., Han, Y. S., Kim, T. H., & Yang, W. (2015). Magnetic properties of SiO_2-coated iron oxide nanoparticles studied by polarized small angle neutron scattering. *Current Applied Physics, 15*, 915-919.

Leng, Y., Ye, G., Bai, F., Wei, J., Wang, J., & Chen, J. (2013). Synthesis of new periodic mesoporous organosilica (PMO) incorporated with macrocyclic host for strontium binding. *Materials Letters, 110*, 212-214.

Lewis, A. E. (2010). Review of metal sulphide precipitation. *Hydrometallurgy, 104*, 222-234.

Li, S., Zhang, T., Tang, R., Qiu, H., Wang, C., & Zhou, Z. (2015). Solvothermal synthesis and characterization of monodisperse superparamagnetic iron oxide nanoparticles. *Journal of Magnetism and Magnetic Materials, 379*, 226-231.

Lien, Y. H., & Wu, T. M. (2008). Preparation and characterization of thermosensitive polymers grafted onto silica-coated iron oxide nanoparticles. *Journal of Colloid and Interface Science, 326*, 517-521.

Liu, H., & Li, W. (2011). Dissolved trace elements and heavy metals from the shallow lakes in the middle and lower reaches of the Yangtze River region, China. *Environmental Earth Sciences, 62*, 1503-1511.

López-García, I., Vicente-Martínez, Y., & Hernández-Córdoba, M. (2015). Determination of ultratraces of mercury species using separation with magnetic core-modified silver nanoparticles and electrothermal atomic absorption spectrometry. *Journal of Analytical Atomic Spectrometry, 30*, 1980-1987.

Machida, M., Fotoohi, B., Amamo, Y., & Mercier, L. (2012). Cadmium (II) and lead (II) adsorption onto hetero-atom functional mesoporous silica and activated carbon. *Applied Surface Science, 258*, 7389-7394.

Mahmoud, M. A. (2015). Kinetics and thermodynamics of aluminum oxide nanopowder as adsorbent for Fe (III) from aqueous solution. *Beni-Suef University Journal of Basic and Applied Sciences, 4*, 142-149.

Mahmoud, M. E. (1999). Selective solid phase extraction of mercury (II) by silica gel-immobilized-dithiocarbamate derivatives. *Analytica Chimica Acta, 398*, 297-304.

Mandal, S., Sahu, M. K., & Patel, R. K. (2013). Adsorption studies of arsenic (III) removal from water by zirconium polyacrylamide hybrid material (ZrPACM-43). *Water Resources and Industry, 4*, 51-67.

Mehdinia, A., Jebeliyan, M., Kayyal, T. B., & Jabbari, A. (2017). Rattle-type Fe_3O_4@ SnO_2 core-shell nanoparticles for dispersive solid-phase extraction of mercury ions. *Microchimica Acta, 184*, 707-713.

Mehmood, R. F., Mehmood, F., Akhtar, J., Shah, S. S., & Khosa, M. A. (2013). Adsorption of Cd (II) by Sol-Gel Silica Doped with N-(dipropylcarbamothioyl) thiophene-2-carboxamide. *Journal of Dispersion Science and Technology, 34*, 153-160.

Mendel, R. R. (2013). Metabolism of molybdenum. In Banci, L. (Ed), *Metallomics and the Cell* (pp. 503-528). Dordrecht: Springer

Mensah, E. K., Afari, E., Wurapa, F., Sackey, S., Quainoo, A., Kenu, E., & Nyarko, K. M. (2016). Exposure of small-scale gold miners in Prestea to mercury, Ghana, 2012. *The Pan African Medical Journal, 25*, 6.

Ministry of Health Malaysia. (2010). *National drinking water quality standard, Engineering Services Division, Ministry of Health, Malaysia*. Retrieved Oktober 09, 2017, from http://kmam.moh.gov.my/public-user/drinking-water-quality-standard.html

Mohan, D., & Singh, K. P. (2002). Single-and multi-component adsorption of cadmium and zinc using activated carbon derived from bagasse—an agricultural waste. *Water Research, 36*, 2304-2318.

Monier, M., & Abdel-Latif D. A. (2012). Preparation of cross-linked magnetic chitosan-phenylthiourea resin for adsorption of Hg(II), Cd(II) and Zn(II) ions from aqueous solutions. *Journal of Hazardous Materials, 209-210*, 240-249.

Monteiro, D. A., Rantin, F. T., & Kalinin, A. L. (2013). Dietary intake of inorganic mercury: bioaccumulation and oxidative stress parameters in the neotropical fish Hoplias malabaricus. *Ecotoxicology, 22*, 446-456.

Mubarak, N. M., Sahu, J. N., Abdullah, E. C., & Jayakumar, N. S. (2014). Removal of heavy metals from wastewater using carbon nanotubes. *Separation & Purification Reviews, 43*, 311-338.

Mudasir, M., Karelius, K., Aprilita, N. H., & Wahyuni, E. T. (2016). Adsorption of mercury (II) on dithizone-immobilized natural zeolite. *Journal of Environmental Chemical Engineering, 4*, 1839-1849.

Muliwa, A. M., Leswifi, T. Y., Onyango, M. S., & Maity, A. (2016). Magnetic adsorption separation (MAS) process: An alternative method of extracting Cr (VI) from aqueous solution using polypyrrole coated Fe_3O_4 nanocomposites. *Separation and Purification Technology, 158*, 250-258.

Muresan, B., Pernet-Coudrier, B., Cossa, D., & Varrault, G. (2011). Measurement and modeling of mercury complexation by dissolved organic matter isolates from freshwater and effluents of a major wastewater treatment plant. *Applied Geochemistry, 26*, 2057-2063.

Mureseanu, M., Reiss, A., Cioatera, N., Trandafir, I., & Hulea, V. (2010). Mesoporous silica functionalized with 1-furoyl thiourea urea for Hg (II) adsorption from aqueous media. *Journal of Hazardous Materials, 182*, 197-203.

Mushtaq, M., Bhatti, H. N., Iqbal, M., & Noreen, S. (2016). Eriobotrya japonica seed biocomposite efficiency for copper adsorption: isotherms, kinetics, thermodynamic and desorption studies. *Journal of Environmental management, 176*, 21-33.

Najafi, M., Yousefi, Y., & Rafati, A. A. (2012). Synthesis, characterization and adsorption studies of several heavy metal ions on amino-functionalized silica nano hollow sphere and silica gel. *Separation and Purification Technology, 85*, 193-205.

Nanseu-Njiki, C. P., Tchamango, S. R., Ngom, P. C., Darchen, A., & Ngameni, E. (2009). Mercury (II) removal from water by electrocoagulation using aluminium and iron electrodes. *Journal of Hazardous Materials, 168*, 1430-1436.

Naveedullah, M. Z. H., Yu, C., Shen, H., Duan, D., Shen, C., Lou, L., & Chen, Y. (2014). Concentrations and human health risk assessment of selected heavy metals in surface water of the siling reservoir watershed in Zhejiang province, China. *Polish Journal of Environmental Studies, 23*, 801-811.

Nestora, S., Merlier, F., Prost, E., Haupt, K., Rossi, C., & Bui, B. T. S. (2016). Solid-phase extraction of betanin and isobetanin from beetroot extracts using a dipicolinic acid molecularly imprinted polymer. *Journal of Chromatography A, 1465*, 47-54.

Nethaji, S., Sivasamy, A., & Mandal, A. B. (2013). Adsorption isotherms, kinetics and mechanism for the adsorption of cationic and anionic dyes onto carbonaceous particles prepared from Juglans regia shell biomass. *International Journal of Environmental Science and Technology, 10*, 231-242.

Niu, Y., Liu, H., Qu, R., Liang, S., Chen, H., Sun, C., & Cui, Y. (2015). Preparation and characterization of thiourea-containing silica gel hybrid materials for Hg (II) adsorption. *Industrial & Engineering Chemistry Research, 54*, 1656-1664.

Nouri, J., Mahvi, A. H., & Bazrafshan, E. (2010). Application of electrocoagulation process in removal of zinc and copper from aqueous solutions by aluminum electrodes. *International Journal of Environmental Research, 4*, 201-208.

Onwudiwe, D. C., & Ajibade, P. A. (2011). Synthesis, characterization and thermal studies of Zn (II), Cd (II) and Hg (II) complexes of N-Methyl-N-Phenyldithiocarbamate: the single crystal structure of $[(C_6H_5)(CH_3)NCS_2]_4Hg_2$. *International Journal of Molecular Sciences, 12*, 1964-1978.

Orlikova, B., Tasdemir, D., Golais, F., Dicato, M., & Diederich, M. (2011). Dietary chalcones with chemopreventive and chemotherapeutic potential. *Genes & Nutrition, 6*, 125-147.

Panhwar, Q. K., & Memon, S. (2014). Synthesis, characterisation, and antioxidant study of Cr (III)-rutin complex. *Chemical Papers, 68*, 614-623.

Park, J. D., & Zheng, W. (2012). Human exposure and health effects of inorganic and elemental mercury. *Journal of Preventive Medicine and Public Health, 45*, 344-352.

Patil, C. B., Mahajan, S. K., & Katti, S. A. (2009). Chalcone-A versatile molecule. *Journal of Pharmaceutical Sciences and Research, 1*, 11-22.

Picciano, A. L., & Vaden, T. D. (2013). Complexation between Cu (II) and curcumin in the presence of two different segments of amyloid β. *Biophysical Chemistry, 184*, 62-67.

Pillay, K., Cukrowska, E. M., & Coville, N. J. (2013). Improved uptake of mercury by sulphur-containing carbon nanotubes. *Microchemical Journal, 108*, 124-130.

Poon, W. C., Herath, G., Sarker, A., Masuda, T., & Kada, R. (2016). River and fish pollution in Malaysia: A green ergonomics perspective. *Applied Ergonomics, 57*, 80-93.

Pourjavid, M. R., Sehat, A. A., Arabieh, M., Yousefi, S. R., Hosseini, M. H., & Rezaee, M. (2014). Column solid phase extraction and flame atomic absorption spectrometric determination of manganese (II) and iron (III) ions in water, food and biological samples using 3-(1-methyl-1H-pyrrol-2-yl)-1H-pyrazole-5-carboxylic acid on synthesized graphene oxide. *Materials Science and Engineering: C, 35*, 370-378.

Prado, A. G., Sales, J. A., Carvalho, R. M., Rubim, J. C., & Airoldi, C. (2004). Immobilization of 5-amino-1, 3, 4-thiadiazole-thiol onto silica gel surface by heterogeneous and homogeneous routes. *Journal of Non-Crystalline Solids, 333*, 61-67.

Prasadarao, K., & Mohan, S. (2012). Synthesis, characterization and antimicrobial activity of some chalcones. *International Journal of Pharmacy and Technology, 4*, 4060-4066.

Prasanna, M. V., Praveena, S. M., Chidambaram, S., Nagarajan, R., & Elayaraja, A. (2012). Evaluation of water quality pollution indices for heavy metal contamination monitoring: a case study from Curtin Lake, Miri City, East Malaysia. *Environmental Earth Sciences, 67*, 1987-2001.

Puanngam, M., & Unob, F. (2008). Preparation and use of chemically modified MCM-41 and silica gel as selective adsorbents for Hg (II) ions. *Journal of Hazardous Materials, 154*, 578-587.

Pytlakowska, K. (2016). Dispersive micro solid-phase extraction of heavy metals as their complexes with 2-(5-bromo-2-pyridylazo)-5-diethylaminophenol using graphene oxide nanoparticles. *Microchimica Acta, 183*, 91-99.

Qu, R., Zhang, Y., Qu, W., Sun, C., Chen, J., Ping, Y., ... & Niu, Y. (2013). Mercury adsorption by sulfur-and amidoxime-containing bifunctional silica gel based hybrid materials. *Chemical Engineering Journal, 219*, 51-61.

Radi, S., Tighadouini, S., El Massaoudi, M., Ben Hadda, T., Zaghrioui, M., Bacquet, M., ... & Warad, I. (2014). Synthesis of 1-(Pyrrol-2-yl) imine modified silica as a new sorbent for the removal of toxic metals from aqueous solutions. *Journal of Materials and Environmental Science, 5*, 1280-1287.

Rahman, I. A., & Padavettan, V. (2012). Synthesis of silica nanoparticles by sol-gel: size-dependent properties, surface modification, and applications in silica-polymer nanocomposites-A review. *Journal of Nanomaterials, 2012*, 132424.

Rahman, M. S., Molla, A. H., Saha, N., & Rahman, A. (2012). Study on heavy metals levels and its risk assessment in some edible fishes from Bangshi River, Savar, Dhaka, Bangladesh. *Food Chemistry, 134*, 1847-1854.

Rahman, M. S., Saha, N., & Molla, A. H. (2014). Potential ecological risk assessment of heavy metal contamination in sediment and water body around Dhaka export processing zone, Bangladesh. *Environmental Earth Sciences, 71*, 2293-2308.

Ramos-Ramírez, E., Ortega, N. L. G., Soto, C. A. C., & Gutiérrez, M. T. O. (2009). Adsorption isotherm studies of chromium (VI) from aqueous solutions using sol–gel hydrotalcite-like compounds. *Journal of Hazardous Materials, 172*, 1527-1531.

Ren, X., Li, J., Tan, X., & Wang, X. (2013). Comparative study of graphene oxide, activated carbon and carbon nanotubes as adsorbents for copper decontamination. *Dalton Transactions, 42*, 5266-5274.

Reza, R., & Singh, G. (2010). Heavy metal contamination and its indexing approach for river water. *International Journal of Environmental Science & Technology, 7*, 785-792.

Ríos, Á., & Zougagh, M. (2016). Recent advances in magnetic nanomaterials for improving analytical processes. *TrAC Trends in Analytical Chemistry, 84*, 72-83.

Ripp, J. (Ed.). (1996). *Analytical detection limit guidance & laboratory guide for determining method detection limits*. Madison, WI: Wisconsin Department of Natural Resources, Laboratory Certification Program.

Rofouei, M. K., Rezaei, A., Masteri-Farahani, M., & Khani, H. (2012). Selective extraction and preconcentration of ultra-trace level of mercury ions in water and fish samples using Fe_3O_4-magnetite-nanoparticles functionalized by triazene compound prior to its determination by inductively coupled plasma-optical emission spectrometry. *Analytical Methods, 4*, 959-966.

Roohani, N., Hurrell, R., Kelishadi, R., & Schulin, R. (2013). Zinc and its importance for human health: An integrative review. *Journal of Research in Medical Sciences: The Official Journal of Isfahan University of Medical Sciences, 18*, 144-157.

Saad, B., Chong, C. C., Ali, A. S. M., Bari, M. F., Ab Rahman, I., Mohamad, N., & Saleh, M. I. (2006). Selective removal of heavy metal ions using sol–gel immobilized and SPE-coated thiacrown ethers. *Analytica Chimica Acta, 555*, 146-156.

Sadeek, S. A., Negm, N. A., Hefni, H. H., & Wahab, M. M. A. (2015). Metal adsorption by agricultural biosorbents: Adsorption isotherm, kinetic and biosorbents chemical structures. *International Journal of Biological Macromolecules, 81*, 400-409.

Saka, C. (2012). BET, TG–DTG, FT-IR, SEM, iodine number analysis and preparation of activated carbon from acorn shell by chemical activation with $ZnCl_2$. *Journal of Analytical and Applied Pyrolysis, 95*, 21-24.

Santhosh, P., & Sridevi, A. (2013). A lab-scale study on reduction of heavy metals from electroplating effluent using conventional chemical precipitation. *Journal of Environmental Research and Development, 8*, 102-108.

Say, R., Birlik, E., Erdemgil, Z., Denizli, A., & Ersöz, A. (2008). Removal of mercury species with dithiocarbamate-anchored polymer/organosmectite composites. *Journal of Hazardous Materials, 150*, 560-564.

Sciancalepore, C., Bondioli, F., & Messori, M. (2017). Non-hydrolytic sol–gel synthesis and reactive suspension method: an innovative approach to obtain magnetite–epoxy nanocomposite materials. *Journal of Sol-Gel Science and Technology, 81*, 69-83.

Selin, N. E. (2009). Global biogeochemical cycling of mercury: A review. *Annual Review of Environment and Resources, 34*, 43-63.

Sendrayaperumal, V., Pillai, S. I., & Subramanian, S. (2014). Design, synthesis and characterization of zinc–morin, a metal flavonol complex and evaluation of its antidiabetic potential in HFD–STZ induced type 2 diabetes in rats. *Chemico-biological Interactions, 219*, 9-17.

Seo, J. W., & Park, T. J. (2008). Magnesium metabolism. *Electrolyte & Blood Pressure, 6*, 86-95.

Shawky, H. A., El-Aassar, A. H. M., & Abo-Zeid, D. E. (2012). Chitosan/carbon nanotube composite beads: Preparation, characterization, and cost evaluation for mercury removal from wastewater of some industrial cities in Egypt. *Journal of Applied Polymer Science, 125*, E93-E101.

Shen, X., Wang, Q., Chen, W., & Pang, Y. (2014). One-step synthesis of water-dispersible cysteine functionalized magnetic Fe_3O_4 nanoparticles for mercury (II) removal from aqueous solutions. *Applied Surface Science, 317*, 1028-1034.

Shirkhanloo, H., Khaligh, A., Mousavi, H. Z., & Rashidi, A. (2016). Ultrasound assisted-dispersive-micro-solid phase extraction based on bulky amino bimodal mesoporous silica nanoparticles for speciation of trace manganese (II)/(VII) ions in water samples. *Microchemical Journal, 124*, 637-645.

Singh, P., Anand, A., & Kumar, V. (2014). Recent developments in biological activities of chalcones: A mini review. *European Journal of Medicinal Chemistry, 85*, 758-777.

Singh, R., Gautam, N., Mishra, A., & Gupta, R. (2011). Heavy metals and living systems: an overview. *Indian Journal of Pharmacology, 43*, 246-253.

Sobhi, H. R., Ghambarian, M., Esrafili, A., & Behbahani, M. (2017). A nanomagnetic and 3-mercaptopropyl-functionalized silica powder for dispersive solid phase extraction of Hg (II) prior to its determination by continuous-flow cold vapor AAS. *Microchimica Acta, 184*, 2317-2323.

Song, H., Shao, J., He, Y., Liu, B., & Zhong, X. (2012). Natural organic matter removal and flux decline with PEG–TiO_2-doped PVDF membranes by integration of ultrafiltration with photocatalysis. *Journal of Membrane Science, 405*, 48-56.

Soto, R. J., Yang, L., & Schoenfisch, M. H. (2016). Functionalized mesoporous silica via an aminosilane surfactant ion exchange reaction: controlled scaffold design and nitric oxide release. *ACS Applied Materials & Interfaces, 8*, 2220-2231.

Stein, E. D., Cohen, Y., & Winer, A. M. (1996). Environmental distribution and transformation of mercury compounds. *Critical Reviews in Environmental Science and Technology, 26*, 1-43.

Strode, S. A., Jaeglé, L., Selin, N. E., Jacob, D. J., Park, R. J., Yantosca, R. M., ... & Slemr, F. (2007). Air-sea exchange in the global mercury cycle. *Global Biogeochemical Cycles, 21*, GB1017.

Sumesh, E., Bootharaju, M. S., & Pradeep, T. (2011). A practical silver nanoparticle-based adsorbent for the removal of Hg^{2+} from water. *Journal of Hazardous Materials, 189*, 450-457.

Sun, X., Qu, R., Sun, C., Zhang, Y., Sun, S., Ji, C., & Yin, P. (2014). Sol–gel preparation and Hg (II) adsorption properties of silica-gel supported low generation polyamidoamine dendrimers polymer adsorbents. *Industrial & Engineering Chemistry Research, 53*, 2878-2888.

Tadayon, F., Saber-Tehrani, M., & Motahar, S. (2013). Selective removal mercury (II) from aqueous solution using silica aerogel modified with 4-amino-5-methyl-1,2,4-triazole-3(4H)-thion. *Korean Journal of Chemistry Engineering, 30*, 642-648.

Tadjarodi, A., Jalalat, V., & Zare-Dorabei, R. (2015). Adsorption of La (III) in aqueous systems by N-(2-hydroxyethyl) salicylaldimine-functionalized mesoporous silica. *Materials Research Bulletin, 61*, 113-119.

Tavares, D. S., Daniel-da-Silva, A. L., Lopes, C. B., Silva, N. J., Amaral, V. S., Rocha, J., ... & Trindade, T. (2013). Efficient sorbents based on magnetite coated with siliceous hybrid shells for removal of mercury ions. *Journal of Materials Chemistry A, 1*, 8134-8143.

Teh, C. Y., Budiman, P. M., Shak, K. P. Y., & Wu, T. Y. (2016). Recent advancement of coagulation–flocculation and its application in wastewater treatment. *Industrial & Engineering Chemistry Research, 55*, 4363-4389.

Tiwari, S., Ready, K. V., & Bajpai, A. (2015) IR spectra studies of coordination polymers prepared by urea bisdithicarbamates. *International Journal of Advanced Technology in Engineering and Science, 3*, 608-615.

Trewyn, B. G., Slowing, I. I., Giri, S., Chen, H. T., & Lin, V. S. Y. (2007). Synthesis and functionalization of a mesoporous silica nanoparticle based on the sol–gel process and applications in controlled release. *Accounts of Chemical Research, 40*, 846-853.

Turanov, A. N., Karandashev, V. K., Sukhinina, N. S., Masalov, V. M., & Emelchenko, G. A. (2016). Adsorption of lanthanides and scandium ions by silica sol-gel material doped with novel bifunctional ionic liquid, trioctylmethylammonium 1-phenyl-3-methyl-4-benzoyl-5-onate. *Journal of Environmental Chemical Engineering, 4*, 3788-3796.

Tzvetkova, P., & Nickolov, R. (2012). Modified and unmodified silica gel used for heavy metal ions removal from aqueous solutions. *Journal of the University of Chemical Technology and Metallurgy, 47*, 498-504.

United State Environmental Protection Agency. (2004). *Understanding the Safe Drinking Water Act*, EPA 816-F-04-030. EPA, Washington, DC.

United State Environmental Protection Agency. (2009). National primary drinking water regulation, EPA 816-F-09-004. EPA, Washington, DC.

Venkatesan, K. A., Srinivasan, T. G., & Rao, P. V. (2003). Removal of complexed mercury by dithiocarbamate grafted on mesoporous silica. *Journal of Radioanalytical and Nuclear Chemistry, 256*, 213-218.

Venkatesan, K. A., Srinivasan, T. G., & Vasudeva Rao, P. R. (2002). Removal of complexed mercury from aqueous solutions using dithiocarbamate grafted on silica gel. *Separation Science and Technology, 37*, 1417-1429.

Wajima, T., & Sugawara, K. (2011). Adsorption behaviors of mercury from aqueous solution using sulfur-impregnated adsorbent developed from coal. *Fuel Processing Technology, 92*, 1322-1327.

Wang, M., Bi, W., Huang, X., & Chen, D. D. Y. (2016). Ball mill assisted rapid mechanochemical extraction method for natural products from plants. *Journal of Chromatography A, 1449*, 8-16.

Wang, N., Liu, C. Q., Wen, B., Wang, H. L., Liu, S. M., & Chai, W. P. (2014). Enhanced optical and electrical properties of NiO thin films prepared by rapid radiation pyrolysis method based on the sol–gel technique. *Materials Letters, 122*, 269-272.

Wang, Z., Lim, B., & Choi, C. (2011). Removal of Hg^{2+} as an electron acceptor coupled with power generation using a microbial fuel cell. *Bioresource Technology, 102*, 6304-6307.

Wanninger, S., Lorenz, V., Subhan, A., & Edelmann, F. T. (2015). Metal complexes of curcumin–synthetic strategies, structures and medicinal applications. *Chemical Society Reviews, 44*, 4986-5002.

Water Environment Partnership in Asia. (2006). *National water quality standards in Malaysia*. Retrieved October 10, 2017, from http://www.wepa-db.net/policies/law/malaysia/eq_surface.htm

Weiss-Penzias, P. S., Gay, D. A., Brigham, M. E., Parsons, M. T., Gustin, M. S., & ter Schure, A. (2016). Trends in mercury wet deposition and mercury air concentrations across the US and Canada. *Science of the Total Environment, 568*, 546-556.

Wells, M. J. (2003). Principles of extraction and the extraction of semivolatile organics from liquids. In Mitra, S. (Ed), *Sample Preparation Techniques in Analytical Chemistry* (pp. 37-138). Hoboken, New Jersey: John Wiley & Sons, Inc.

Wen, S., & Zhu, X. (2014). Speciation analysis of Mn (II)/Mn (VII) in tea samples using flame atomic absorption spectrometry after room temperature ionic liquid-based dispersive liquid–liquid microextraction. *Food Analytical Methods, 7*, 291-297.

Wen, Z., Dai, C., Zhu, Y., & Zhang, Y. (2015). Arsenate removal from aqueous solutions using magnetic mesoporous iron manganese bimetal oxides. *RSC Advances, 5*, 4058-4068.

Wierucka, M., & Biziuk, M. (2014). Application of magnetic nanoparticles for magnetic solid-phase extraction in preparing biological, environmental and food samples. *TrAC Trends in Analytical Chemistry, 59*, 50-58.

Wilbers, G. J., Becker, M., Sebesvari, Z., & Renaud, F. G. (2014). Spatial and temporal variability of surface water pollution in the Mekong Delta, Vietnam. *Science of the Total Environment, 485*, 653-665.

World Health Organization, & United Nations Children's Fund. (2014). *Progress on sanitation and drinking water: 2014 update*. Geneva: World Health Organization.

World Health Organization. (2005). *Mercury in drinking-water*. Geneva: World Health Organization.

World Health Organization. (2011). *Guidelines for drinking-water quality*. Geneva: World Health Organization.

World Health Organization. (2017). *Drinking water*. Retrieved October 09, 2017, from http://www.who.int/mediacentre/factsheets/fs391/en/

Wu, P., Wang, G., Chen, R., Guo, Y., Ma, X., & Jiang, D. (2016). Enhanced visible light absorption and photocatalytic activity of $[KNbO_3]_{1-x}[BaNi_{0.5}Nb_{0.5}O_{3-\delta}]_x$ synthesized by sol–gel based Pechini method. *RSC Advances, 6*, 82409-82416.

Wu, X., Luo, L., Chen, Z., & Liang, K. (2016). Syntheses, characterization and adsorption properties for Pb^{2+} of silica-gel functionalized by dendrimer-like polyamidoamine and 5-sulfosalicylic acid. *Applied Surface Science, 364*, 86-95.

Wu, Z., Zhong, H., Yuan, X., Wang, H., Wang, L., Chen, X., ... & Wu, Y. (2014). Adsorptive removal of methylene blue by rhamnolipid-functionalized graphene oxide from wastewater. *Water Research, 67*, 330-344.

Xian, Y., Wu, Y., Dong, H., Guo, X., Wang, B., & Wang, L. (2017). Dispersive micro solid phase extraction (DMSPE) using polymer anion exchange (PAX) as the sorbent followed by UPLC–MS/MS for the rapid determination of four bisphenols in commercial edible oils. *Journal of Chromatography A, 2517*, 35-43.

Xiang, G., Li, L., Jiang, X., He, L., & Fan, L. (2013). Thiol-modified magnetic silica sorbent for the determination of trace mercury in environmental water samples coupled with cold vapor atomic absorption spectrometry. *Analytical Letters, 46*, 706-716.

Xie, L., Liu, S., Han, Z., Jiang, R., Liu, H., Zhu, F., ... & Ouyang, G. (2015). Preparation and characterization of metal-organic framework MIL-101 (Cr)-coated solid-phase microextraction fiber. *Analytica Chimica Acta, 853*, 303-310.

Yan, L. G., Qin, L. L., Yu, H. Q., Li, S., Shan, R. R., & Du, B. (2015). Adsorption of acid dyes from aqueous solution by CTMAB modified bentonite: kinetic and isotherm modeling. *Journal of Molecular Liquids, 211*, 1074-1081.

Yang, T., Liu, L. H., Liu, J. W., Chen, M. L., & Wang, J. H. (2012). Cyanobacterium metallothionein decorated graphene oxide nanosheets for highly selective adsorption of ultra-trace cadmium. *Journal of Materials Chemistry, 22*, 21909-21916.

Yilmaz, E., & Soylak, M. (2014). Solid phase extraction of Cd, Pb, Ni, Cu, and Zn in environmental samples on multiwalled carbon nanotubes. *Environmental Monitoring and Assessment, 186*, 5461-5468.

Yokoi, T., Yoshitake, H., & Tatsumi, T. (2004). Synthesis of amino-functionalized MCM-41 via direct co-condensation and post-synthesis grafting methods using mono-, di-and tri-amino-organoalkoxysilanes. *Journal of Materials Chemistry, 14*, 951-957.

Yost, T. L., Fagan, B. C., Allain, L. R., Barnes, C. E., Dai, S., Sepaniak, M. J., & Xue, Z. (2000). Crown ether-doped sol-gel materials for strontium (II) separation. *Analytical Chemistry, 72*, 5516-5519.

Zaitoun, M., Momania, K., Jaradat, Q., Momani, I., & Qurashi, I. (2014). Synthesis of an organic chelate doped sol gel filter to remove Cu (II) ions from aqueous solutions. *Jordan Journal of Chemistry, 9*, 81-*96*.

Zawisza, B., Baranik, A., Malicka, E., Talik, E., & Sitko, R. (2016). Preconcentration of Fe (III), Co (II), Ni (II), Cu (II), Zn (II) and Pb (II) with ethylenediamine-modified graphene oxide. *Microchimica Acta, 183*, 231-240.

Zewail, T. M., & Yousef, N. S. (2015). Kinetic study of heavy metal ions removal by ion exchange in batch conical air spouted bed. *Alexandria Engineering Journal, 54*, 83-90.

Zhai, G. Y., Qu, W. T., Yan, Z. T., Zhu, W., Duan, Y. D., & Wang, J. P. (2014). Synthesis, spectral and antioxidant properties of Tin (II)-Rutin complex. *Chemistry of Natural Compounds, 50*, 624-628.

Zhai, Y., He, Q., Yang, X., & Han, Q. (2010). Solid phase extraction and preconcentration of trace mercury (II) from aqueous solution using magnetic nanoparticles doped with 1, 5-diphenylcarbazide. *Microchimica Acta, 169*, 353-360.

Zhang, B. T., Zheng, X., Li, H. F., & Lin, J. M. (2013). Application of carbon-based nanomaterials in sample preparation: A review. *Analytica Chimica Acta, 784*, 1-17.

Zhang, W. B., Sun, C. X., & Yang, X. A. (2014). Magnetic solid-phase extraction combined with in situ slurry cold vapor generation atomic fluorescence spectrometry for preconcentration and determination of ultratrace mercury. *Analytical Methods, 6*, 2876-2882.

Zhang, X., Siddiqi, Z., Song, X., Mandiwana, K. L., Yousaf, M., & Lu, J. (2012). Atmospheric dry and wet deposition of mercury in Toronto. *Atmospheric Environment, 50*, 60-65.

Zhang, Z., Li, J., Song, X., Ma, J., & Chen, L. (2014). Hg^{2+} ion-imprinted polymers sorbents based on dithizone–Hg^{2+} chelation for mercury speciation analysis in environmental and biological samples. *RSC Advances, 4*, 46444-46453.

Zhao, Y., Zhai, S. R., Zhai, B., & An, Q. D. (2012). Heavy metal removal of tri-amino-functionalized sol–gel hybrids with tailored characteristics. *Journal of Sol-gel Science and Technology, 62*, 177-185.

Zhou, L., Zou, H., Wang, Y., Liu, Z., Huang, Z., Luo, T., & Adesina, A. A. (2016). Adsorption of uranium (VI) from aqueous solution using phosphonic acid-functionalized silica magnetic microspheres. *Journal of Radioanalytical and Nuclear Chemistry, 310*, 1155-1163.

Zhou, Q., Xing, A., & Zhao, K. (2014). Simultaneous determination of nickel, cobalt and mercury ions in water samples by solid phase extraction using multiwalled carbon nanotubes as adsorbent after chelating with sodium diethyldithiocarbamate prior to high performance liquid chromatography. *Journal of Chromatography A, 1360*, 76-81.

Zhu, J., Yang, J., & Deng, B. (2009). Enhanced mercury ion adsorption by amine-modified activated carbon. *Journal of Hazardous Materials, 166*, 866-872.

LIST OF PUBLICATIONS AND PAPERS PRESENTED

1. Publication

   Khor, S. W., Lee, Y. K., Abas, M. R. B., & Tay, K. S. (2017). Application of chalcone-based dithiocarbamate derivative incorporated sol–gel for the removal of Hg (II) ion from water. *Journal of Sol-Gel Science and Technology*, *82*(3), 834-845.

2. Poster presented

   Khor Soo Wei, Mhd Radzi Bin Abas, Tay Kheng Soo, Chalcone Derived Ligand Incorporated Sol-gel for Mercury (II) Ion Removal in Water. Poster Presentation at UM#111-Chemistry Symposium. 3rd March 2016, Department of Chemistry, Faculty of Science, University of Malaya.